DISSERTATION

Submitted to the

Combined Faculties for the Natural Sciences and for Mathematics of the Ruperto-Carola University of Heidelberg, Germany

for the degree of

Doctor of Natural Sciences

presented by

Luis Alberto Castillo-Ramirez, MSc.

born in: Monterrey, Mexico

Oral-examination: 14th February 2017

Development of an early life stress model in larval zebrafish and analysis of stress-induced transcriptomic changes in hypothalamic cells

Referees: Prof. Dr. Jan Lohmann

Prof. Dr. Soojin Ryu

ABSTRACT

The Hypothalamic-Pituitary-Adrenal (HPA) axis and its final effector, glucocorticoids (GCs), are important players in maintaining homeostasis of an organism upon stress exposure. However, overexposure to GCs during early life is involved in developmental programming of the HPA axis and is linked to detrimental effects in health. The hypothalamus is a key target for developmental programming due to its pivotal role as an integrator of input signals coming from sensory systems and other brain regions and as a translator of neuronal signals into endocrine signals. Yet, little is known about the molecular mechanisms involved in hypothalamic programming mediated by stressful experiences during early life. Elucidation of these mechanisms is essential for understanding the link between early life stress, dysregulation of the stress response, and detrimental health in later stages.

Here, I used the zebrafish model to elucidate the molecular correlates of early adverse experience in hypothalamic cells. First, I developed a stimulation protocol using vortex flows to activate the hypothalamic-pituitary-interrenal (HPI) axis, the homolog of the HPA axis in teleost, and characterized the stress response at early stages by measuring cortisol (the main GC in zebrafish) and behavioral correlates. I then identified a critical time window in which HPI axis activity matures. Subsequently, I established an early life stress protocol to induce hypercortisolic states and alter stress response maturation. Endocrinological, behavioral, and cellular characterization of the early life stress paradigm showed an overall downregulation of the stress response with attenuated locomotor and cortisol response to subsequent stressful events as well as reduced calcium activity and expression of stress related peptides (AVP, CRH, and OXT) in hypothalamic cells. To dissect the molecular correlates of early adverse experience, I then performed transcriptomic analysis of hypothalamus-specific cell populations after exposure to the early life stress paradigm. Candidate molecules involved in the adaptive process occurring in hypothalamic cells were identified. Moreover, gene ontology and pathway analysis showed that lipid metabolism and molecular transport pathways were downregulated after zebrafish larvae were subjected to the early life stress protocol. In contrast, cellular movement and inflammatory response pathways were upregulated. Finally, I characterized the cortisol profiles of optogenetic and targeted transgenic tools which have been generated to manipulate the

HPI axis activity in freely swimming larvae. Here, I show evidence of altered levels of endogenous cortisol in larvae that were manipulated at any of the three levels of the HPI axis.

Altogether, the main contributions of this thesis are: 1) establishment of a novel stress protocol to activate the HPI axis in zebrafish larvae in a highly controlled and strength-dependent manner; 2) characterization of the cortisol response of developing zebrafish and identification of a critical time window of stress response maturation; 3) development of an early life stress paradigm and elucidation of the effects of early adverse experience at the cellular, behavioral, and endocrinological level; 4) identification of candidate molecules and metabolic pathways in hypothalamic cells involved in adaptive processes after early adverse experience, and 5) characterization of the cortisol profiles of optogenetic and genetic tools to manipulate the HPI axis activity at any of its three levels (hypothalamus, pituitary, and interrenal gland).

ZUSAMMENFASSUNG

Die Hypothalamic-Pituitary-Adrenal (HPA)-Achse und ihre Endsignalstoffe, die Glucocorticoide (GCs), sind wichtige Spieler bei der Aufrechterhaltung der Homöostase eines Organismus unter Stresseinwirkung. Allerdings ist eine übermäßige Einwirkung von GCs früh im Leben an der Programmierung der HPA-Achse während ihrer Entwicklung beteiligt und wird mit gesundheitsschädlichen Effekten in Verbindung gebracht. Der Hypothalamus ist ein Hauptziel für Programmierung während der Entwicklung aufgrund seiner entscheidenden Rolle als Integrator von einkommenden Signalen der sensorischen Systeme und anderer Hirnregionen, und als Übersetzer neuronaler Signale in endokrine Signale. Dennoch ist wenig über die durch stressige frühe Erfahrungen vermittelten molekularen Mechanismen bekannt, die an hypothalamischer Programmierung beteiligt sind. Eine Aufklärung dieser Mechanismen ist entscheidend für das Verständnis der Verbindungen zwischen Stress früh im Leben, Fehlregulation der Stressantwort, und Gesundheitsschäden in späteren Stadien.

In der vorliegenden Arbeit benutzte ich den Zebrafisch als Modell, um die molekularen Korrelate von frühen negativen Erlebnissen in hypothalamischen Zellen aufzuklären. Zuerst habe ich ein Stimulationsprotokoll mit Wirbelströmungen entwickelt, um die Hypothalamic-Pituitary-Interrenal (HPI)-Achse zu aktivieren, die in Teleostei homolog zur HPA-Achse ist, und habe die Stressantwort in frühen Entwicklungsstadien durch Messung von Cortisol (des primären GCs im Zebrafisch), und korrelierendes Verhalten charakterisiert. Weiterhin habe ich ein kritisches Zeitfenster identifiziert, in dem die Aktivität der HPI-Achse ausreift. Anschließend habe ich ein Protokoll für Stress früh im Leben etabliert, um hypercortisolische Zustände zu erzeugen und die Reifung der Stressantwort zu verändern. Endokrinologische, verhaltensbiologische und zelluläre Charakterisierung dieses „early life stress paradigms“ zeigte eine generelle Herabregulierung der Stressantwort mit gedämpften lokomotorischen und Cortisolantworten auf nachfolgende Stressereignisse, und verringerte Calciumaktivität und Expression stressrelevanter Peptide (AVP, CRH und OXT) in hypothalamischen Zellen. Um molekulare Korrelate früher negativer Erlebnisse zu untersuchen, habe ich danach eine Transkriptomanalyse von Hypothalamus-spezifischen Zellpopulationen nach Einwirkung des „early life stress paradigms“ durchgeführt. Kandidatenmoleküle wurden identifiziert, die im

Anpassungsprozess involviert sind und in hypothalamischen Zellen vorkommen. Außerdem zeigte eine Gen-Ontologie- und Signalweganalyse, dass Lipidmetabolismus und molekulare Transportwege herunterreguliert wurden, nachdem Zebrafischlarven dem „early life stress“-Protokoll ausgesetzt waren; andererseits wurden Zellmotilitäts- und Entzündungsreaktionswege heraufreguliert. Schließlich habe ich die Cortisolprofile von optogenetischen und genetischen Werkzeugen charakterisiert, die zur Manipulation der HPI-Achsenaktivität in freischwimmenden Larven entwickelt wurden. Hier zeige ich Nachweise veränderter endogener Cortisolspiegel in Larven, die auf jeder der drei Ebenen der HPI-Achse manipuliert wurden.

Zusammenfassend sind die hauptsächlichen Beiträge dieser Arbeit: 1) Etablierung eines neuartigen Stressprotokolls zur Aktivierung der HPI-Achse in Zebrafischlarven auf hochgradig kontrollierte und stärkeabhängige Weise; 2) Charakterisierung der Cortisolantwort von sich entwickelnden Zebrafischen und Identifizierung eines kritischen Zeitfensters der Stressantwortreifung; 3) Entwicklung eines „early life stress paradigms“ und Aufklärung der Effekte früher negativer Erlebnisse auf der zellulären, endokrinologischen und Verhaltensebene; 4) Identifizierung von Kandidatenmolekülen und metabolischen Signalwegen in Hypothalamuszellen, die in Anpassungsprozesse nach früher negativer Erfahrung involviert sind, und 5) Charakterisierung von Cortisolprofilen optogenetischer und genetischer Werkzeuge zur Manipulation der HPI-Achsenaktivität auf jeder ihrer drei Ebenen (Hypothalamus, Hypophyse und Interrenalorgan).

PUBLICATIONS and PRESENTATIONS

This work has contributed to the following publications:

De Marco, R. J., Groneberg, A. H., Yeh, C. M., **Castillo-Ramirez, L. A.**, Ryu, S. 2013. Optogenetic elevation of endogenous glucocorticoid level in larval zebrafish. Front Neural Circuits, 7.

Gutierrez-Triana, J. A., Herget, U., Lichtner, P., **Castillo-Ramírez, L. A.**, Ryu, S. 2014. A vertebrate-conserved cis-regulatory module for targeted expression in the main hypothalamic regulatory region for the stress response. BMC Developmental Biology, 14, 41.

Gutierrez-Triana, J. A., Herget, U., **Castillo-Ramirez, L. A.**, Lutz, M., Yeh, C. M., De Marco, R. J., Ryu, S. 2015. Manipulation of Interrenal Cell Function in Developing Zebrafish Using Genetically Targeted Ablation and an Optogenetic Tool. Endocrinology, 156, 3394-401.

Results of this work were presented in:

Castillo-Ramirez, L. A., Developmental programming of the HPI axis: physiological and behavioral correlates of stress during early life stages of zebrafish. Talk, Neuroendocrine Immune Networks in Ageing (NINA) Fellows Workshop, Paris, 2012.

Castillo-Ramirez, L. A., Optogeneitc manipulation of endogenous cortisol levels during development in zebrafish, Danio rerio. Talk, Neuroendocrine Immune Networks in Ageing (NINA) Fellows Workshop, Amsterdam, 2013.

Castillo-Ramírez, L. A., De Marco, R. J., Gutierrez-Triana, A., Herget, U., Ryu, S. Early life stress exposure alters stress response axis activity in larval zebrafish, *Danio rerio*. Poster, 9th FENS meeting, Milan, 2014.

TABLE OF CONTENTS

1. INTRODUCTION

1.1 Stress response and the Hypothalamic-Pituitary-Adrenal axis

The stress response is defined as a set of physiological and behavioral processes which are elicited in order for an animal to cope with any environmental cue perceived as a threat to the internal homeostasis of an organism (Selye, 1956). Upon the perception of a stressful event, different brain circuits are activated depending on the nature of the stressor (Herman and Cullinan, 1997). While stressors representing a physiological threat (physical or systemic stressors) are processed by the brainstem (Palkovits, 1999), stressors which need to be interpreted by higher brain structures (psychological or processive stressors) are processed by limbic structures such as the amygdala, hippocampus, prefrontal cortex (PFC), and bed nucleus of the stria terminalis (BNST) (Herman and Cullinan, 1997, Bains et al., 2015). In both cases, information coming from physical or psychological stressors is then integrated in the paraventricular nucleus of the hypothalamus (PVN) (Figure 1.1). This brain area organizes the physiological and behavioral response to the stressor by activating the sympathetic nervous system (first response wave) and the Hypothalamic-Pituitary-Adrenal (HPA) axis (second response wave) (Sapolsky et al., 2000, Joels et al., 2006, Cicchetti, 2013).

During the first response wave, adrenalin is secreted from the adrenal medulla having immediate effects at the systemic level by increasing heart rate, elevating blood glucose levels, and suppressing digestive and reproductive systems to avoid unnecessary energy expenditure and facilitate coping with the stressor (Sapolsky et al., 2000, Ulrich-Lai and Herman, 2009). The second response wave, orchestrated by the HPA axis, modulates the physiological changes induced by the first response wave (Sapolsky et al., 2000). The HPA axis is considered as the key regulatory system, for it is a physiological and anatomical link between the central nervous system and the endocrine system, represented by the hypothalamus and pituitary, respectively (Löhr and Hammerschmidt, 2011). Activation of the HPA axis is mediated by hypothalamic neurons expressing corticotropin releasing hormone (CRH) in the PVN. Within seconds after activation, CRH and arginine vasopressin (AVP) are released from the PVN and stimulate adrenocorticotropic hormone (ACTH) secretion from the corticotroph cells located at the anterior lobe of the pituitary gland. ACTH binds to the melanocortin receptors 2 (MC2R) located in the adrenal glands at the top of the kidneys and

stimulates glucocorticoid (GC) release, with cortisol and corticosterone being the main GCs in humans and rodents, respectively (Charmandari et al., 2005) (Figure 1.1).

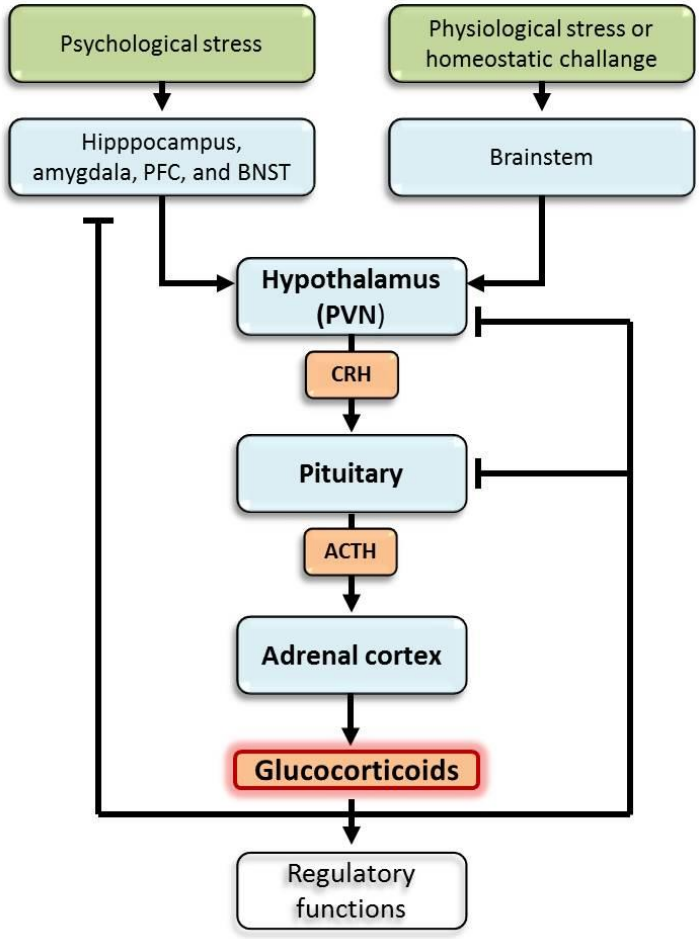

Figure 1.1. Schematic representation of the stress response. Psychological and physiological stressors are processed by different brain structures which further direct information to the main integrational brain center located in the paraventricular nucleus of the hypothalamus (PVN). Neurons expressing corticotropin releasing hormone (CRH) orchestrate the stress response by secreting this hormone, which binds to the CRH receptors (CRHR) in the pituitary and stimulates adrenocorticotropic hormone (ACTH) synthesis and secretion. ACTH then binds to melanocortin 2 receptors located in the adrenal glands and stimulates glucocorticoids (GCs) synthesis and secretion into the general circulation. GCs have a wide range of peripheral functions which induce adaptive changes aiming to maintain homeostasis, including negative feedback on the hypothalamus-pituitary axis, as well as on higher brain centers such as the hippocampus, prefrontal cortex (PFC), and amygdala.

GCs are the final effectors of the stress response having pleiotropic effects, both genomic and non-genomic, in several target tissues. Among a wide variety of functions, they play an important role on glucose mobilization from muscle and liver and in anti-inflammatory process which allows directing valuable energy to essential functions involved in coping with a stressful event and maintaining homeostasis (Sapolsky et al.,

2000, Tasker and Herman, 2011). Moreover, GCs exert a wide range of effects on neurons in a temporal and spatial-dependent manner, affecting brain function such as cognition, behavior, and mood (De Kloet et al., 1998, de Kloet et al., 2005, Sandi and Haller, 2015). They also interact with hypothalamic cells in the PVN and corticotrophs in the anterior pituitary to form a negative loop that represses CRH and ACTH secretion (Johnson et al., 1992, Groeneweg et al., 2011) (Figure 1.1). In mammals, the changes in hormone levels in response to a stressor are in the range of minutes; however, some genomic effects of GCs in target tissues as a result of a stress response may occur with a delay of hours or even days (Sapolsky et al., 2000).

1.2 Glucocorticoid and mineralocorticoid receptors mediate the effects of glucocorticoids.

The genomic effects of GCs are mediated by the glucocorticoid receptor (GR; low affinity) and/or the mineralocorticoid receptor (MR; high affinity) (De Kloet et al., 1998, Kadmiel and Cidlowski, 2013). In the brain, the GRs are strongly expressed in regions related to HPA axis activity, such as the hypothalamus and pituitary corticotrophs. The MRs are also expressed in hypothalamic regions involved in osmoregulation; however, the highest expression of MRs is located in the hippocampus, the brain region involved in learning and memory processes (Reul and de Kloet, 1985, De Kloet et al., 1998). Both receptors are members of the nuclear receptor family and are located in the cytosolic space of cells, where they bind to their ligands that diffuse through the cell membrane. Due to the high affinity to GCs, around 80% of the MRs are occupied even at relatively low concentrations of GCs under basal conditions. Hence, it has been proposed that GCs exert a tonic influence through hippocampal MRs. In contrast, GRs occupancy occurs when higher GCs levels are reached after HPI axis activation and therefore their actions are linked, among other functions, to feedback mechanisms to restore homeostasis (De Kloet et al., 1998, Eberwine, 1999). In this way, the function of MRs is more likely to be limited by the number of receptors rather than by its level of occupancy. On the other hand, the GR function is more dependent on fluctuations of GCs levels occurring after HPI axis activation.

After binding to GCs, GRs translocate to the nucleus as homodimers. They modify gene transcription via transactivation. In this process, GRs bind glucocorticoid-responsive elements (GRE) on the DNA, culminating in enhanced or repressed gene transcription of target genes. Activated GRs also interfere with the transcriptional

activity of transcription factors through protein-protein interactions, resulting in indirect regulation of target genes expression, a process denominated as transrepression. Moreover, heterodimerization between GRs and MRs is also possible, resulting in changes in the transcription rate of target genes (Beato and Sanchez-Pacheco, 1996, De Kloet et al., 1998, Newton and Holden, 2007, Datson et al., 2008).

In addition, GCs exert rapid non-genomic effects in a wide variety of target tissues. Of especial interest are the rapid effects of GCs on brain regions involved in the stress response. These rapid effects facilitate or inhibit signaling of ion channels, receptors, and/or neurotransmitters, culminating in altered cell activity (Groeneweg et al., 2011). While increased excitability has been observed in hippocampus, amygdala and PFC shortly after an increase in GC levels, other brain regions such as the hypothalamus showed decreased excitability (Zhu et al., 1998, Di et al., 2003, Karst et al., 2005, Karst et al., 2010, Groeneweg et al., 2011).

The receptors and mechanisms mediating the rapid non-genomic effects of GCs in the brain are not completely known. Studies have shown that these effects involve member-bound receptors and G-protein-coupled signaling. Although some studies have shown that rapid effects are mediated by classical GRs and MRs bound to the membrane (Solito et al., 2003, Karst et al., 2005, Karst et al., 2010, Roozendaal et al., 2010), others have shown that administration of GR or MR receptor antagonists do not block the rapid effect of GCs (Di et al., 2003, Di et al., 2009). Moreover, G-protein-coupled signaling was also observed in these cases, indicating that a yet unknown membrane-bound G-protein-coupled receptor is involved in some non-genomic effects of GCs. This is the case in PVN cells, where rapid non-genomic effects on glutamatergic signaling mediated by GCs require endocannabinoid signaling (Di et al., 2003, Evanson et al., 2010). After administration of GCs, a putative membrane-bound G-protein-coupled receptor is activated and stimulates the synthesis of the endocannabinoids anandamide (AEA) and 2-arachidonoylglycerol (2-AG) in postsynaptic neurons; these endocannabinoids are secreted and bind to the endocannabinoid receptor type 1 (CB1) at the presynaptic terminal, which culminates in reduced secretion of glutamatergic vesicles. In this way, rapid non-genomic effects of GCs are involved in the fast termination of the stress response at the level of the hypothalamus, maintaining homeostasis and preventing the complete depletion of stress hormones to allow the organism to respond to potential subsequent threats.

1.3 The paraventricular nucleus (PVN), acute stress, and glucocorticoid effects.

The PVN is one of the most important neuronal nuclei for orchestrating neuroendocrine and autonomic functions. Being located in the periventricular zone, in the anterior and tuberal region of the hypothalamus, the PVN has a highly integrative functional role involved in a wide variety of physiological functions (Swanson and Sawchenko, 1980) (Figure 1.2A-B). It controls the activity of the HPA axis, thyroid axis, and reproductive axis, as well as growth and development, body fluid balance, and gastrointestinal and cardiovascular function (Coote, 1995, Kalra et al., 1999, Williams et al., 2000, Buijs et al., 2003, Ferguson et al., 2008). To exert regulation over these functions, the PVN neurons project to other brain regions such as the median eminence (parvocellular neurons) and pituitary (magnocellular neurons). Moreover, projections from the PVN to caudal medullary and spinal autonomic control centers exert autonomic regulatory control (Swanson and Sawchenko, 1983, Ferguson et al., 2008, Herman et al., 2008) (Figure 1.2C).

Depending on the type of cells activated and the region to which they project, there are three main effector pathways regulated by the PVN neurons: 1) the HPA axis, through CRH-expressing neurons in the dorsomedial parvocellular (PVNmpd) and anterior parvocellular (PVNap) regions of the nucleus; 2) neurohypophysial peptide signals, through AVP- and OXT-expressing magnocellular neurons in the anterior, medial, and posterior magnocellular regions (PVNam, PVNmm, PVNpm, respectively); and 3) autonomic regulation, through neurons in the lateral (PVNlp), dorsal (PVNsp), and ventromedial (PVNmpv) parvocellular regions which project to the brainstem and spinal cord (Swanson and Sawchenko, 1983, Herman et al., 2008) (Figure 1.2C). Importantly, integrative glutamatergic and GABAergic neurons have been located within the PVN and in the halo zone surrounding the PVN, respectively, indicating the high complexity of integrational regulation onto the PVN (Ferguson et al., 2008).

Exposure to acute stress rapidly activates parvocellular neurosecretory neurons within the PVN, inducing phosphorylation of cyclic AMP response element binding protein (CREB) and mitogen activated protein (MAP) kinase, as well as increased transcription of *Crh* and *Avp* (Kovacs and Sawchenko, 1996, Khan and Watts, 2004, Herman et al., 2008, Herman et al., 1992, Herman, 1995). Moreover, acute stress (immobilization) also activates OXT-magnocellular neurons resulting in OXT release

(Jezova et al., 1995, Herman et al., 2008). Importantly, induction of *c-fos* mRNA in magnocellular neurons after mild stress exposure (restraint, swim, novelty) occurs in a delayed manner, suggesting that under these conditions, these cells respond to the physiological effects of stress, rather than to the stressor (Cullinan et al., 1995, Herman et al., 2008).

GCs play an essential role on the delayed effects of stress in the PVN. Strong expression of GRs is present in PVN neurons and their intracellular localization (whether in the nucleus or cytoplasm) depends on the presence of GCs, suggesting GC-dependent transcriptional activity (Fuxe et al., 1985, Liposits et al., 1987, Aronsson et al., 1988, Uht et al., 1988). In primary cultures of hypothalamic cells, synthesis and release of CRH, AVP and OXT are inhibited by acute exposure to GCs (Hu et al., 1992, Hellbach et al., 1998, Kim et al., 2001). Consistent with this, *in vivo* studies have shown that the negative feedback exerted by the GC stress response in parvocellular neurons limits the stress-induced up-regulation of AVP in a cyclic AMP dependent-manner (Herman, 1995, Kuwahara et al., 2003). Similarly, CRH expression levels in PVN neurons are regulated by GCs and stress (Imaki et al., 1991); in mice, adrenalectomy results in increased CRH and AVP expression in PVN neurons; this effect can be inhibited with GC implants around this brain region (Davis et al., 1986, Kovacs et al., 1986, Kovacs and Mezey, 1987, Sawchenko, 1987, Ma and Aguilera, 1999, Kovacs et al., 2000).

In this way, acute stress and exposure to GCs exert transcriptional changes in PVN neurons, altering its functionality and activating adaptive processes that allow the organism to maintain or restore homeostasis. However, persistent activation of PVN neurons and/or overexposure to GCs may induce maladaptive transcriptional changes. Due to the complex integrative function of these neurons, and the essential role they play on regulating HPA axis activity and exposure to GCs, dysregulations in any function of PVN cells may contribute to the development of a wide variety of pathologies such as cardiovascular, metabolic, and neurodegenerative diseases (Herman et al., 2008, Popoli et al., 2011).

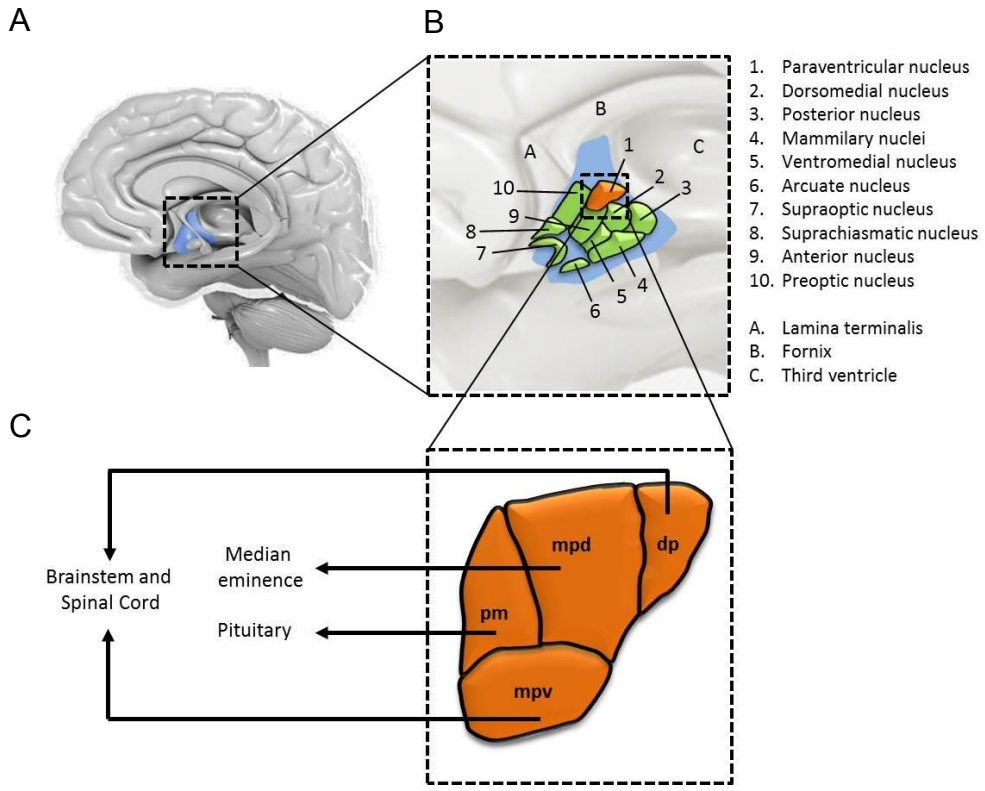

Figure 1.2. Schematic representation of the hypothalamus and its nuclei. A. The hypothalamus is part of the limbic system and it is located ventrally to the diencephalon. It is a major integrational brain center which plays a key role in maintaining body homeostasis by controlling body temperature, hunger, sleep, thirst, stress-reactivity, and circadian rhythms. The image was generated using the FINR Brain Atlas, by Florida Institute for Neurologic Rehabilitation, Inc., http://www.finr.net/. **B.** Schematic magnification of the hypothalamus showing its nuclei. **C.** Schematic magnification of the paraventricular nucleus of the hypothalamus (PVN) showing its subdivisions. Neurons located in the dorsal parvocellular (dp) and ventral division of the medial parvocellular regions (mpv) project to autonomic regulatory control centers in the brainstem and spinal cord. Neurons in the dorsal division of the medial parvocellular zone (mpd) project to the median eminence and orchestrate ACTH synthesis and release during the stress response. Neurons in the posterior magnocellular (pm) subdivision project to the pituitary and regulate peptide signals.

1.4 Chronic stress and the PVN

Chronic activation of the HPA axis and overexposure to GCs lead to changes at the transcriptional and protein level in PVN neurons (Herman et al., 2008). In contrast to the effects of acute stress and acute exposure to GCs on the PVN cells, chronic stress paradigms such as immobilization, footshock, chronic unpredictable stress, or chronic social stress, lead to increased expression of *Crh* and *Avp* mRNA in parvocellular neurons (Herman et al., 1995, Makino et al., 1995, Albeck et al., 1997). Moreover, magnocellular neurons respond to chronic stress with increased AVP and OXT expression in a stressor-dependent manner (Kiss and Aguilera, 1993, Herman et al.,

1995, Albeck et al., 1997, Glasgow et al., 2000). Importantly, elevations of AVP in magnocellular PVN neurons are linked to increased anxiety behavior after chronic stress, providing further evidence for the essential role the PVN neurons play on adaptive processes triggered by stress (Landgraf et al., 2007, Choleris et al., 2013).

Furthermore, chronic stress induces down-regulation of GR in PVN neurons (Herman et al., 1995, Ulrich-Lai and Herman, 2009). As described in section 1.2, GR is involved in the rapid termination of the acute stress response as well as in the delayed transcriptional changes occurring during adaptive processes to maintain homeostasis after a stressful event. Hence, downregulation of GR leads to a wide variety of changes in PVN neurons at a transcriptional and functional level.

There is also evidence of altered PVN neuron activity after chronic stress. Expression of neurotransmitter receptors for both glutamatergic (excitatory) and GABAergic (inhibitory) signaling is changed after chronic stress (Cullinan, 2000, Verkuyl et al., 2004, Herman et al., 2008, Ziegler et al., 2005). While beta subunits of GABA-A receptor are down-regulated after chronic variable stress in PVN neurons (Cullinan, 2000), the GluR5 subunit of the kainate-preferring glutamate receptor is up-regulated (Herman et al., 2008). Moreover, NMDA-receptor subunits are also altered, leading to enhanced calcium permeability and therefore to increased glutamate signaling (Ziegler et al., 2005). These changes may be involved in the mechanisms mediating enhanced activity of PVN neurons that leads to hyperactivity of the HPA axis and overexposure to endogenous GCs after chronic stress exposure. Importantly, chronic stress and depletion of GC exposure by adrenalectomy also alters morphological plasticity of parvocellular PVN neurons by increasing glutamate innervation of CRH-cells (Herman et al., 2008).

Overall, chronic stress exerts changes in PVN neurons at the transcriptional, morphological, and functional level, leading to altered HPA axis activity. This may culminate in chronic dysregulation of the stress response and therefore lead to the development of stress-related pathologies. Many questions still remain open concerning the mechanisms mediating the changes in PVN cells after chronic stress. While some studies have shown that the changes are dependent on GC (as described above), little is known about the interaction between activity dependent changes in neuroplasticity due to increased excitatory input into the PVN cells, and the delayed effects of GCs on these

phenomena. Hence, further research is needed to dissect the dynamics and interactions between these processes.

1.5 Early Life Experience and Developmental Programming

GCs play a critical role both in development and in coping with a specific environmental challenge to the homeostasis of the organism (Wendelaar Bonga, 1997, Cottrell and Seckl, 2009, Nesan and Vijayan, 2012). However, when an adverse environment is present during early life and the HPA axis is activated, an overexposure to GCs may occur. Stress experiences and overexposure to GCs during early life modulate reconfigurations in neuronal circuits at the molecular, cellular, and physiological level mediated by gene-environment interactions, a process referred as developmental programming. This culminates in changes in emotional, cognitive and behavioral adaptations which define the individual's fitness to cope with subsequent stressful events (Russo et al., 2012). Early life exposure to strong or prolonged adverse experience is linked to vulnerability to disease and detrimental effects in health such as cardiovascular and metabolic disease, and brain disorders (Seckl and Meaney, 2004, Reynolds, 2013). In contrast, mild predictable stress inoculation in early life stages has been shown to enhance stress resilience by facilitating the individual's ability to adapt its phenotype and increasing its stress coping fitness in similar environmental conditions (Schmidt, 2010, Taylor, 2010, Khulan and Drake, 2012, Daskalakis et al., 2013).

Because the HPA axis plays a fundamental role in the regulation of metabolic, cardiovascular, reproductive, and neurological systems, dysregulation in any of its functions may trigger the development of pathologies. Hence, developmental programming of the HPA axis has been identified as a critical link between early life adverse experience and the development of chronic disease later in adulthood (Reynolds, 2013, Moisiadis and Matthews, 2014); however, the molecular mechanisms mediating these changes are poorly understood.

Epigenetics is a key player in the long lasting changes induced by early adverse experience that culminate in altered neurobiology, behavior, and potential pathologies. Changes in DNA methylation, posttranslational histone modifications, and regulation by micro-RNA (miRNA) of genes involved in the stress response occur after early adverse experience in animal models and in humans (Murgatroyd et al., 2009, Murgatroyd and Spengler, 2011, Jawahar et al., 2015). Among the stress-related genes showing altered

epigenetic profiles are: a) GR; increased methylation in the GR promoter region culminates in reduced GR mRNA in hippocampus of both pups with low nursing mothers and humans exposed to childhood abuse (Weaver et al., 2004, McGowan et al., 2009, Jawahar et al., 2015); b) *Crh*; decreased methylation of the *Crh* promoter has been observed in PVN and hippocampal neurons of maternally deprived animals, which results in increased gene expression (Chen et al., 2012, Wang et al., 2014); c) *Avp*; decreased methylation of the *Avp* enhancer sequence has been observed in PVN neurons of maternally-deprived animals, resulting in increased gene expression (Murgatroyd et al., 2009). Moreover, other genes outside the HPA axis involved in the stress response such as *Bdnf*, serotonin transporter (5-HTT, S*lc6a4*), and estrogen receptor-α (ERα), also show epigenetic alterations which culminate in long lasting transcriptional changes after early adverse experience and potentially contribute to developing stress-related pathologies (Champagne et al., 2006, Lee et al., 2007, Roth et al., 2009, Jawahar et al., 2015).

Importantly, not only epigenetic, but also long-lasting transcriptional changes of stress-related genes such as *Crh* and *Avp* induced by early adverse experience are linked to altered coping fitness later in life (Korosi et al., 2010, Singh-Taylor et al., 2015, Murgatroyd et al., 2009); although this may be mediated by epigenetic changes, the exact molecular mechanisms of this process have been difficult to elucidate due to its high complexity. Among the factors involved in developmental programming after early adverse experience, there are three which may have repercussion on whether an organism will develop long-lasting adaptive changes that may culminate in dysfunction and disease: a) the nature of the stressor, b) the severity of the adverse experience, and c) the developmental time window in which the adverse experience is delivered (Bale, 2015, Gee and Casey, 2015).

Neurodevelopmental programing mainly occurs during sensitive periods, in which environmental influences on brain development is facilitated due to increased neuroplasticity (Moriceau and Sullivan, 2006, Callaghan and Richardson, 2011, Gee and Casey, 2015). This is the case during highly dynamic brain development periods, such as gestation, infancy, and adolescence (Bale, 2015, Gee and Casey, 2015). Since epigenetic processes are key players of neurodevelopment and maturation, any threat to the homeostasis of the organism during this critical time window may culminate in epigenome reprograming, and therefore potentially into long-lasting transcriptional,

functional, and behavioral changes (Daskalakis et al., 2013, Jawahar et al., 2015, Bale, 2015). Adaptive changes resulting from this reprograming process, which is mediated by the environment, may increase the organism's fitness to cope with subsequent adversities; however, if there is a mismatch between the environment in which the organisms developed and the one in later stages of life, a potential dysfunction may arise, culminating in disease (Nederhof and Schmidt, 2012, Daskalakis et al., 2013).

A critical time window with increased vulnerability to long-lasting programming effects of stress and inflammation occurs prenatally, during early stages of gestation (Brown et al., 2009, Goines et al., 2011, Bale, 2015). Moreover, chronic stress presented at early postnatal stages also induces long-lasting epigenetic, functional, and structural changes in the hippocampus and the hypothalamus (Korosi et al., 2010, McClelland et al., 2011, Ivy et al., 2010). Interestingly, the effects on epigenetic reprogramming observed after postnatal chronic stress are of opposite direction relative to those observed in prenatal-stress models (Korosi et al., 2010, Mueller and Bale, 2008). This shows the high complexity of developmental programming mechanisms and highlights the need to elucidate the critical time windows in which neurodevelopment, and in particular the HPA axis, is more vulnerable to developmental programming. Furthermore, it remains to be explored whether epigenetic alterations are mediated by increased GC exposure or by activity-dependent mechanisms in neurons.

Additionally, synaptic-plasticity mechanisms activated during acute or chronic stress responses (section 1.4) may play an important role in the adaptive changes occurring in hypothalamic neuroendocrine cells after early adverse experience (Herman et al., 2008, Bains et al., 2015). This may culminate in long lasting functional changes of hypothalamic neurons and therefore of the HPA axis. Little is known about the role of GCs in mediating these phenomena in the context of developmental programming. It is not known whether these mechanisms act during early life stages in maturing neurons and whether this culminates in long lasting changes still detectable in adulthood; however, synaptic-plasticity mechanisms are strong candidates to be mediators of the programming effects observed after early adverse experience.

Further research is needed to dissect the mediators of early adverse experience effects on HPA axis function. Two main factors need to be taken into consideration: 1) delayed/transcriptional effects of increased GCs levels, which may orchestrate neuronal

circuits reconfigurations, and 2) activity-dependent synaptic plasticity mechanisms mediated by the increased excitatory input into the hypothalamic neuroendocrine cells, which may lead to long lasting changes in cell function. In both process, epigenetics may play an essential role. Dissecting these mechanisms requires tools that allow for the manipulation of the HPA axis function. To achieve this, the effects of increased excitatory input into hypothalamic cells should be studied in the absence of endogenous GCs either by inhibiting GCs secretion or by avoiding GR signaling. On the other hand, to study the effects of GC exposure on developmental programming of the HPA axis, overexposure to endogenous GCs should be achieved without activating hypothalamic cells. This task has been particularly difficult to achieve in the current mammalian models for stress research due to the lack of non-invasive ways to perform such manipulations.

1.6 Zebrafish as a model organism for HPI axis research

Most of the studies about the role of the HPA axis in developmental programming have been performed using animal models such as monkeys, rats, and mice. The use of these models has facilitated the understanding of mainly the physiological and behavioral correlates after early life stress, but the molecular mechanisms driving early life programming are largely unknown (Weaver et al., 2002, Seckl and Meaney, 2004, Schmidt, 2010). Although the use of these models has provided valuable information about HPA axis development and the impact of GCs in early life programming, they also present limitations. Current methods to induce activation of the HPA axis or exposure to GCs in mammals during early life include maternal separation, confinement, or systematic injection of substances (Schmidt et al., 2011); these methods are highly invasive making it difficult to draw conclusions about the manipulation effects.

Zebrafish, *Danio rerio*, is a promising animal model to dissect the complex actions of GCs during early life programming of the stress axis as well as the molecular mechanisms involved in this process. The Hypothalamic-Pituitary-Interrenal (HPI) axis in zebrafish regulates the stress response and is highly conserved across phyla, with cortisol being the final GC effector (Alsop and Vijayan, 2008). The hypothalamic neurosecretory preoptic area (NPO) in zebrafish is homologous to the PVN in mammals (Herget et al., 2014); neurons expressing CRH and arginine vasopressin protein (AVP)

are found in this region and project innervations to the pituitary, establishing a direct connection between these two structures (Pogoda and Hammerschmidt, 2007, Herget et al., 2014).

Importantly, the HPI axis in zebrafish larvae matures early in development, being able to increase cortisol levels as a response to an acute stressor after 97 hpf (Alsop and Vijayan, 2008). Moreover, the stress paradigms in the zebrafish model are less complex than those used in mammalian models, reducing significantly animal handling and invasive procedures; this allows a more accurate manipulation of the HPI axis activation (Macri and Wurbel, 2006). Furthermore, the immersion paradigm, although absorption dynamics need to be performed, facilitates the use of synthetic GC and pharmacological substances (Steenbergen et al., 2011).

Another advantage of the zebrafish model is its transparency during early stages of development. This characteristic combined with molecular tools available nowadays which allow gene expression manipulation, facilitates the elucidation of molecular and cellular mechanisms under different conditions by performing *in vivo* imaging; this allows the observation of internally developing structures without the need of invasive procedures (Burne et al., 2011). Moreover, transparent larvae are remarkably suited for the application of optogenetic tools that can manipulate the activity of specific cell populations in developing freely-behaving zebrafish larvae (Simmich et al., 2012, De Marco et al., 2013).

Besides these strengths, when compared with mammalian models, zebrafish present other advantages; they are relatively small and are easy to maintain under laboratory conditions. Moreover, each female is able to give from 100 to 500 eggs per week, allowing high-throughput analysis. All this together makes zebrafish a promising animal model to study maturation of the HPI axis and early life programming. Zebrafish can facilitate the generation of new insights into the molecular mechanisms involved in early life stress and its consequence later in life. Moreover, the role of overexposure to either endogenous or synthetic GCs in HPI axis development can be studied under highly controlled conditions, which is difficult to achieve in mammalian models. Altogether, zebrafish is a valuable complement to the existing mammalian models in stress research.

1.7 Activation of the HPI axis in zebrafish

Zebrafish embryos acquire the ability to synthesize and secrete basal cortisol levels around hatching time (2 days post-fertilization (dpf)). However, stress-induced cortisol response starts between 3 and 5 days post-fertilization, depending on the nature and intensity of the stressor, suggesting that there is a hyporesponsive period similar to that reported in other vertebrates (Alsop and Vijayan, 2008, Schmidt, 2010, Steenbergen et al., 2012). Nevertheless, there is a need for further characterization of the HPI axis activity of zebrafish between the larval and juvenile stages, since most of the studies have reported HPI axis activity at developmental stages not later than 5 dpf. Our understanding of the changes in stress response activity after this stage is still poor. Important aspects of this process such as basal activity, stress-induced response maturation, negative feedback maturation, and response to repeated stress, are largely unexplored.

A wide range of stressors has been used in order to activate the HPI axis in both larval and adult zebrafish; like mammals and other vertebrates, larval and adult zebrafish respond with increased cortisol levels to a wide variety of stressors such as net handling, osmotic shock, pH change, light intensity changes, temperature change, heavy metals, predator exposure, crowding, restraint, air exposure, swirling or turbulent water (bubbles), and novel environment (Ramsay et al., 2006, Barcellos et al., 2007, Alsop and Vijayan, 2008, Alderman and Bernier, 2009, Alsop and Vijayan, 2009, Ramsay et al., 2009, von Krogh et al., 2010, Clark et al., 2011, Yeh et al., 2013, De Marco et al., 2013). Although all these stressors have been used successfully to increase cortisol levels, most of them do not allow precise control of input delivery. Acute and transient delivery of a stressor becomes difficult for some types of stressors such as osmotic shock or fluctuations in pH, which need sophisticated perfusion systems in order to achieve fast exchange of the incubation solution. Other stressors such as netting or exposure to air do not offer a way to deliver different strengths of the stimulation, an important aspect when studying subtle changes in HPI axis activation.

Exposure to hydrodynamic flows, specifically of cylindrical vortex flows, of different strengths may provide a way to overcome these limitations. When fish and other aquatic organisms are exposed to water currents, they perform a robust and well characterized behavior known as rheotaxis. This behavior is involved in migration,

feeding behaviors, predator avoidance, schooling, and importantly, to reduce energetic costs when coping with strong hydrodynamic flows (Arnold, 1974, Montgomery et al., 1995, Baker et al., 2002, Gardiner and Atema, 2007, Suli et al., 2012). Rheotaxis behavior is multisensory; several sensory inputs including optical, vestibular, tactile, and lateral line cues are integrated and involved in this complex behavior where one sensory input loss can be compensated by other sensory inputs (Bak-Coleman et al., 2013, Baker and Montgomery, 1999, Arnold, 1974, Montgomery et al., 1997). Although it has been widely studied in several species, all studies describe this behavior in the presence of turbulent or laminar flows. To date, there is no report in literature about rheotaxis behavior of zebrafish larvae (or any other species) in the presence of a semi-uniform vortex flow in a cylindrical arena.

Rheotaxis behavior requires energy mobilization; therefore, exposure to vortex flows is expected to induce an increase in cortisol levels. In fact, it has been shown that swirling stimulation induces higher levels of cortisol in both larval and adult zebrafish (Alsop and Vijayan, 2008, Fuzzen et al., 2010); however, a systematic characterization of the effects of such stimulation has not been reported yet. This type of stimulation offers a more naturalistic manner to activate the HPI axis since it is based on exposure to differential speeds of water motion which may mimic the natural habitat of both, larval and adult zebrafish (Engeszer et al., 2007). Moreover, handling effects can be potentially reduced and it is easy to deliver in a transient way, allowing either continuous or repeated presentations of the stimulation in short periods of time. Also, since this type of stimulation is delivered in free swimming larvae, the study of behavioral correlates of HPI axis activation is facilitated.

1.8 Long lasting effects of overexposure to glucocorticoids in zebrafish

It has been shown in other teleost fish that exposure to stress perturbations at early stages of development (eyed, hatching, and yolk resorption) leads to long lasting hypo-activity of the HPI axis in adult fish (Auperin and Geslin, 2008). The same effect was obtained when the embryos were incubated with exogenous cortisol (Auperin and Geslin, 2008). In zebrafish, cortisol incubation during the first 48 hours after fertilization leads to long lasting changes in behavior, specifically, in locomotor activity as a response to a pulse of darkness (Steenbergen et al., 2011). Moreover, prolonged incubation of zebrafish embryos in exogenous cortisol during the first five days post-

fertilization increases whole-body basal cortisol levels, glucocorticoid signaling, and the expression of immune system-related genes. Interestingly, these changes persist into adulthood, culminating in dysfunctional regeneration capacities and increased expression of inflammatory genes which were dysregulated after injury (Hartig et al., 2016). A similar treatment during the same time window but with incubation in dexamethasone, a synthetic GC, also induced long-lasting changes in behavior and metabolism which were still detected in adulthood (Wilson et al., 2016). Less is known about changes in HPI axis activity and function in response to acute or chronic stressors after such treatments, or whether exposure to stressors after 4 dpf, when the HPI axis of larval zebrafish is already able to elicit stress-induced cortisol increase, may disrupt the maturation process of the HPI axis elements. This in turn may lead to altered coping fitness to subsequent stressful events and contribute to the developmental programing effects of early adverse experience. Moreover, to date, there is no study using the zebrafish model addressing the effects of overexposure to GCs and/or early adverse experience on developmental programming of the HPI axis elements in a tissue-specific manner.

1.9 Transcriptomics approach to study developmental programming of the HPI axis in zebrafish.

The transcriptome consists of the complete set of transcripts, and their quantity, present in a cell at any given time and environmental context. Analyzing the transcriptome of a cell or group of cells provides essential information to understand the functional aspects of the genome in a specific temporal and physiological situation (Wang et al., 2009). In the last decade, performing such transcriptomic analyses has become much more accessible with the development of the deep sequencing RNAseq technology. RNAseq provides precise measurements for characterizing genome-wide transcript levels in a quantitative manner. This opens an avenue to study the effects of early adverse experience at the molecular level in specific tissues/cell types, facilitating the dissection of the molecular mechanisms involved in the adaptive processes occurring during developmental programming.

Genome-wide gene expression profiling measures the expression levels of thousands of genes simultaneously. In this way, instead of following a hypothesis-driven approach by investigating candidate genes, it is possible to ask: what are the genes whose expression changes after treatment? After identification and quantification

of transcripts using RNAseq technology, gene expression patterns are identified and candidate genes are further investigated to evaluate their role in cell function and functional contribution to the phenotype that results from the adaptive processes observed after early life adverse experience (Figure 1.3). In zebrafish, gene editing technologies such as CRISPR/Cas9 have been established allowing the generation of transgenic lines in which reverse genetics can be performed (Yin et al., 2016). This facilitates functional studies of candidate genes and the dissection of the molecular mechanisms involved in developmental programming after early adverse experience. Furthermore, with the use of transgenic tools available in zebrafish, such as optogenetic manipulation of the HPI axis, or targeted ablation of HPI axis elements, the mediators that induce the changes in expression of the candidate genes can be elucidated, further dissecting the mechanisms underlying developmental programming after early adverse experience.

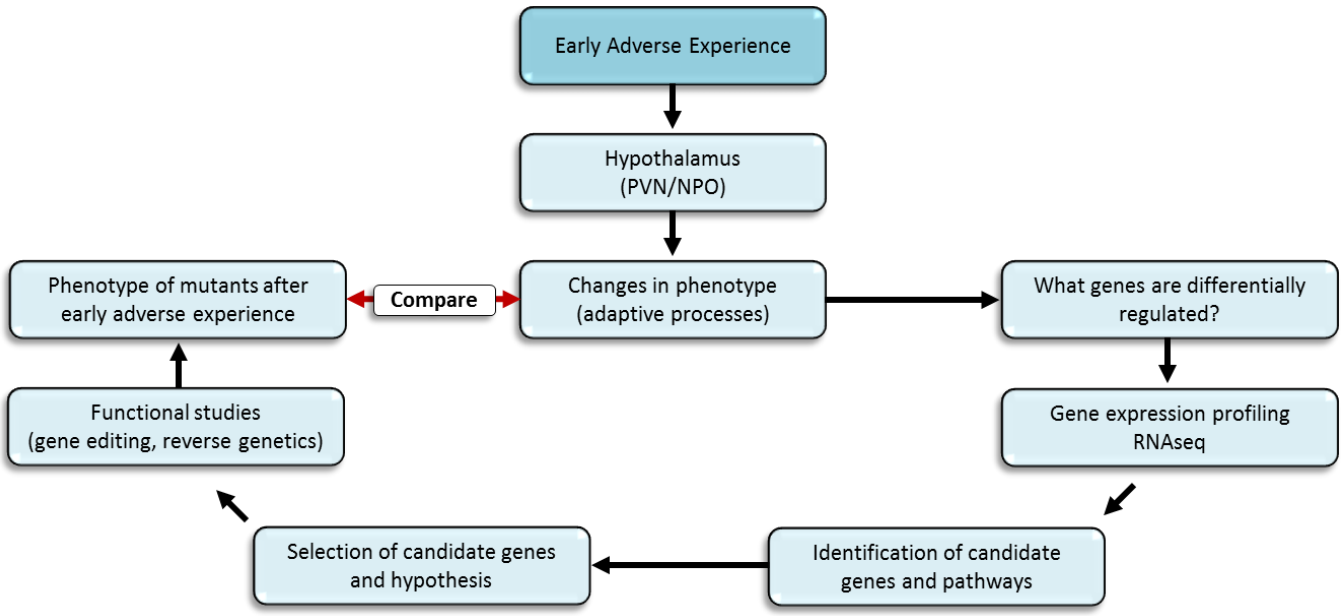

Figure 1.3. Transcriptomic approach. Overview of the transcriptomic approach to identify candidate molecules involved in adaptive changes occurring during developmental programing after early life adverse experience. Note that the scope of this thesis is not represented by this overview.

1.10 Transgenic tools to study the HPI axis in zebrafish

Tissue-specific targeting of the HPI axis elements

Tissue-specific analysis is essential to dissect the effects of early adverse experience on HPI axis function. To achieve this, specific promoter elements can be used to target tissue-specific populations, allowing cell-labeling and directed expression of a specific gene. Labeling cells with fluorescent proteins, such as GFP, is a valuable method to isolate specific-cell populations by using fluorescent activated cell sorting (FACS). To this end, transgenic lines have been generated by our laboratory and by others, in which GFP expression is directed to specific cell populations of all three elements of the HPI axis:

1) NPO cells in the hypothalamus are labeled by driving GFP expression under a conserved *cis*-regulatory NPO-specific enhancer element of the gene orthopedia a (*Otpa*) (*otp*ECR6). This regulatory element drives expression in the NPO region which co-localizes with *crh*, a*vp*, and *oxt* expression (Figure 1.4A-C) (Gutierrez-Triana et al., 2014). 2) Pituitary cells are labeled by driving GFP expression under the proopiomelanocortin (*pomc*) promoter. This promoter drives expression in both anterior and posterior pituitary corticotrophs, which regulate ACTH synthesis and secretion, but not in melanotrophs in the posterior pituitary, which control melanocyte-stimulating hormone synthesis and secretion (Liu et al., 2003). 3) Steroidogenic interrenal cells are labeled by driving GFP expression under a 2kb fragment of the *StAR* promoter. This regulatory element drives expression specifically in steroidogenic interrenal cells, which synthesize and secrete cortisol upon stress exposure, and not in chromaffin cells, which synthesize and secrete catecholamines (Figure 1.4E-F) (Gutierrez-Triana et al., 2015). These same promoter elements can be used to drive expression of molecular tools which allow manipulating and measuring HPI axis activity.

Manipulating HPI axis activity

In order to elucidate the mechanisms mediating the adaptive changes induced by adverse experience during early life in zebrafish, it is necessary to generate non-invasive tools to manipulate the HPI axis activity. In mammalian models (rodents), inducing hyper- or hypocortisolic states is mainly performed by injecting GCs into the

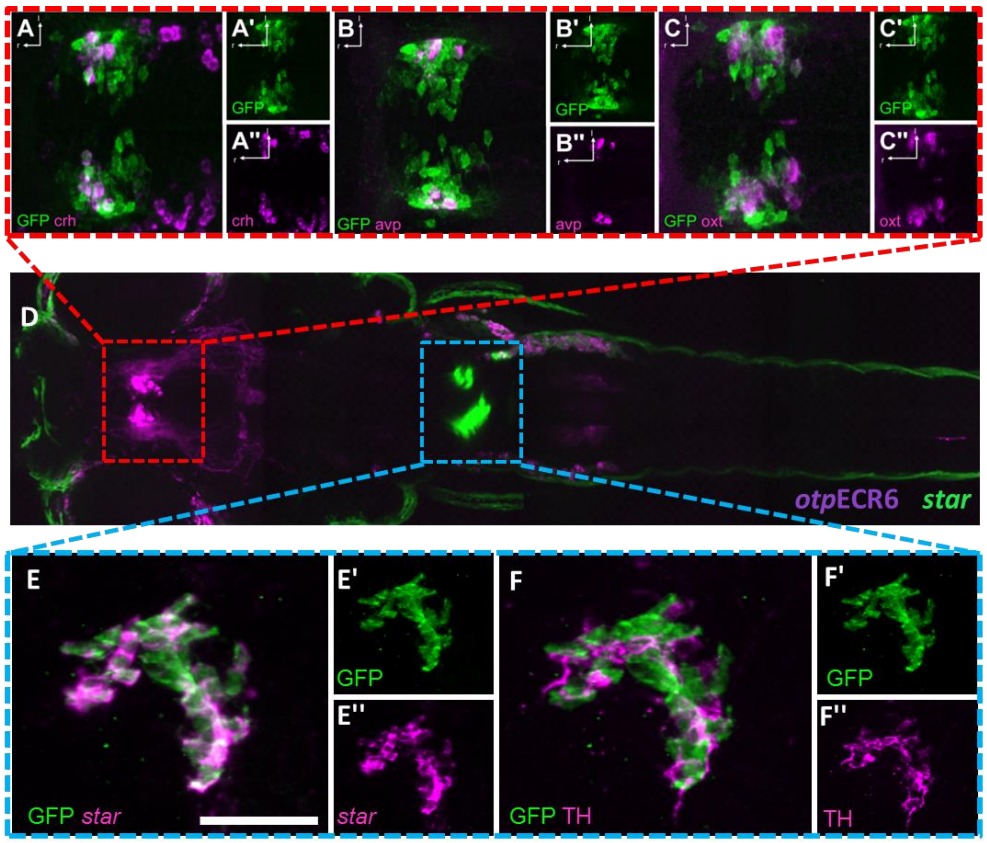

Figure 1.4. Genetic targeting of HPI axis elements. A-C. Maximum intensity projections of confocal stacks show that neurons in the neurosecretory preoptic area (NPO) of zebrafish expressing the stress-related peptides corticotropin releasing hormone (CRH), arginine vasopressin (AVP), and oxytocin (OXT) (fluorescence *in situ* hybridization) are labeled in the *Tg(otpECR6-E1b:mmGFP)*^{hd12} transgenic line, in which GFP expression (immuno-histochemistry) is driven by the conserved promoter module *otp*ECR6. Image courtesy of Dr. Ulrich Herget (Herget, 2015). **D.** Double transgenic zebrafish larvae in which the promoter module *otp*ECR6 and the 2kb regulatory element of the StAR promoter are used to drive expression of the red and green fluorescent proteins (RFP and GFP), respectively (*Tg(otpECR6-E1b:RFP-CAAX)*^{hd13} and *Tg(2kbStARp:GFP)*^{hd17}). Note that the NPO and interrenal gland boxed regions are only for reference of the magnified regions showed in A-C and E-F, but show different transgenic lines expressing different fluorescent marker. Image courtesy of Dr. Ulrich Herget. **E-F.** Maximum intensity projections of confocal stacks show that the expression of GFP in *Tg(2kbStARp:GFP)*^{hd17} transgenic larvae co-localizes with steroidogenic acute regulatory protein (StAR)-expressing cells, but not with tyrosine hydroxylase (TH)-expressing cells. Scale bars: 50 mm. Image courtesy of Dr. Ulrich Herget (Herget, 2015).

blood stream or by adrenalectomy, respectively. Although these methods have been used widely and provided valuable information about the role and function of GCs, they are invasive protocols that may not be suitable for all experimental designs. In the case of the zebrafish model (and specifically in larval stages), none of the above mentioned methods is suitable for manipulating HPI axis activity, remaining as the only available option the incubation of the organisms in water containing GCs. However, the spatial resolution of this method is low, exposing the whole organism to exogenous GCs. Moreover, although the concentration of GCs can be controlled in the media, it is difficult to evaluate the extent to which GCs diffuse into the larval body. In order to extend the repertory of tools for manipulating HPI axis activity in freely swimming zebrafish larvae, Dr. Arturo Gutierrez-Triana, in our laboratory, has developed transgenic lines in which optogenetic and genetically targeted ablation approaches can be used to alter endogenous GCs levels and induce hyper- or hypocortisolic states (De Marco et al., 2013, Gutierrez-Triana et al., 2014, Gutierrez-Triana et al., 2015).

To optogenetically manipulate HPI axis function and induce hypercortisolic states, Dr. Arturo Gutierrez-Triana, in our laboratory, generated transgenic lines where expression of a blue light-photoactivated adenylyl cyclase from the soil bacterium *Beggiatoa* (bPAC) is driven by a fragment of either the *pomc* promoter, resulting in bPAC expression in pituitary corticotroph cells (*Tg(Pomc:bPAC-2A-tdTomato)*^{hd10}) (Ryu et al., 2010, Stierl et al., 2011, De Marco et al., 2013), or by a 2kb regulatory region of the *StAR* promoter, resulting in bPAC expression in the steroidogenic interrenal cells (*Tg(2kbStARp:bPAC-tdTomato)*^{hd19}) (Gutierrez-Triana et al., 2015). Upon stress exposure, CRH binds its receptor (CRHR) in pituitary cells, increasing cAMP levels that culminate in ACTH release and subsequently in cortisol secretion (Fleischer et al., 1969, King and Baertschi, 1990, Wendelaar Bonga, 1997). Since bPAC increases cAMP levels after blue light-photo activation (Ryu et al., 2010), it was hypothesized that expression of bPAC protein in corticotrophs cells would resemble CRH receptor signaling upon blue light illumination by increasing cAMP levels and would then induce higher cortisol levels in response to an otherwise similarly stressful event (Figure 1.5A and C). Similarly, when ACTH binds to its receptor, MC2R, in interrenal gland cells, it increases cAMP levels and Ca^{2+} influx, culminating in cortisol synthesis and release (Gallo-Payet and Payet, 2003). Therefore, following the same rationale, it was hypothesized that expression of bPAC in steroidogenic interrenal cells

would result in increased cortisol secretion upon blue light stimulation (Figure 1.5B, C). To validate these hypotheses, cortisol levels were measured after transgenic larvae of both genotypes (*pomc*:bPAC+ and *StAR*:bPAC+) were exposed to blue light. The characterization of the cortisol response of these transgenic lines is presented in this thesis as well as in (De Marco et al., 2013, Gutierrez-Triana et al., 2015).

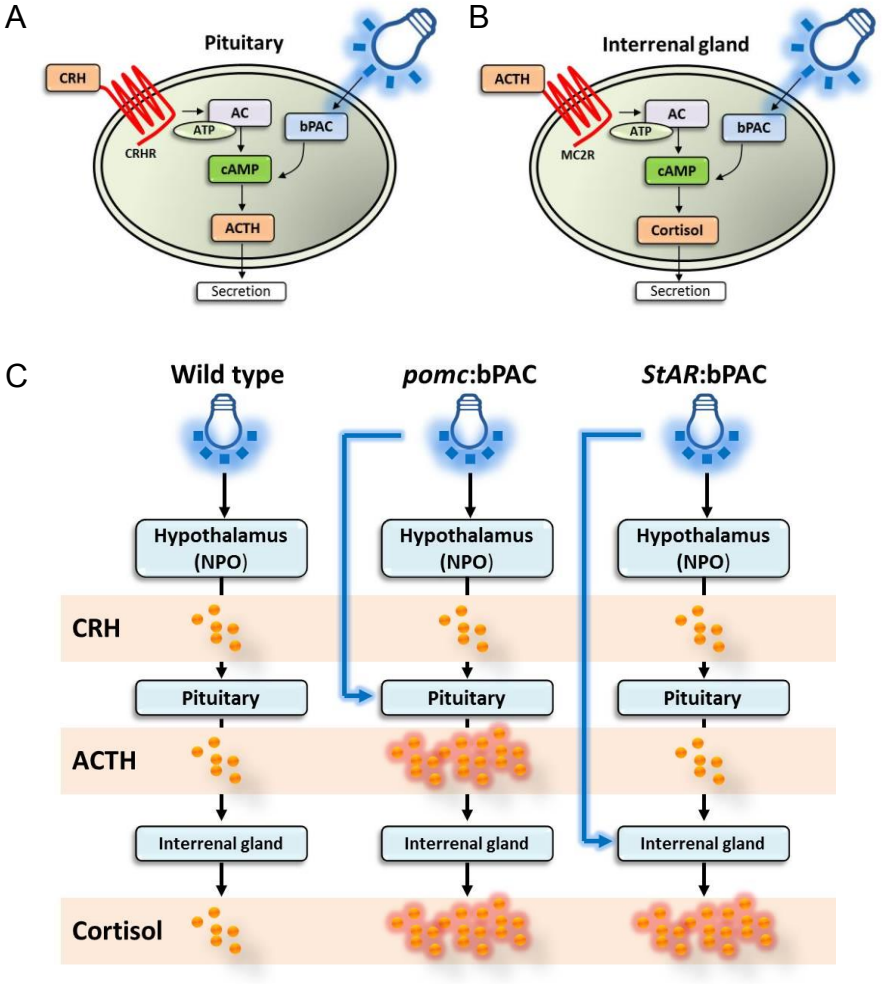

Figure 1.5. Optogenetic manipulation of HPI axis elements to induce hypercortisolic states. **A.** In pituitary corticotrophs, *Beggiatoa* photoactivated adenylyl cyclase (bPAC) increases cAMP levels upon blue light exposure; this culminates in increased ACTH release, resembling CRH signaling. AC, adenylyl cyclase; CRHR, CRH receptor. **B.** In steroidogenic interrenal cells, bPAC is expected to increase cAMP levels upon blue light exposure, resembling ACTH signaling and culminating in cortisol secretion. MC2R, melanocortin 2 receptor. **C.** Overview of the possible outcomes of optogenetic manipulation of the HPI axis activity in wild type and transgenic larvae expressing bPAC either in the corticotrophs (*pomc*:bPAC) or in steroidogenic interrenal cells (*StAR*:bPAC). Blue light exposure in *pomc*:bPAC larvae leads to increased ACTH secretion and therefore increased cortisol secretion. In *StAR*:bPAC larvae, blue light exposure leads to increased cortisol secretion from the interrenal glands.

The most common and effective procedure in mammalian models to deprive the organism of endogenous cortisol and induce hypocortisolic states is by surgically removing the adrenal glands (adrenalectomy). Because of technical limitations to perform such a procedure in zebrafish larvae, alternative protocols to deprive larvae of endogenous cortisol were explored in our laboratory by generating genetically targeted ablation tools. To accomplish this, the conditional nitroreductase-metronidazole (NM) system has been used. The NM system allows conditional targeted cell ablation by directing the expression of bacterial nitroreductase (nfsB) to specific cell type populations and incubating in metronidazole (Mtz), leading to cell ablation only of those cells expressing nfsB (Curado et al., 2007, Gutierrez-Triana et al., 2014, Gutierrez-Triana et al., 2015).

Conditional cell ablation was targeted to the NPO and to steroidogenic interrenal cells, separately. To target cell ablation to hypothalamic cells in the NPO, a transgenic line was generated where the conserved *cis*-regulatory element of *otpa*, *otp*ECR6, was used to drive expression of the *E. coli* nfsB as a GFP fusion protein (*Tg(otpECR6-E1b:nfsB-GFP)*^{hd14}) (Gutierrez-Triana et al., 2014). On the other hand, to target cell ablation to steroidogenic interrenal cells, expression of *E.coli* nfsB fused to GFP was driven by a 2kb regulatory fragment of the *StAR* promoter (*Tg(2kbStARp:nfsB-GFP)*^{hd18}) (Gutierrez-Triana et al., 2015). It was hypothesized that conditional ablation of NPO cells or steroidogenic interrenal cells would result in impaired HPI axis activity and therefore in reduced cortisol levels upon a stressful event (Figure 1.6). The characterization of the cortisol profiles of both transgenic lines (*otp*ECR6:nfsB-GFP and *StAR*:nfsB-GFP) after cell ablation is presented in this thesis and in (Gutierrez-Triana et al., 2014, Gutierrez-Triana et al., 2015).

Non-invasive manipulation of all three elements of the HPI axis facilitates the elucidation of the role that each element plays on the adaptive processes during developmental programming after early life adverse experience. These tools provide a valuable platform to dissect the effects of acute and prolonged exposure to GCs, as well as their rapid and non-rapid functions. Moreover, they can be used to further investigate the regulatory mechanisms of candidate genes identified by transcriptomic analysis after early adverse experience.

Measuring Ca^{2+} activity in vivo in hypothalamic NPO cells

To evaluate the effects of developmental programming after early life adverse experience on cell function of hypothalamic neurons involved in HPA axis activation, it is essential to measure neuronal activity; however, the analysis of real-time CRH neuron activity upon stress exposure in mammalian models has been limited because of difficulties on identifying CRH neurons *in vivo*. Hence, electrophysiological studies of CRH neurons have been performed *ex vivo* in post-stress preparations (Alon et al., 2009, Martin et al., 2010, Wamsteeker Cusulin et al., 2013, Itoi et al., 2014). These studies have provided valuable morphological and functional information of CRH neurons; nonetheless, the study of these aspects in intact animals would provide a more complete understanding of CRH neurons function upon stress exposure, since the activation of the stress response involves integration of information coming from different brain areas and periphery.

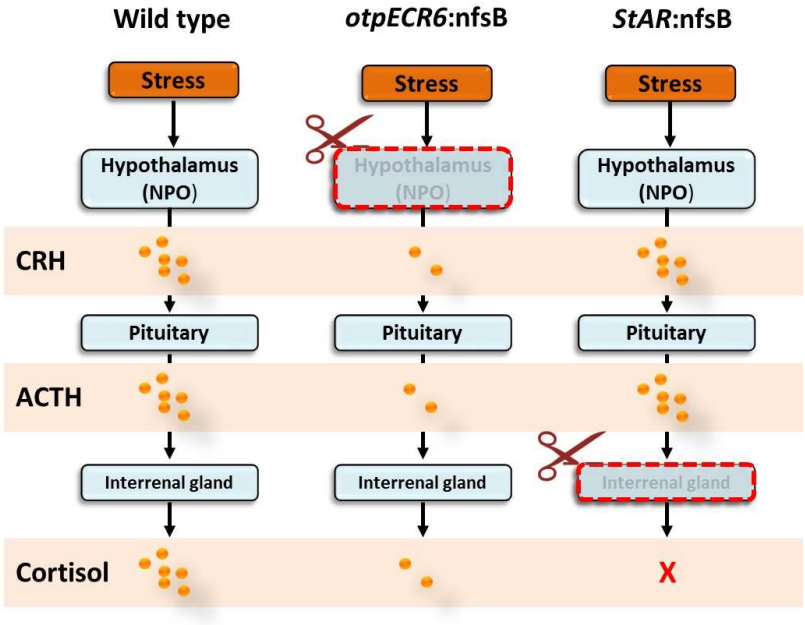

Figure 1.6. Genetically targeted cell ablation of HPI axis elements to induce hypocortisolic states. Overview of the possible outcomes upon stress exposure after metronidazole incubation of wild type and transgenic larvae expressing bacterial nitroreductase (nfsB) either in the NPO (*otp*ECR6:nfsb-GFP) or in steroidogenic interrenal cells (S*tAR*:nfsb-GFP). Ablation of NPO cells results in reduced cortisol response upon stress exposure. Since redundant regulatory mechanisms may play a role in the stress response, a reduced cortisol response may take place even when NPO cells are ablated. Steroidogenic interrenal cell ablation may result in blunted cortisol response upon stress exposure.

To measure *in vivo* CRH neuronal activity in zebrafish, Dr. Colette vom Berg-Maurer, in our laboratory, generated a transgenic line in which expression of the calcium sensor GCaMP3.0 is driven by a promoter element of the *Otpa* transcription factor which contains an evolutionary conserved NPO-specific enhancer module (*Tg(otpa3kb:GCaMP3.0)*^{hd22}) (Vom Berg-Maurer et al., 2016). Additionally, to identify CRH neurons *in vivo*, Dr. vom Berg-Maurer generated a transgenic line in which the expression of the red fluorophore tagRFP is driven by the *crh* promoter (*Tg(crh:RFP)*^{hd21}) (Vom Berg-Maurer et al., 2016). To image CRH neuronal activity, double-transgenic larvae can be used. This allows *in vivo* recording of CRH-positive and CRH-negative cell activity using two-photon calcium imaging in intact larvae (Figure 1.7A).

To perform in vivo calcium imaging in intact double-transgenic larvae, a custom made in vivo imaging chamber has been designed, in which temperature control, electrodes, and a perfusion system have been integrated, facilitating the delivery of osmotic shocks of known strength as threatening signals to activate the stress response in a highly controlled manner (Figure 1.7B) (Vom Berg-Maurer et al., 2016).

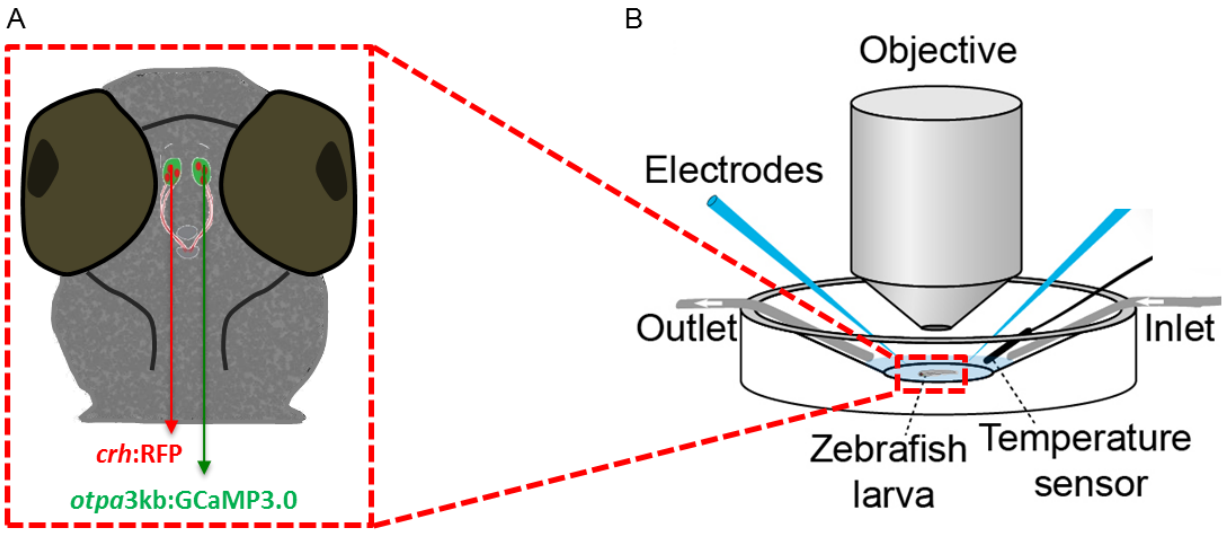

Figure 1.7. Neuronal activity of CRH-positive cells can be measured *in vivo* using two-photon Ca^{2+} imaging. A. Schematic representation of a double transgenic zebrafish larva expressing the calcium sensor GCaMP3.0 in NPO neurons and the red fluorescent protein in CRH-positive cells. **B.** Schematic representation of the *in vivo* Ca^{2+} imaging chamber. Scheme adapted from (Vom Berg-Maurer et al., 2016).

2. AIMS OF THE PROJECT

The aim of this thesis was to identify molecules involved in adaptive processes activated after early life exposure to adverse experiences. Specifically, I aimed to study the molecular changes in hypothalamic cells at the genome-wide level occurring after prolonged activation of the stress response axis. In order to achieve this, four main objectives were set:

- First, I aimed to develop a stimulation protocol to activate the HPI axis of freely swimming larvae in a highly controlled manner and without invasive procedures. Special attention was paid in developing a stress protocol with reduced handling effects and without any unspecific effect of the stimulation on the cortisol response of zebrafish larvae.
- Second, I aimed to characterize the ontogeny of the HPI axis activity in developing larvae by measuring cortisol levels, the final effector of the HPI axis. This was an essential step in order to elucidate the levels of endogenous cortisol to which the larvae are exposed through early development after stress exposure and identify a suitable developmental time window in which exposure to early adverse experience may be more likely to activate glucocorticoid-mediated adaptive mechanisms.
- Third, I aimed to develop an early life stress paradigm in order to evaluate the effects of early adverse experience at the behavioral, endocrinological, and cellular level; subsequently, the goal of the project was to perform a genome-wide transcriptome analysis of hypothalamus-specific cell populations in order to elucidate the molecular correlates of early adverse experience.
- Finally, I characterized the cortisol response profiles of optogenetic and genetically targeted ablation tools that allow the manipulation of all three elements of the HPI axis. This facilitates the subsequent study of the role of glucocorticoids on the adaptive changes induced by early adverse experience.

3. RESULTS

3.1 Vortex flow stimulation as an activator of the HPI axis.

3.1.1 Characterization of the vortex flow stimulation.

To activate the HPI axis of free swimming zebrafish larvae, I developed a stimulation protocol using vortex flows of different strengths. Vortex flows were generated by a commercially available magnetic stirrer plate and a micro-stirrer. Larvae were placed in small petri dishes containing the micro-stirrer and exposed to different strengths of magnetic field inversion delivered by the magnetic stirrer plate (Figure 3.1A). The generated vortex flow created a pattern of water motion that depended on the strength of the stimulation (Figure 3.1B-D). To analyze the trajectories of water flow elicited by the vortex, single anesthetized larvae were exposed to the stimulation; larvae were placed half the distance between the vortex origin and the edge of the petri dish and the magnetic stirrer plate was turned on. Anesthetized larvae exposed to water flows generated by the micro-stirrer followed an irregular trajectory underlain by the differential speed of the water flow inside the container, which depends on the distance to the vortex origin (Figure 3.1B-D). As expected, higher speeds reached by the anesthetized larvae were found in the proximity of the vortex origin. This was true for all the stimulation strengths tested; moreover, anesthetized larvae exposed to higher strengths of the magnetic field inversion reached higher absolute values of speed (Figure 3.1C). Importantly, the strength of the magnetic field inversion determined the mean speed of the anesthetized larvae exposed to different strengths of vortex flow (Figure 3.1D). This allows controlling quantitatively the strength of the input delivered to the larvae and facilitates subsequent analysis of HPI axis activity.

3.1.2 Exposure to vortex flow stimulation correlates with behavioral outputs.

Vortex flow stimulation allows behavioral analysis in free swimming larvae. In order to characterize behavioral output during and after the stimulation, zebrafish larvae were filmed and tracked to measure locomotor activity and body orientation. Locomotor activity, as expected, was transiently increased immediately after the onset of the vortex flow stimulation (Figure 3.2A, C). Importantly, the increased locomotor activity of larvae exposed to the vortex flow stimulation was strength-dependent (Figure 3.2C), suggesting a link between the locomotor response to vortex flow onset and the speed of the vortex flow (Figure 3.1D).

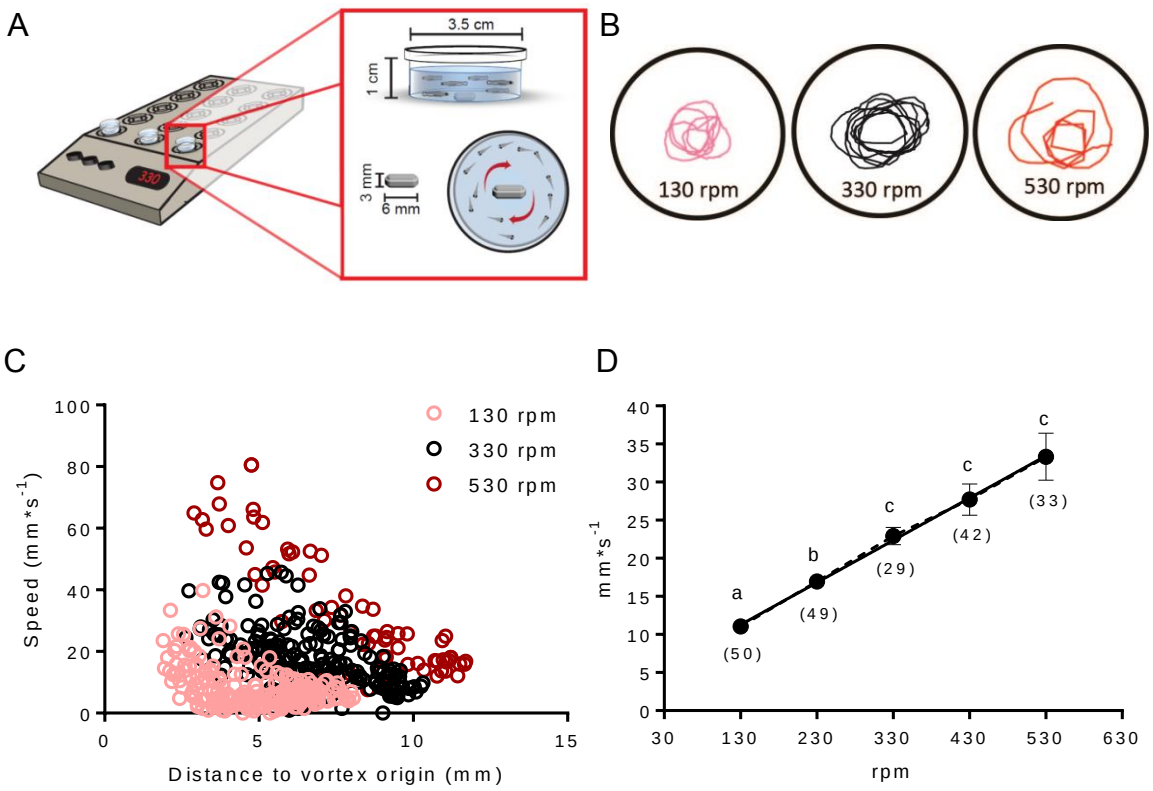

Figure 3.1. Characterization of vortex flow stimulation using anesthetized larvae. **A:** Schematic representation of the magnetic stirrer plate and the micro-stirrer. **B:** Exemplary trajectories followed by a single anesthetized larva when exposed to vortex flow of different strengths. **C:** The speed of an anesthetized larva depends on the distance to the vortex origin during vortex flow stimulation. **D:** The mean speed of an anesthetized larva (30 frames) exposed to vortex flow depends on the strength of the magnetic field inversion (Kruskal-Wallis test: $H = 92.79$, $p<0.0001$; Dunn's post-test: $^{abc}p<0.05$; sample size indicated in parenthesis).

To evaluate whether acute exposure to vortex flow stimulation leads to altered locomotor activity immediately after the stimulation, distance swam after stimulation offset was measured. Interestingly, a strength-dependent decrease in locomotor activity was observed at the offset of a three-minute long vortex flow stimulation, leading to almost no motion when the strongest stimulation was used (Figure 3.2D). In the same way, this suggests a link between the speed of the vortex flow to which the larvae are exposed and the levels of locomotor activity reached after the offset of the stimulation (Figure 3.1D and 3.2D). It is important to note that some individuals exposed to the strongest stimulation showed a transient decreased ability to maintain equilibrium of their body axes immediately after the vortex stimulation offset (data not shown). This suggests that higher strengths of vortex flow stimulation are likely to lead to exhaustion and potentially transient depletion of energy.

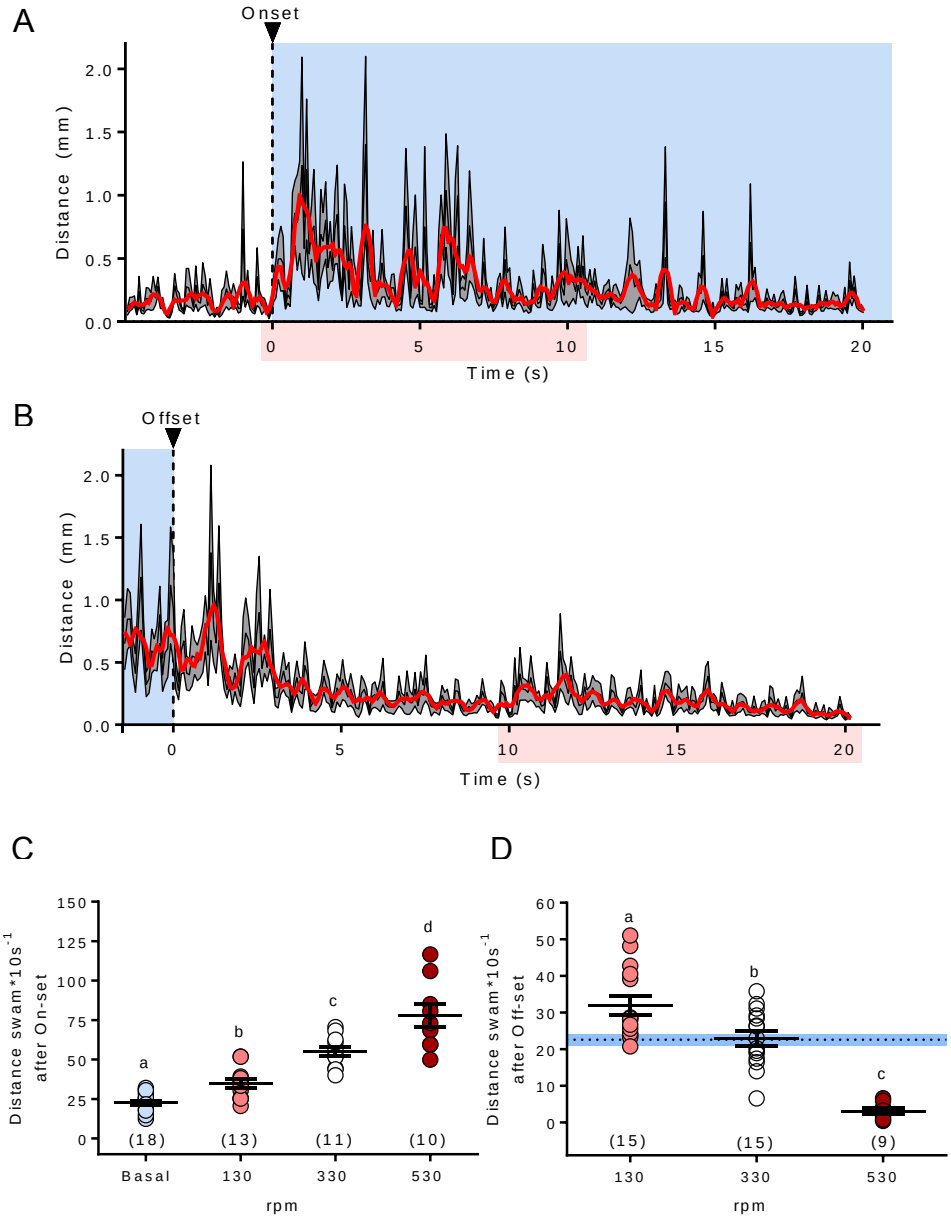

Figure 3.2. Vortex flow stimulation induces locomotor activity changes. A: Example of a trace showing the distance swam by larvae exposed to vortex flow stimulation with strength of 330 rpm. Note that the distance swam increases immediately after stimulation onset. The mean of the distance swam in a time window of 10 seconds after stimulation onset (colored box in x-axis) was selected to compare the locomotor response to the onset of vortex flow stimulation of different strengths. **B:** Example of a trace showing the distance swam after the offset of vortex flow stimulation with strength of 330 rpm. The mean of the distance swam in a time window of 10 seconds after stimulation offset (colored box in x-axis) was selected to compare the locomotor activity after stimulation offset of vortex flow stimulation of different strengths. **C:** The increase in locomotor activity induced by vortex flow stimulation onset depends on the strength of the stimulation (One-way ANOVA: $F(3,47) = 48.46$, $p<0.0001$; Turkey's post-test: ^{abcd} $p<0.05$; sample size indicated in parenthesis). **D:** The distance swam immediately after vortex flow stimulation offset depends on the strength of the stimulation (One-way ANOVA: $F(2,36) = 38.07$, $p<0.0001$; Turkey's post-test: ^{abcd} $p<0.05$; sample size indicated in parenthesis). Basal levels of locomotion measured before onset of vortex flow stimulation are represented by the blue line.

Rheotaxis is a well characterized behavior in both larval and adult zebrafish. Generally, a fish showing rheotaxis behavior would face against an upcoming current and swim in that direction in order to efficiently maintain a position without being swept by the current. Swimming against a current would also allow the fish to maximize the distance between its position and the source of the generated current, potentially a predator. Although vortex flows are not uniform linear flows, they create continuous water currents around the vortex origin. Rheotaxis behavior of zebrafish larvae as a response to this type of currents has not been described before. Therefore, I characterized rheotaxis behavioral output of 6 dpf larvae during vortex flow stimulation. First, to test the hypothesis that zebrafish larvae would re-orientate their body axis during vortex flow stimulation, I measured change in body angle orientation as a response to the vortex flow stimulation onset. Larvae showed a brief and transient increase in change of body angle immediately after the onset of the vortex flow stimulation (Figure 3.3A). To reveal whether this is a directed response, I measured the position of the larvae with respect to the vortex origin right after the stimulation onset. To measure the position of the larvae, the petri dish was virtually divided in three concentric rings (Figure 3.3C-E). The proportion of larvae located in the most inner ring, close to the vortex origin, significantly decreases after vortex flow onset and is accompanied with an increased number of larvae positioned in the two outer rings. In line with this, the mean distance to the vortex origin of a population of larvae is significantly increased after vortex flow onset (Figure 3.3B).

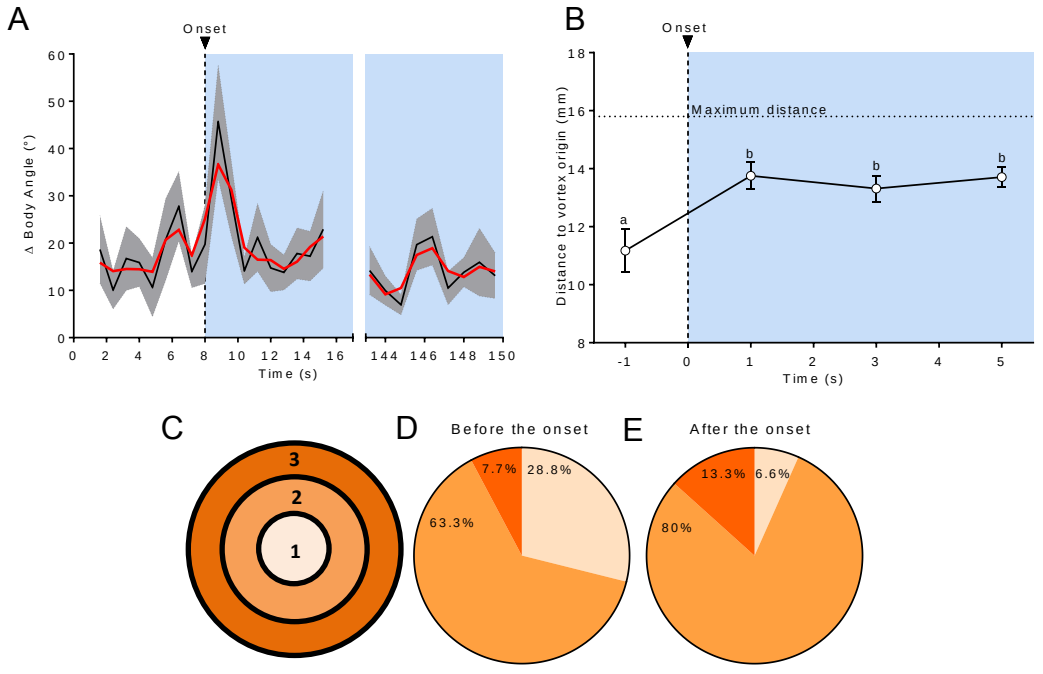

Figure 3.3. Larvae re-orientate their body axis and move away from the vortex origin after vortex flow stimulation onset. A: Change of body angle increases transiently immediately after vortex flow onset (N=10). **B:** Mean distance to the vortex origin of a population of larvae increases after vortex flow onset (Kruskal-Wallis test: H = 11.98, p=0.0075; Dunn's post-test: [ab] p<0.05; N=30). **C:** Schematic representation of the petri dish division. **D-E:** Proportion of larvae positioned in each of the three concentric rings before (D) and after (E) vortex stimulation onset (N=30).

Rheotaxis behavior is characterized by the orientation of the fishes' body axis with the water flow. This requires a specific body angle orientation and maintenance of that position. To analyze these aspects in zebrafish larvae exposed to vortex flow stimulation, I measured the proportion of larvae facing the direction of the flow and the frequency distribution of body angles shown by a larvae population after two minutes of vortex flow stimulation (Figure 3.4A-D). In line with typical rheotaxis behavior, the proportion of larvae facing against the water flow was strength-dependent. For the lowest strength of vortex flow stimulation, the proportion of larvae facing against the water flow was not different from 50%; however, higher strengths led to higher proportion of larvae facing against the water flow (Figure 3.4A).

When larvae were exposed to the highest strength of vortex flow stimulation, 97% of the larvae faced against the water flow (Figure 3.4A). Since water currents are not linear during vortex flow stimulation, the larvae showed a wide distribution of body angles during the stimulation. Interestingly, the frequency distribution of body angles shown by the larvae during the stimulation was strength-dependent, being wider for basal conditions and low strengths of vortex flow stimulation and more restricted for the highest strength (530 rpm), where the median angle was around 55.1° (Figure 3.4C-F). Another important aspect of rheotaxis behavior is the maintenance of a specific orientation. To assess whether larvae maintain a specific orientation during vortex flow stimulation, I measured the change in body angle after 2 minutes of vortex flow stimulation of different strengths. Higher strengths of vortex flow stimulation led to a decreased change in body angle, suggesting that the strength of the stimulation correlates with the extent to which the larvae maintain a specific orientation during vortex flow stimulation (Figure 3.4B).

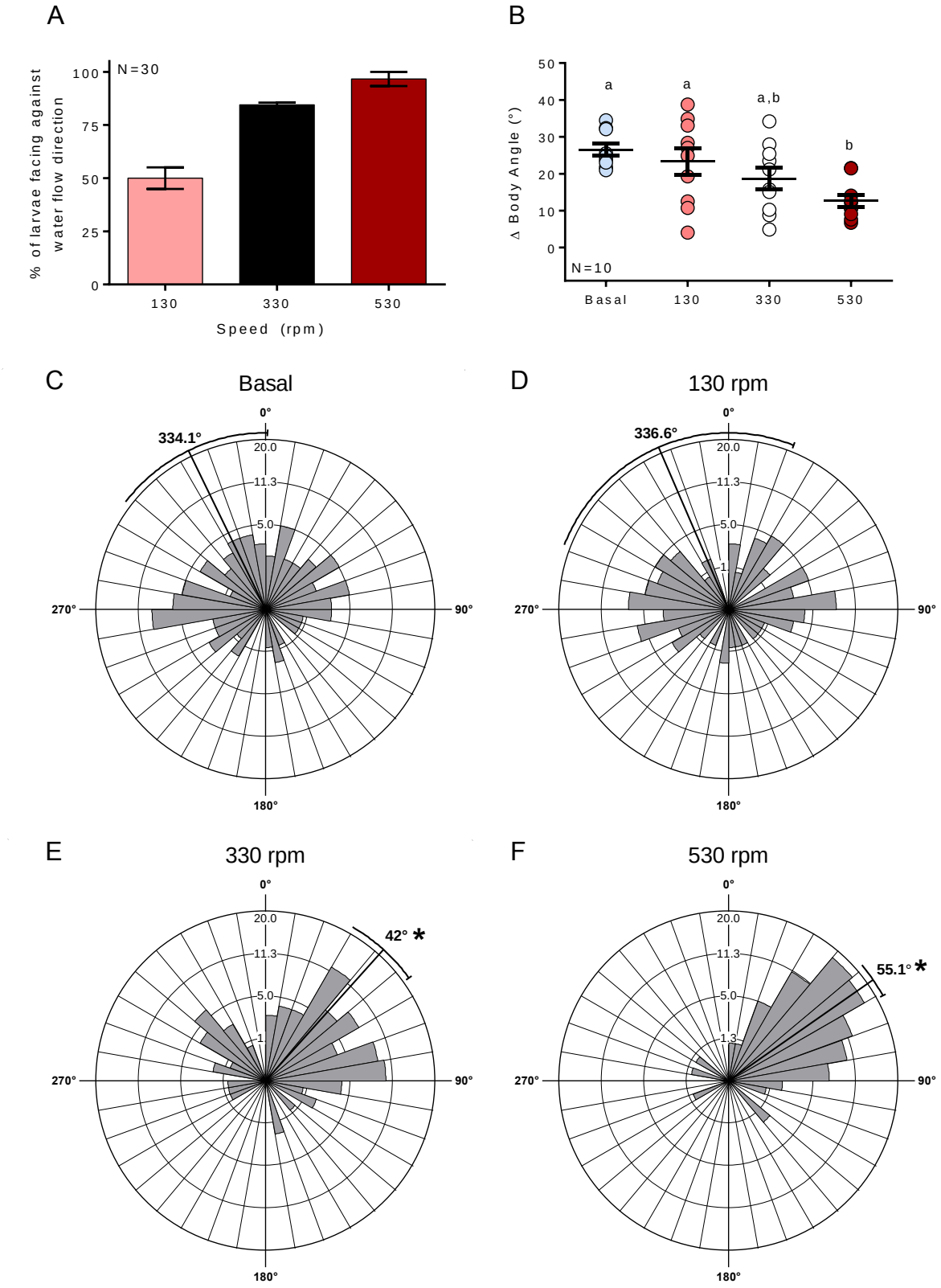

Figure 3.4. Larvae show rheotaxis behavior in a strength-dependent manner by facing against the water flow and maintaining that position. A: Proportion of larvae facing against the water flow after 2 minutes of vortex flow stimulation onset. **B:** Change of body angle after 2 minutes of vortex flow stimulation onset was decreased when larvae were exposed to the highest strength of vortex flow stimulation (One-way ANOVA: F (3,35) = 5.115, p=0.0049; Turkey's post-test: [ab] p<0.05). **C-F:** Circular representation of the frequency distribution of body

angles showed by larvae at basal conditions or after 2 minutes of vortex flow stimulation onset (130, 330, or 530 rpm). Mean angle is represented with a line and the arcs extending to either side represent the 95% confidence limits. Note that higher strengths of the vortex flow stimulation show a narrower frequency distribution. Significant differences when compared to basal conditions are indicated by an asterisk (*) next to the mean angle (Watson-Williams F-test: Basal vs 130 rpm: F = 0.022, p=0.882, Basal vs 330 rpm: F = 30.57, p<0.0001, Basal vs 530 rpm: F = 57.74, p<0.0001; N=90).

3.1.3 Exposure to vortex flow stimulation activates the HPI axis

Vortex flow stimulation elicits behavioral output in zebrafish larvae (Section 3.1.2): a) increased locomotor activity, b) active re-orientation of the body axis, and c) maintenance of a particular orientation. It is reasonable to assume that these three behavioral changes require energy mobilization. Since activation of the HPI axis and its final effectors, glucocorticoids, are involved in energy mobilization, I therefore hypothesized that exposure to vortex flow stimulation would activate this axis and increase cortisol levels, facilitating behavioral coping strategies. To test this, I used the highest strength of vortex flow stimulation as the input signal to activate the HPI axis and measured whole body cortisol as the output signal for HPI axis activation. Cortisol levels were increased 4-fold after vortex flow stimulation, suggesting that this stimulation activates the HPI axis (Figure 3.5A). Importantly, handling-induced cortisol levels of vortex flow stimulation are not different from basal cortisol levels of un-stimulated larvae. To exclude any potential unspecific effects on HPI axis activation by electromagnetic field exposure, larvae were exposed to different magnetic field inversion strengths in the absence of the magnetic stirrer and cortisol levels were measured. Exposure to the magnetic field inversion of different strengths did not elicit a cortisol response (Figure 3.5B).

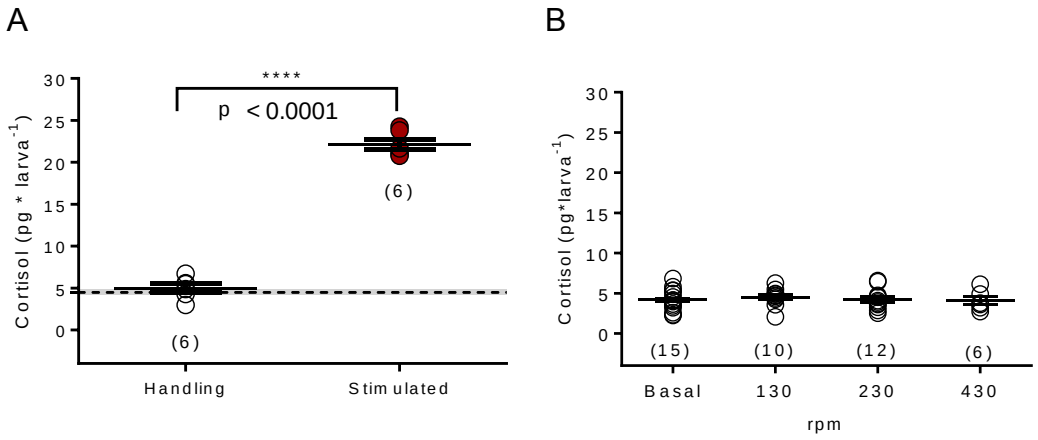

Figure 3.5. Vortex flow stimulation induces a cortisol response. A: Acute vortex flow exposure (1 min) increases cortisol levels in 6 dpf larvae. Samples were collected 10 minutes after stimulation onset (t-test, **** $p<0.0001$; sample sized indicated in parenthesis) **B:** exposure to magnetic fields of different strengths without the magnetic stirrer failed to elicit a cortisol response in 6 dpf larvae (One-way ANOVA: $F(3,46) = 0.2948$, $p=0.8290$; sample sized indicated in parenthesis).

As described in section 3.1.2, behavioral correlates depend on the strength of the vortex flow stimulation. To evaluate whether HPI axis is also activated in a strength-dependent manner by vortex flow stimulation, larvae were exposed to different strengths of vortex flow stimulation and peak cortisol levels were measured. Indeed, the cortisol levels reached after the stimulation were different depending on the strength to which they were exposed. Higher strengths of the stimulation induced higher cortisol levels (Figure 3.6A).

To evaluate the effect of the duration of the vortex flow stimulation and its potential interaction with the strength of the stimulation, larvae were exposed to one, three, or six minutes of continuous stimulation of high (330 rpm) and low (130 rpm) strength and cortisol levels were measured after 10 minutes of stimulation onset. All treatments increased cortisol levels significantly (Figure 3.6B). High strength stimulation induced higher cortisol levels in all conditions when compared to the cortisol levels induced by the low strength stimulation. Different exposure time to the low strength vortex flow stimulation did not have an effect on cortisol levels. On the other hand, exposure to the high strength stimulation for three minutes induced higher cortisol levels than the ones reached after one minute of exposure. This effect was not significant when the duration of the stimulation was increased to six minutes. Moreover, two-way ANOVA analysis revealed an interaction between the duration and strength of the stimulation (Figure 3.6B).

In order to evaluate the degree of correlation between the behavioral output and the HPI axis activation after vortex flow stimulation, locomotor activity and maintenance of body orientation in the presence of vortex flows were plotted against cortisol levels reached after vortex flow exposure (Figure 3.7A, B). As described before in section 3.1.2, higher strengths of vortex flow stimulation led to an increased locomotor response immediately after vortex flow onset; this correlates with cortisol levels induced by vortex flow exposure ($r^2=0.88$). Similarly, increased maintenance of a specific body orientation after two minutes of high-strength vortex flow stimulation

correlated with higher levels of cortisol (r^2= 0.99). These correlations suggest a link between cortisol release and behavioral coping strategies performed by larvae after vortex flow stimulation.

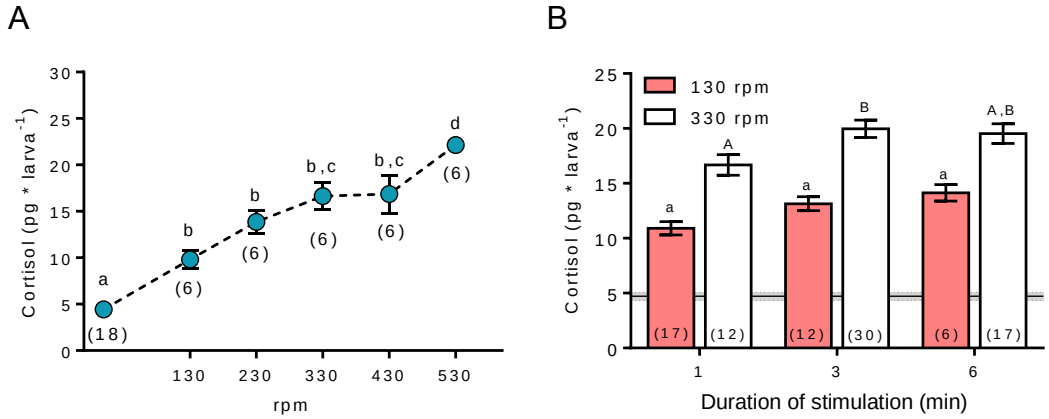

Figure 3.6. Activation of the HPI axis by vortex flow stimulation depends on the strength and duration of the stimulation. A: Vortex flow stimulation (1 minute exposure) increased cortisol levels in 6 dpf zebrafish larvae in a strength-dependent manner (One-way ANOVA: F (5,41) = 56.52, p=0.0001; Turkey's post-test: ^{abcd} p<0.05; sample size indicated in parenthesis). **B:** Cortisol levels reached by zebrafish larvae after 1, 3, or 6 minutes of exposure to vortex flow stimulation of low (130 rpm) or high (330 rpm) strength (Two-way ANOVA: duration: $F_{(3,122)}$=112.9, p<0.0001; strength: $F_{(1,122)}$=59.07, p<0.0001; duration x strength: $F_{(3,122)}$=8.75, p<0.0001; Tukey's post-test: comparison of duration within each strength: ^{ab}p<0.05, indicated with lower case letters for low strength (130 rpm) and uppercase letters for high strength (330 rpm)). Basal cortisol levels ± standard error of the mean (SEM) are indicated by the black/gray line.

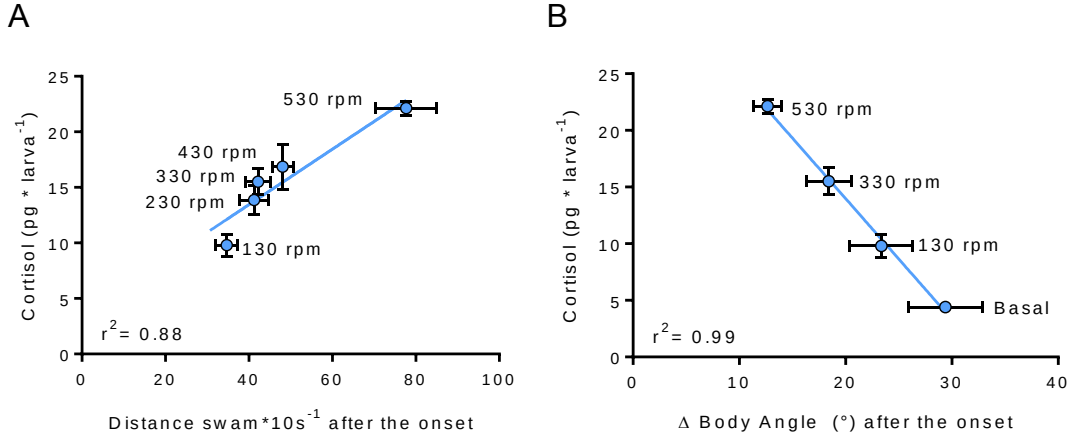

Figure 3.7. Activation of the HPI axis correlates with behavioral output after vortex flow stimulation. A: Correlation analysis showing that strength-dependent cortisol response correlates with locomotor activity after vortex flow onset (Pearson analysis, r^2 = 0.88, p=0.0195). **B:** Correlation analysis showing that strength-dependent cortisol response negatively correlates with change in body angle orientation after vortex flow onset (Pearson analysis, r^2 = 0.99, p=0.0019). Cortisol values used for correlation analysis are also shown in Figure 3.6A.

3.2 Activation of the HPI axis during early life stages of zebrafish larvae.

To characterize the ontogeny of the HPI axis activity during early life stages, I determined the changes in HPI axis activity of zebrafish larvae between 2 and 8 dpf. I quantified basal activity, acute activation, and responses to repeated stress during early development using vortex flow stimulation and osmotic shock as threatening input signals, and cortisol as the output measure of HPI axis activity.

3.2.1 Basal cortisol levels and profiles of acute HPI axis activation after vortex flow stimulation change with age.

To evaluate basal activity of the HPI axis through development, cortisol levels at resting conditions of unstimulated larvae of different developmental stages were measured. As expected, overall cortisol levels increased throughout the time window between 2 and 8 dpf (Figure 3.8). According to previous studies and based on these changes in basal cortisol levels, it is reasonable to hypothesize that the HPI axis of larvae at these developmental stages is still under maturation. To test this, I screened the effects of vortex flow stimulation on cortisol levels in 4, 6, and 8 dpf larvae. The larvae were exposed to different strengths of vortex flow stimulation (ranging from 130 to 430 rpm) for either 1, 3, or 6 minutes. The aim of such a screening was threefold: 1) to identify when and how the cortisol-response profiles change through development; 2) to define appropriate conditions of the vortex flow stimulation for subsequent experiments to disrupt the maturation of the HPI axis activity, and 3) to define appropriate conditions of the stimulation that could be used to detect changes in stress-induced cortisol profiles after disruption of HPI axis activity maturation.

Figure 3.9 shows an overall representation of the cortisol mean values measured after the larvae were exposed to the different conditions of the vortex flow stimulation (note that different colors in figure 3.9 do not represent significant differences). In all developmental stages, the highest mean cortisol value was observed after larvae were exposed to the highest strength (430 rpm) for 6 minutes. In general, absolute mean values of cortisol were lower in 4 dpf larvae. Moreover, 8 dpf larvae showed a smaller range of cortisol mean values as a response to different conditions of vortex flow stimulation.

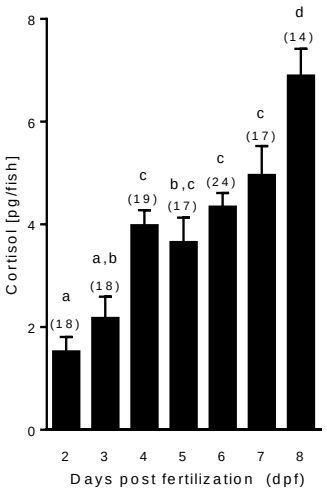

Figure 3.8. Basal cortisol levels of zebrafish larvae from 2 to 8 dpf. Cortisol levels at basal conditions change with age (One-way ANOVA: F (6,120) = 17.72, p<0.0001; Turkey's post-test: ^{abcd} p<0.05; sample size indicated in parenthesis).

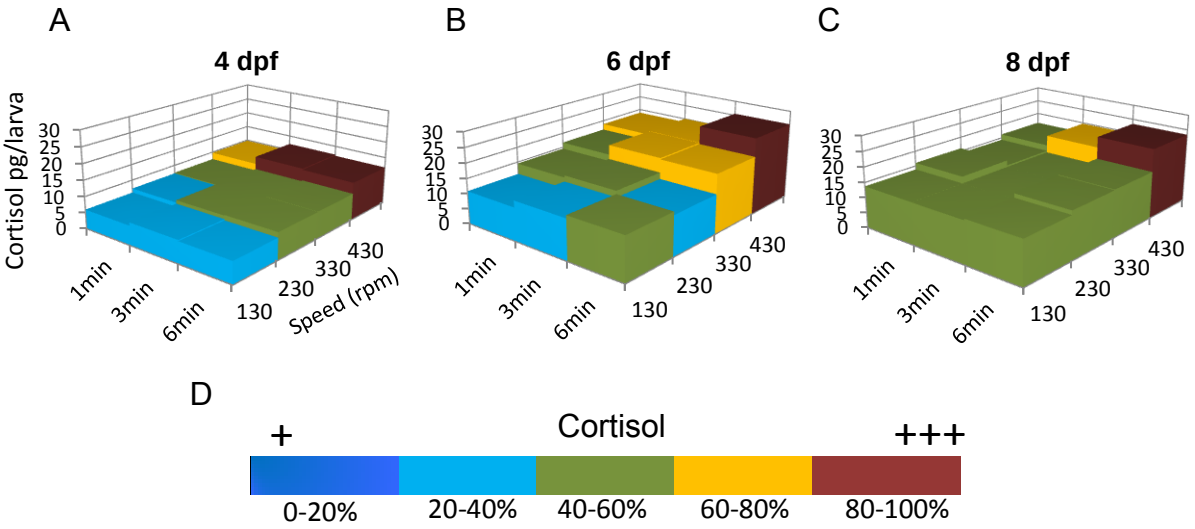

Figure 3.9. Acute HPI axis activity through development. A-C: mean cortisol levels reached by 4, 6, or 8 dpf larvae after exposure to vortex flow stimulation of different strengths (130 to 340 rpm) for either 1, 3, or 6 minutes. Bars are depicted in different colors according to the color code described in D. Note that different colors do not represent statistical significance, but only different category based on cortisol mean values. **D:** color code of cortisol levels depending on the percentage of cortisol change, where 0% is basal cortisol level for a particular age, and 100% is the maximum cortisol value observed in that particular age.

To determine whether the developmental stage had an effect on the strength-dependent cortisol profiles induced by the vortex flow stimulation, first, the data was grouped according to the duration of the vortex flow stimulation. The cortisol values of each developmental stage were normalized according to the basal cortisol levels (0%) and to the maximum cortisol value observed in each condition of duration of vortex

flow stimulation (1, 3, or 6 minutes) for that particular age (100%) (Figure 3.10). Normalization allowed analyzing the effects of age on the strength-dependent cortisol response without taking into account the differences in absolute values of cortisol observed at different developmental stages. Interestingly, Two-way ANOVA analysis revealed that the developmental stage had a significant effect on the strength-dependent cortisol response observed after the larvae were exposed to the vortex flow stimulation for 1 and 3 minutes, but not when exposed for 6 minutes (Figure 3.10).

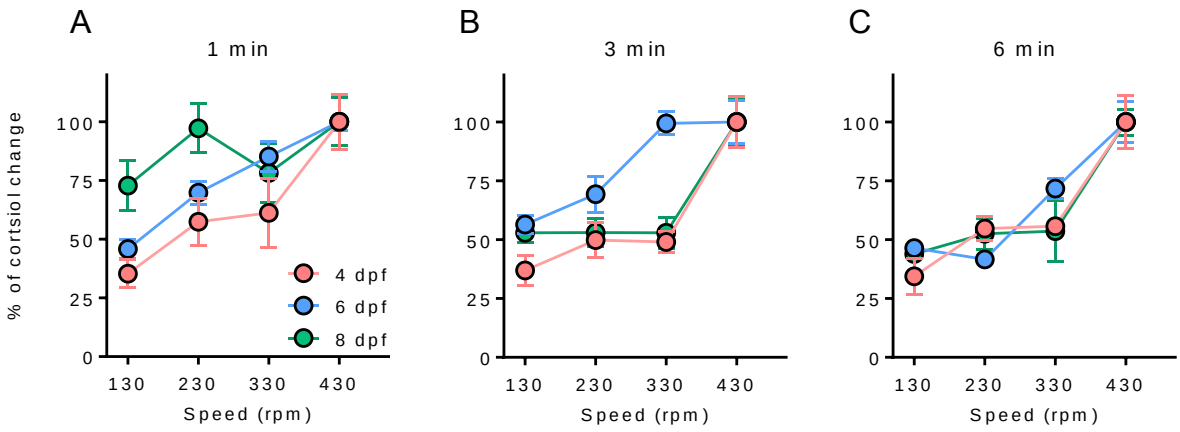

Figure 3.10. Strength-dependent cortisol response to acute vortex flow stimulation changes with age. A-C: cortisol response of 4, 6, and 8 dpf larvae, which were exposed to acute vortex flow stimulation of different strengths (130-430 rpm) for either 1, 3, or 6 minutes, respectively. Different developmental stages showed differences in cortisol profiles when exposed to the vortex flow stimulation for 1 or 3 minutes. Exposure to vortex flow stimulation for 6 minutes did not induce differences in cortisol profiles among the different developmental stages (A: ^{1min}Two-way ANOVA: strength: $F_{(3,125)}=10.68$, $p<0.0001$; age: $F_{(2,125)}=4.759$, $p=0.0102$; strength x age: $F_{(6,125)}=1.059$, $p=0.3908$. B: ^{3min}Two-way ANOVA: strength: $F_{(3,131)}=14.11$, $p<0.0001$; age: $F_{(2,131)}=66.53$, $p<0.0001$; strength x age: $F_{(6,131)}=4.745$, $p=0.0002$. C: ^{6min}Two-way ANOVA: strength: $F_{(3,89)}=7.252$, $p=0.0002$; age: $F_{(2,89)}=2.855$, $p=0.0628$; strength x age: $F_{(6,89)}=0.5201$, $p=0.7917$).

To dissect further the differences in cortisol response at different developmental stages, I selected two strengths of stimulation: low and high. Low strength stimulation consisted of exposure to vortex flow stimulation of 130 rpm strength for 1 minute. High strength stimulation consisted of exposure to the stimulation of 330 rpm strength for 3 minutes. These conditions were selected based on cortisol response data of 6 dpf larvae (Figure 3.9 and 3.10). The conditions for the low strength stimulation are the lowest which elicited a significant increase in cortisol levels when compared to basal levels (t test, $T = 9.235$, $p<0.0001$). The conditions for the high strength stimulation induced a

high increase of cortisol levels without reaching the maximum levels of cortisol observed when higher stimulation strengths were used. This avoids potential saturation/exhaustion of the cortisol response, which may mask subtle changes in cortisol profiles. Moreover, these conditions induced a cortisol response of clearly different magnitude among different developmental stages (One-way ANOVA ^{3min330rpm}4dpf, ^{3min330rpm}6dpf, ^{3min330rpm}8dpf: $F(2,67) = 65.35$, $p<0.0001$).

The cortisol levels induced by vortex flow stimulation of low and high strength in 4 to 8 dpf larvae are shown in Figure 3.11A. High strength stimulation induced a high increase in cortisol levels at 6 dpf (Figure 3.10B and Figure 3.11A), which gradually decreased at 7 and 8 dpf. This increase was not detected when low strength stimulation was used. I then asked whether the pattern of cortisol response induced by vortex flow stimulation throughout development was stressor-specific. To evaluate this, 4 to 8 dpf larvae were exposed to an osmotic shock of low (50 mM NaCl) and high (250 mM NaCl) strengths and cortisol levels were measured. Similar to the cortisol response to vortex flow stimulation, zebrafish larvae elicited a higher cortisol response to a strong osmotic shock at 6 dpf (Figure 3.11A-B). Two-way ANOVA analysis revealed that for both type of stimulations the developmental stage, strength of the stimulation, and the interaction between these two factors, have a significant effect on the stress-induced cortisol levels (Figure 3.11A-B). Although the same general trend can be seen in cortisol response to both osmotic shock and vortex flow stimulations, some differences were found. Cortisol response to low strength vortex flow stimulation increased slightly after 5 dpf; in the case of low strength osmotic shock, there were no differences in cortisol response among the different developmental stages tested. Although cortisol response to a high strength stimulation of both types decreased gradually after 6 dpf, the cortisol response elicited by low- and high-strength osmotic shock stimulation was still significantly different at 8 dpf (Mann-Whitney test: $U=2.5$, $p=0.0011$); in contrast, the difference in cortisol response elicited by low- and high-strength of vortex flow stimulation in 8 dpf larvae was not detectable anymore (t test: $T=0.5986$, $p=0.5559$). In order to evaluate whether the decline in cortisol response to high strength stimulations after 6 dpf was due to a compromised energetic state or to limited nutritional resources, 8 dpf larvae to which a feeding protocol was delivered starting from day 6 were exposed to the same stress protocol using vortex flow stimulation of low and high strengths

(Figure 3.11C). No significant difference in cortisol response was observed between fed and unfed 8 dpf larvae.

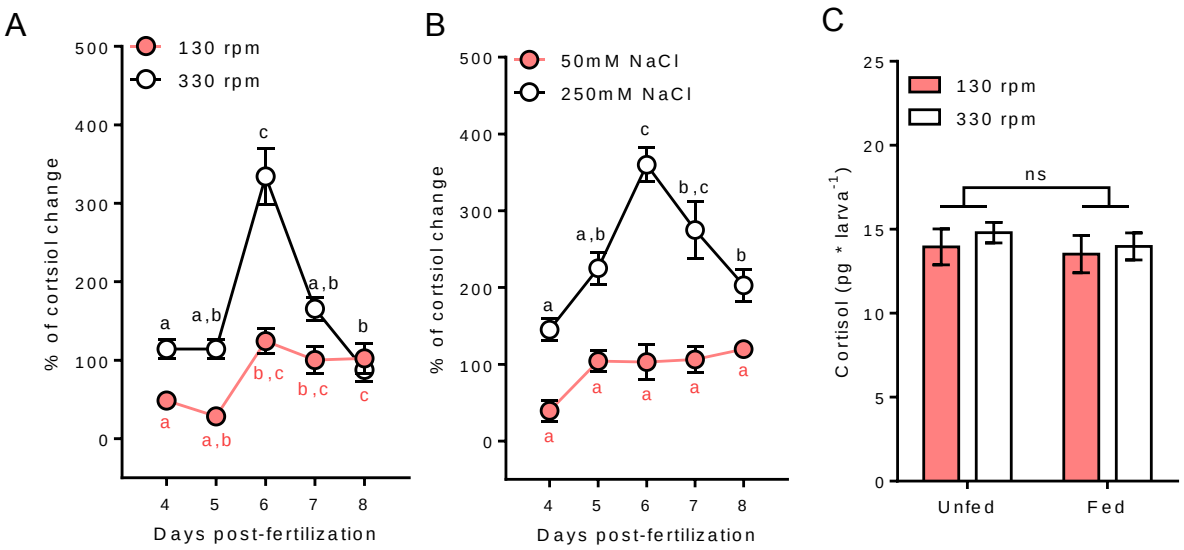

Figure 3.11. Cortisol response profiles to acute stress in zebrafish larvae change with age. **A:** Cortisol levels reached after exposure to acute vortex flow stimulation of low (1 minute, 130 rpm) or high (3 minutes, 330 rpm) strength at different developmental stages (4 to 8 dpf) (Two-way ANOVA: age: $F_{(4,98)}$=37.64, p<0.0001; strength: $F_{(1,98)}$=27.12, p<0.0001; age x strength: $F_{(4,98)}$=10.76, p<0.0001; Tukey's post-test: comparison of age within each strength: ^{abc} p<0.05, indicated with lower case letters). **B:** Cortisol levels reached after acute osmotic shock exposure of low (50 mM NaCl) or high (250 mM NaCl) strength at different developmental stages (4 to 8 dpf). Samples were collected 10 minutes after stimulation onset (Two-way ANOVA: age: $F_{(4,82)}$=4.95, p=0.0013; strength: $F_{(1,82)}$=55.19, p<0.0001; age x strength: $F_{(4,82)}$=2.49, p<0.049; Tukey's post-test: comparison among age groups within each strength: ^{abc} p<0.05, indicated with lower case letters). **C:** Cortisol levels reached after acute exposure to vortex flow stimulation of low (1 minute, 130 rpm) or high (3 minutes, 330 rpm) strength in either fed or unfed 8 dpf larvae. No difference was observed between fed or unfed larvae (Two-way ANOVA: strength: $F_{(1,42)}$=0.4413, p=0.5101; feeding condition: $F_{(1,42)}$=0.4046, p=0.5282; strength x feeding condition: $F_{(1,42)}$=0.03809, p=0.8462).

3.2.2 Profiles of HPI axis activation after repeated exposure to vortex flow change with age.

Termination of the stress response is achieved by activation of the HPI axis negative feedback, in which the stress-induced cortisol feeds back to the hypothalamus and pituitary via the glucocorticoid receptor. Efficiency of the HPI axis negative feedback is therefore important for an appropriate stress response. Based on the data described in section 3.2.1, it is reasonable to hypothesize that the HPI axis negative feedback dynamics mature through the early stages of development tested: from 4 to 8 dpf. In order to evaluate this, cortisol response after a repeated exposure to vortex flow stimulation was measured. The magnitude of a cortisol response to a second

perturbation delivered at either 30 or 60 minutes after the first stimulation was used as an indicator of HPI axis negative feedback activation. I evaluated the effects of the developmental stage on cortisol response to repeated vortex flow stimulation considering the strength of the stimulation and the inter-trial interval in between subsequent stimulations (Figure 3.12A and B).

When low-strength vortex flow stimulation was used, a second stimulation of the same strength with either 30 or 60 minutes of inter-trial interval failed to elicit a cortisol response comparable in magnitude to the one elicited after the first presentation (Figure 3.12A). Two-way ANOVA analysis revealed neither an effect of the developmental stage nor of the inter-trial interval on the cortisol levels induced by the repeated stimulations.

A different result was found when high-strength vortex flow stimulation was used. In this case, Two-way ANOVA analysis revealed a significant effect of both the developmental stage and the inter-trial interval on the cortisol levels induced by the repeated vortex flow stimulation of high strength (Figure 3.12B). Larvae of 4 and 6 dpf failed to elicit a cortisol response comparable to the one reached after the first stimulation when the inter-trial interval was set to 30 minutes. However, 8 dpf larvae did elicit a cortisol increase of similar magnitude than the one induced after the first stimulation, suggesting that at this developmental stage a faster recovery occurs (Figure 3.12B). When the inter-trial interval was increased to 60 minutes, 4 dpf larvae responded with a cortisol increase of similar magnitude than the one elicited after the first vortex flow stimulation (Figure 3.12B). This was different from 6 dpf larvae, where the maximum cortisol levels reached after the second perturbation were not of the same magnitude than the ones reached after the first stimulation (Figure 3.12B). Interestingly, a tendency was found in 8 dpf larvae to respond to a second perturbation with even higher cortisol levels than the ones reached after the first vortex flow stimulation when the inter-trial interval was set to 60 minutes (Figure 3.12B).

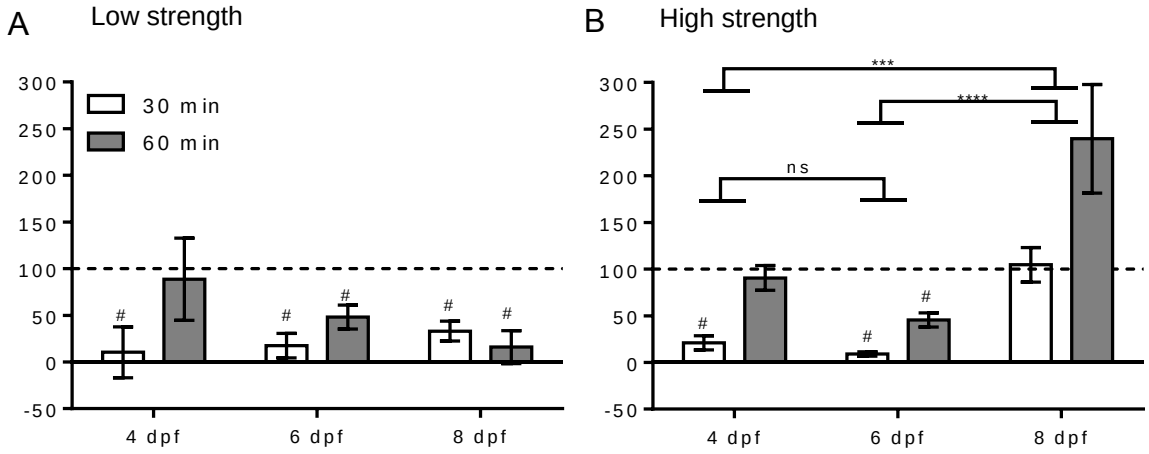

Figure 3.12. Cortisol response profiles after repeated vortex flow stimulation change with age. A: Cortisol response of 4, 6 and 8 dpf larvae to a repeated vortex flow stimulation of low strength (1 minute, 130 rpm) with an inter-trial interval of either 30 or 60 minutes (Two-way ANOVA: age: $F_{(2,30)}$=0.5648, p=0.5744; inter-trial interval: $F_{(1,30)}$=2.450, p=0.128; age x inter-trial interval: $F_{(2,30)}$=1.976, p=0.1563; # indicates significant difference from 100 after one-sample t-test, p<0.5; N=6). **B:** Cortisol response of 4, 6 and 8 dpf larvae to a repeated vortex flow stimulation of high strength (3 minutes 330 rpm) with an inter-trial interval of either 30 or 60 minutes (Two-way ANOVA: age: $F_{(2,41)}$=24.88, p<0.0001; inter-trial interval: $F_{(1,41)}$=18.98, p<0.0001; age x inter-trial interval: $F_{(2,41)}$=2.702, p=0.0790; # indicates significant difference from 100 after one-sample t-test, p<0.05; N=6, except ^{30min}6dpf: 12, and ^{30min}8dpf: 11). All samples were collected after 10 minutes of the second stimulation onset.

In order to evaluate whether the decreased cortisol response to repeated stimulations is mediated by the negative feedback via glucocorticoid receptor, 4, 6 or 8 dpf larvae were stimulated with repeated vortex flow stimulation (30 minutes inter-trial interval) in the presence of the glucocorticoid receptor antagonist mifepristone (Figure 3.13A-C). 4 dpf larvae showed an enhanced cortisol response to a second vortex flow stimulation when incubated with mifepristone (Figure 3.13A). 6 dpf larvae incubated with mifepristone responded to the repeated stimulation with cortisol levels of the same magnitude than the first stimulation (Figure 3.13B). Similarly, 8 dpf larvae incubated with the GR antagonist responded to the repeated perturbation with cortisol levels even higher than the ones reached after the first cortisol response (Figure 3.13C). These data together suggest that the decreased cortisol response to repeated vortex flow stimulation is mediated, at least partially, by the negative feedback via glucocorticoid receptor and that it is already present in 4 dpf larvae.

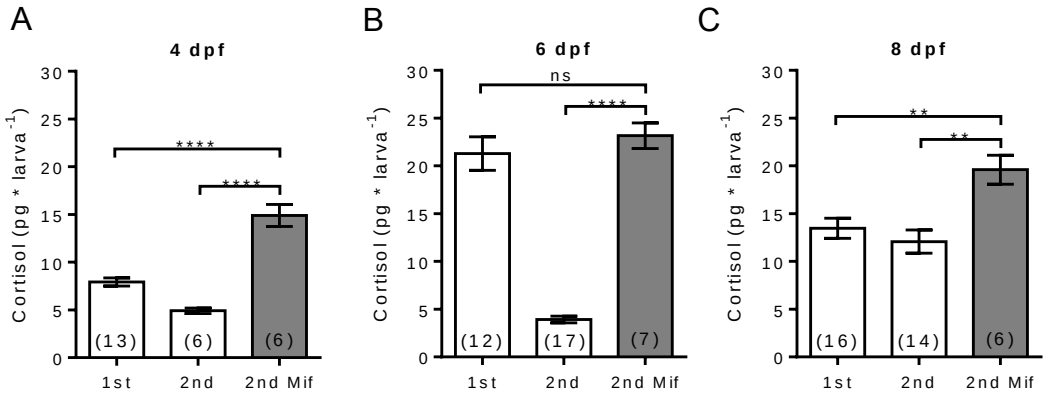

Figure 3.13. Decreased cortisol response after repeated exposure to vortex flow is mediated by the glucocorticoid receptor. A-C: Cortisol response of 4, 6, and 8 dpf larvae to repeated vortex flow stimulation of high strength (330 rpm) with an inter-trial interval of 30 minutes in the presence of the glucocorticoid receptor antagonist mifepristone. At all developmental stages, larvae elicited a cortisol response to a repeated acute stimulation in the presence of mifepristone. This response was of the same magnitude or higher than the cortisol response to the first stimulation (4 dpf: t test 1st vs 2nd Mif, T = 7.054, p<0.0001, t test 2nd vs 2nd Mif, T = 8.468, p<0.0001, ****p<0.0001; 6 dpf: t test 1st vs 2nd Mif, T = 0.7430, p=0.4676, t test 2nd vs 2nd Mif, T = 19.15, p<0.0001, ****p<0.0001; 8 dpf: t test 1st vs 2nd Mif, T = 3.105, p=0.0056, t test 2nd vs 2nd Mif, T = 3.573, p=0.0022, **p<0.01; sample size is indicated in parenthesis).

3.3 Development of an early life stress model using vortex flow stimulation.

3.3.1 Prolonged exposure to vortex flow stimulation induces a hypercortisolic state.

To evaluate the effects of early life experience on the maturation of the HPI axis and subsequent stress response, larvae were exposed to prolonged vortex flow stimulation during development. Based on data described in section 3.2.1, zebrafish larvae are able to elicit a cortisol response as early as 4 dpf. At 6 dpf, larvae showed higher cortisol response to vortex flow and osmotic shock stimulation (Figure 3.11A, B). These data indicates that the cortisol response induced by external stimuli increases from 4 to 6 dpf. To disrupt this process of maturation, I aimed to activate the HPI axis in a prolonged manner by exposing the larvae to prolonged continuous vortex flow stimulation during this developmental window. The prolonged stimulation consisted of 9 continuous hours of vortex flow stimulation (330 rpm). First, in order to characterize behavioral and cortisol outputs to the prolonged vortex flow stimulation, 5 dpf larvae were exposed to the stimulation and locomotor activity, body orientation, and cortisol levels were measured. At this developmental stage, larvae showed decreased locomotor activity

during the prolonged continuous vortex flow stimulation (Figure 3.14A-B). Together with this, larvae showed increased maintenance of body orientation as shown by decreased body angle change during the stimulation (Figure 3.14C-D). These changes in behavioral outputs were observed during the entire stimulation. Based on the correlation between the maintenance of body orientation and the vortex flow-induced cortisol levels (Figure 3.7B), it was predicted that prolonged vortex flow stimulation would induce a sustained hypercortisolic state. To evaluate this, cortisol levels were measured at different time points during the 9 hours of prolonged vortex flow stimulation (Figure 3.15). Cortisol levels increased as an initial acute response, reaching its peak at 10 minutes after the vortex flow onset; after this time, cortisol levels started to decrease gradually. At 60 minutes after the vortex flow onset, cortisol levels reached a steady state for a prolonged period of time, remaining higher than those of the control group. This hypercortisolic state was maintained for around 4 hours before it reached again normal basal levels which did not differ from those showed by the control group.

3.3.2 Prolonged exposure to vortex flow stimulation attenuates the stress response only when delivered at early life stages.

As described in the previous section, the HPI axis response to the vortex flow stimulation changes with age. To disrupt this process, 4 to 7 dpf larvae were exposed to prolonged vortex flow stimulation. To study the effects of prolonged vortex flow exposure on cortisol response to subsequent acute homotypic stress, a 3 minutes pulse of vortex flow stimulation (330 rpm) was delivered on the day following the prolonged stimulation and cortisol levels were measured. Prolonged exposure to the vortex flow stimulation attenuated the cortisol response to subsequent acute homotypic stress on the following day (Figure 3.16A-D). Interestingly, the attenuation of the cortisol response was observed when the prolonged exposure to vortex flow stimulation was delivered at 4 to 6 dpf, but it failed to induce cortisol response changes when delivered at 7 dpf (Figure 3.16D).

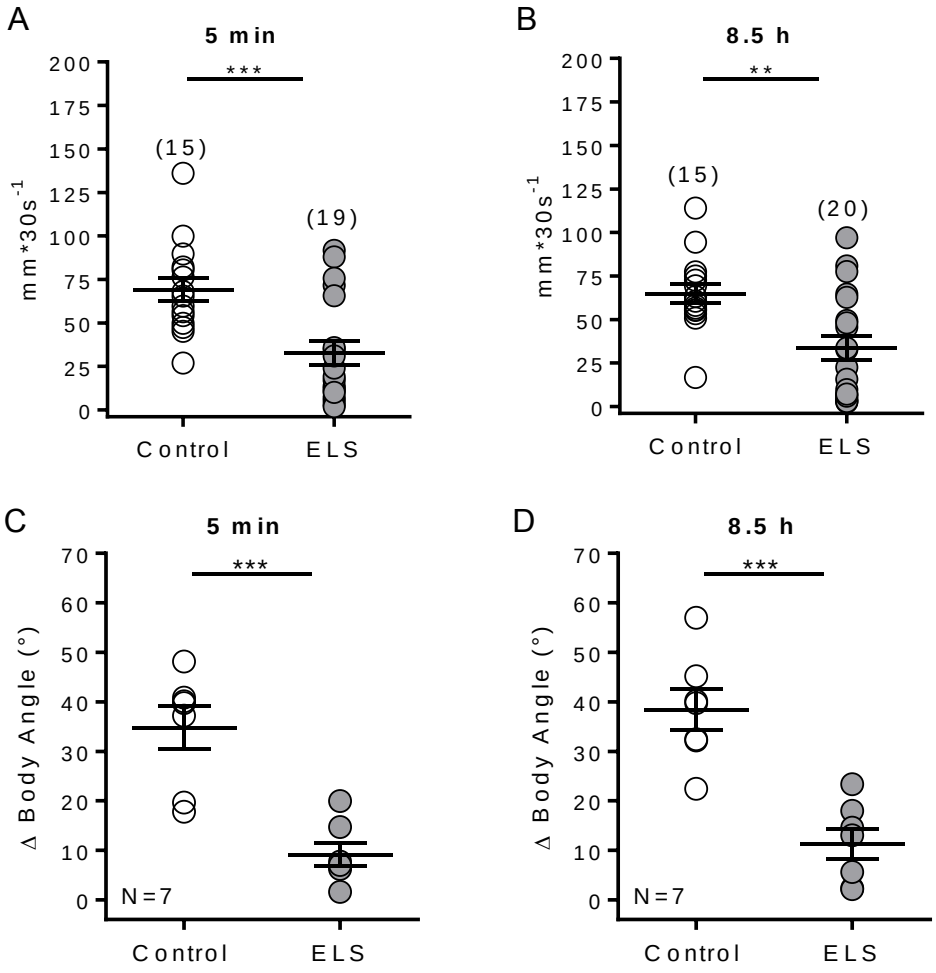

Figure 3.14. Five-dpf larvae respond with reduced locomotor activity and change in body angle to continuous vortex flow stimulation A-B: distance swam in a time window of 30 seconds after 5 minutes or 8.5 hours of continuous vortex flow stimulation, respectively. Distance swam is decreased after 5 minutes of stimulation onset; the same effect is still detected after 8.5 hours of continuous stimulation (t test: $^{5min}T = 3.692$, $p=0.0008$; $^{8.5h}T = 3.385$, $p=0.0019$, *$p<0.05$, **$p<0.01$, ***$p<0.001$; sample size is in parenthesis); prolonged vortex flow stimulation consisted of 9 hours of exposure to 330 rpm on day 5. **C-D:** Change in body angle orientation after 5 minutes or 8.5 hours of continuous vortex flow stimulation, respectively. Reduced body angle change is observed already after 5 minutes of continuous vortex flow stimulation onset; the same effect is observed after 8.5 hours of stimulation onset (t test: $^{5min}T = 5.206$, $p=0.0002$; $^{8.5h}T = 5.248$, $p=0.0002$, *$p<0.05$, **$p<0.01$, ***$p<0.001$; sample size is indicated by "N"); prolonged stimulation as described in A-B.

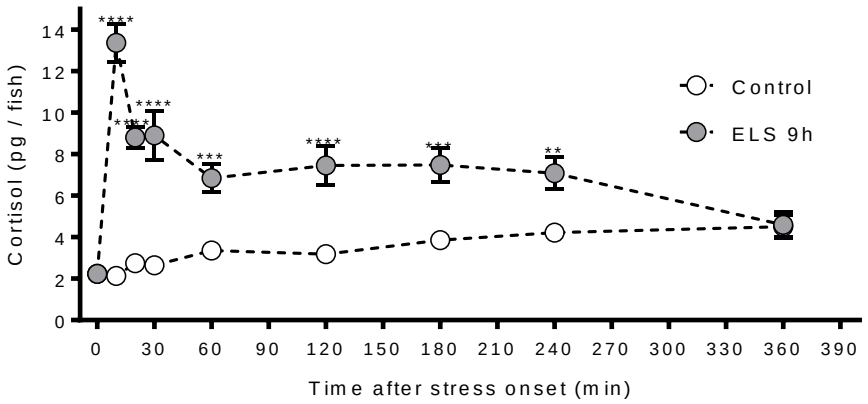

Figure 3.15. Cortisol levels as a function of time after onset of continuous vortex flow stimulation in 5 dpf larvae. Samples of 5 dpf larvae which were either exposed to continuous vortex flow stimulation (330rpm) or unstimulated controls were collected at different time points during the 9 hours of the prolonged vortex flow stimulation protocol and cortisol levels were measured. Onset of prolonged stimulation is at time 0. Prolonged vortex flow stimulation induced a hypercortisolic state which peaked at 10 minutes and was maintained for at least four hours before cortisol levels were not different from unstimulated larvae (Data generated jointly with Laura Flores) (Two way ANOVA: time: $F_{(8,86)}$=13.55, p<0.0001; treatment: $F_{(1,86)}$=246.9, p<0.0001; time x treatment: $F_{(8,86)}$=18.96, p<0.0001; Sidak's post-test: effect of treatment for each time point: *p<0.05, **p<0.01, ***p<0.001, ****p<0.0001; N=6, except $^{ELS9h\text{-}20min}$N=4, $^{ELS\ 9h\text{-}180min}$N=5).

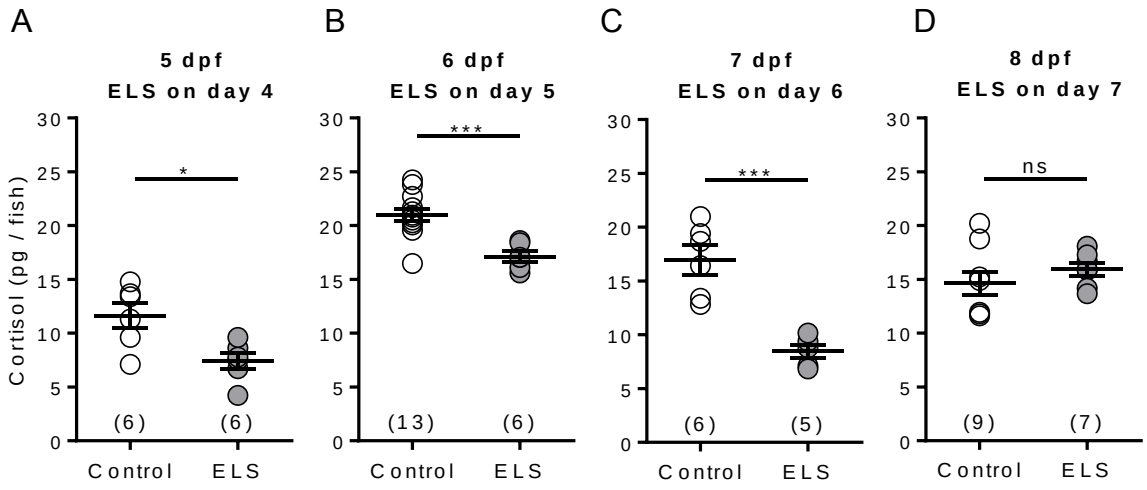

Figure 3.16. Cortisol response to an acute homotypic stressor is attenuated on the day following a prolonged exposure to vortex flow stimulation. A-D: Cortisol response measured 10 minutes after onset of an acute vortex flow stimulation of 330 rpm for 3 minutes in 5 to 8 dpf larvae. Larvae were pre-exposed to 9 hours of continuous vortex flow stimulation (330 rpm) on the previous day of the measurement. Note that 5 to 7 dpf larvae, but not 8 dpf, presented an attenuated cortisol response after treatment (Data generated jointly with Laura Flores) (t test: 5 dpf: T = 3.022, p=0.0128; 6 dpf: T = 4.331, p=0.0005; 7 dpf: T = 5.279, p=0.0005; 8 dpf: T = 0.9989, p=0.3348; *p<0.05, ***p<0.001; sample size is indicated in parenthesis; ELS: early life stress, dpf: days post-fertilization).

3.3.3 Prolonged exposure to vortex flow induces long lasting changes in cortisol response profiles.

Prolonged exposure to vortex flow stimulation during early developmental stages attenuated subsequent cortisol response to a homotypic stressor (Figure 3.16). To evaluate the effect of the strength of the prolonged stimulation on the subsequent cortisol response, different protocols of prolonged vortex flow exposure were presented to 5 dpf larvae. This developmental stage was selected based on data described in section 3.2.1, which suggests that the ability of the larvae to respond with endogenous cortisol to an external stimulus increases from 4 to 6 dpf (Figure 3.11). Since glucocorticoids play a key role in developmental programming of the HPI axis, overexposure to endogenous cortisol elicited by prolonged vortex flows stimulation at this developmental stage (Figure 3.15) may facilitate changes in HPI axis activity induced by early life experience. The early life stress (ELS) protocol consisted on variations of the pulse-length of the vortex flow stimulation which were delivered to the larvae at day 5: either 5 or 30 minutes pulses with an inter-trial interval of 60 minutes or continuous stimulation (Figure 3.17A). The strength of the magnetic field inversion was fixed to 330 rpm and the total length in which the larvae were treated was 9 hours in all cases. On the following day of the treatment, cortisol levels were measured either at basal conditions or at different time points during 60 minutes after an acute vortex flow stimulation of 3 minutes length.

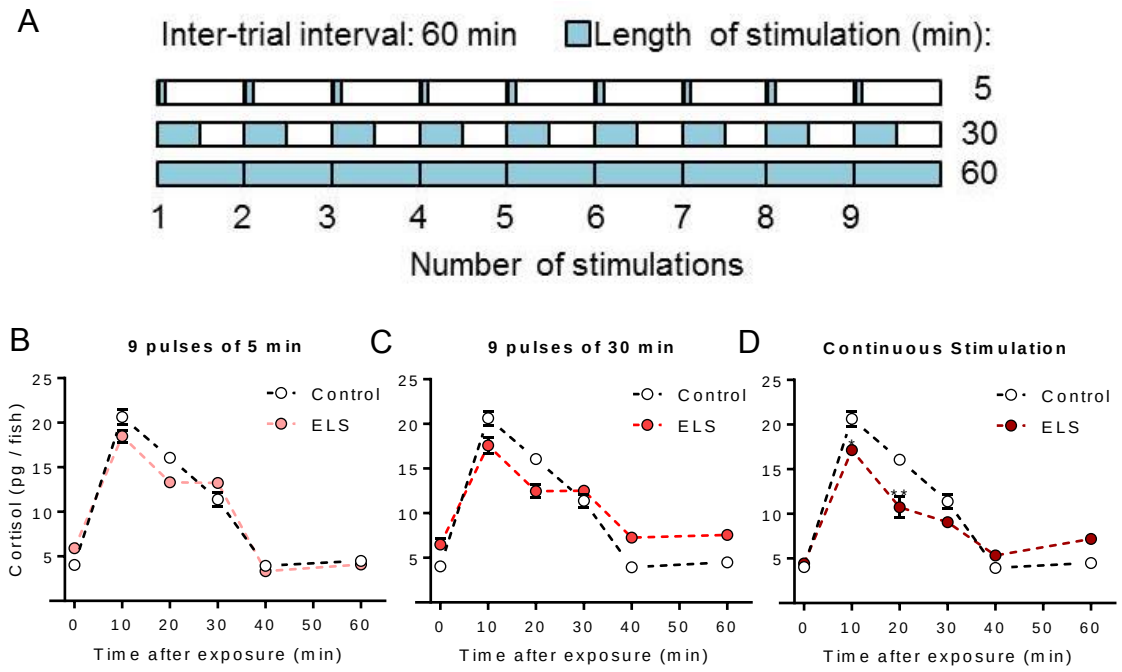

Figure 3.17. Exposure to prolonged vortex flow stimulation at 5 dpf induces changes in cortisol response profiles depending on the structure of the prolonged stimulation (frequency and duration of vortex flow pulses) A: Schematic representation of the different protocols of prolonged vortex flow stimulation used. **B-D:** Cortisol profiles as a function of time after acute stimulation onset in 6 dpf larvae pre-exposed to prolonged vortex flow stimulation (330 rpm) on day 5 consisting of 9 pulses of 5 or 30 minutes, or continuous stimulation, respectively. Note that a tendency for an attenuated cortisol response was observed in larvae pre-exposed to 9 pulses of 5 minutes or 30 minutes delivered at 5 dpf; however, only larvae pre-exposed to 9 continuous hours of vortex flow stimulation showed a significantly reduced cortisol response to an acute homotypic stimulation ($^{9pulses\ 5\ min}$Two-way ANOVA: time: $F_{(5,138)}$=103.1, p<0.0001; treatment: $F_{(1,138)}$=0.4370, p=0.5097; time x treatment: $F_{(5,138)}$=2.159, p=0.0621; Sidak's post-test: effect of treatment for each time point: non-significant; $^{9pulses\ 30\ min}$Two-way ANOVA: time: $F_{(5,138)}$=75.32, p<0.0001; treatment: $F_{(1,138)}$=1.029, p=0.3123; time x treatment: $F_{(5,138)}$=5.336, p=0.0002; Sidak's post-test: effect of treatment for each time point: non-significant; ^{Continuous}Two-way ANOVA: time: $F_{(5,138)}$=79.53, p<0.0001; treatment: $F_{(1,138)}$=4.012, p=0.0471; time x treatment: $F_{(5,138)}$=5.095, p=0.0003; Sidak's post-test: effect of treatment for each time point: *p<0.05, **p<0.01; N=6 for ELS treatments, $^{0min\ control}$N=20, $^{10min\ control}$N=36, $^{20min\ control}$N=13, $^{30min\ control}$N=16, $^{40min\ control}$N=17, $^{60min\ control}$N=12; ELS: early life stress).

The cortisol response profiles after acute stimulation showed that prolonged exposure to vortex flow stimulation induces changes in cortisol response (Figure 3.17B-D). Larvae exposed to the 5 or 30 minutes long pulses of vortex flow stimulation showed higher cortisol levels at basal conditions (t-test: ^{Control}Basal vs $^{9pulses\ 5min}$Basal, T=4.115, p=0.0004; ^{Control}Basal vs $^{9pulses\ 30min}$Basal, T=4.805, p<0.0001); interestingly, when the larvae were exposed to the continuous vortex flow stimulation, no effect on basal cortisol levels was observed (t-test: ^{Control}Basal vs ^{Continuous}Basal, T=0.9683, p=0.3426). The cortisol peak was reached 10 minutes after the onset of the acute vortex flow stimulation in all cases. Larvae previously exposed to the prolonged continuous vortex flow stimulation showed an attenuated cortisol peak (Figure 3.17D). Although a similar tendency was observed in larvae exposed to the prolonged vortex flow stimulation consisting of 5 or 30 minutes pulses, the difference was not significant; The attenuated cortisol response of larvae previously exposed to the continuous stimulation was still detectable at 20 minutes after the acute stimulation onset and was no longer detectable at 30 minutes after stimulation onset (Figure 3.17D).

Based on the changes in cortisol response seen at 6 dpf, the continuous and the 30 minutes-pulses prolonged stimulations were selected. These two strengths were used to evaluate whether the changes in cortisol response induced by prolonged exposure to vortex flow stimulation during day 5 were maintained through development. Larvae

were exposed to these two protocols of prolonged stimulation on day 5 and then raised for 5 more days. At 10 dpf, larvae were exposed to an acute 3 minutes-pulse of vortex flow stimulation and cortisol profiles were evaluated (Figure 3.18A-B). No differences were found in cortisol levels at basal conditions among the different treatments. Only the continuous prolonged stimulation induced long lasting changes in acute cortisol response profiles still detectable at 10 dpf. Similarly to the cortisol profile changes found in 6 dpf larvae previously exposed to prolonged vortex flow stimulation on day 5, treatment of continuous exposure to vortex flow stimulation on day 5 induced an attenuated cortisol response to acute vortex flow stimulation in 10 dpf larvae; the attenuated response was detected at 10 and 20 minutes after the onset of an acute vortex flow stimulation and no longer detected at 30 minutes after stimulation onset (Figure 3.18B). Cortisol response to a repeated homotypic stimulation of the same strength was also attenuated only in larvae pre-exposed to the continuous vortex flow stimulation on day 5 (Figure 3.18A)

Since prolonged exposure to a homotypic stressor may induce a habituation process, I asked whether the cortisol profile changes observed after prolonged exposure to vortex flow stimulation were stressor specific (which may suggest that a habituation process is occurring) or whether the changes in cortisol response can be observed regardless of the nature of the stressor. To evaluate this, larvae previously exposed to either 9 continuous hours or 30 minutes-pulses of vortex flow stimulation (330 rpm) on day 5 were challenged on the following day with an osmotic shock of low (50 mM NaCl) or high (250mM NaCl) strength and cortisol levels were measured (Figure 3.18C). Although a tendency of an attenuated cortisol response to the low strength osmotic shock was observed in the larvae exposed to the prolonged stimulation consisting of 30 minutes-pulses, only the continuous prolonged stimulation induced significant changes in cortisol response (Figure 3.18C). On the other hand, both prolonged stimulation protocols induced detectable changes in cortisol response to the high strength osmotic shock, indicating that altered cortisol response induced by prolonged vortex flow stimulation is also present when the larvae respond to a heterotypic stressor. For further experiments, the continuous vortex flow stimulation (9 hours, 330 rpm) was used.

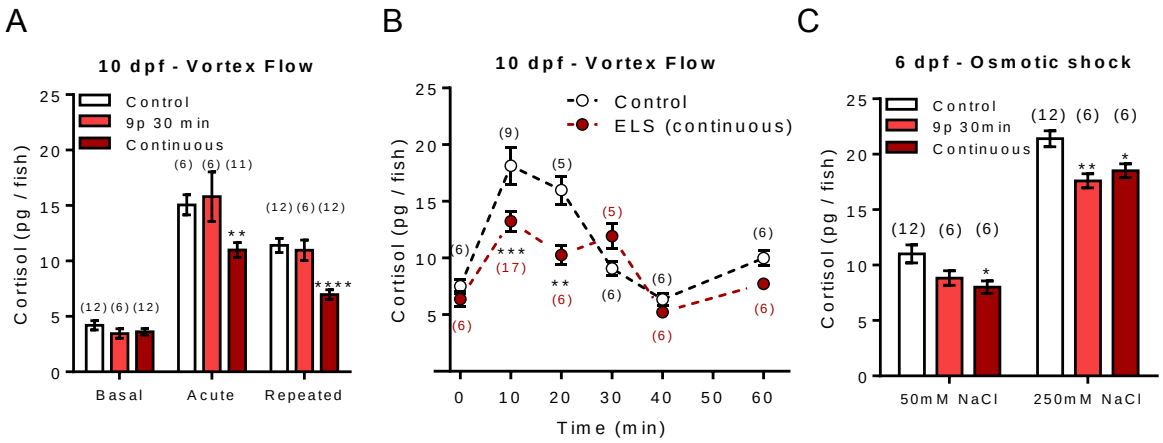

Figure 3.18. Changes in cortisol profiles induced by prolonged vortex flow stimulation are long lasting and non-stressor specific. A: Cortisol levels of 10 dpf under three different conditions: 1) basal conditions, 2) acute response to 3 minutes of vortex flow stimulation (330 rpm), and 3) repeated response to acute homotypic vortex flow stimulation (330 rpm) with 30 minutes of inter-trial interval; larvae were treated with either 9 pulses of 30 minutes or 9 hours of continuous vortex flow stimulation (330 rpm) on day 5. Continuous exposure to vortex flow stimulation at day 5 resulted in attenuation of cortisol response to acute and repeated stimulations. 9p 30 min: 9 pulses of 30 minutes; (Data generated jointly with Laura Flores) (t test: **p<0.01, ****p<0.0001 compared to control group; sample size indicated in parenthesis). **B:** Cortisol response profile as a function of time after acute (3 min) vortex flow stimulation onset in 10 dpf larvae previously exposed to 9 hours of continuous vortex flow stimulation on day 5. Attenuated cortisol levels can be detected at 10 and 20 minutes after stimulation onset. ELS: early life stress; (Data generated jointly with Laura Flores) (Two-way ANOVA: time: $F_{(5,72)}$=29.59, p<0.0001; treatment: $F_{(1,72)}$=10.27, p=0.0020; time x treatment: $F_{(5,72)}$=3.915, p=0.0034; Sidak's post-test for multiple comparison, **p<0.01,***p<0.001; sample size is indicated in parenthesis) **C:** Cortisol response to an osmotic shock using either 50 or 250 mM of NaCl in 6 dpf larvae previously exposed to prolonged vortex flow stimulation consisting of 9 pulses of 30 minutes or 9 hours of continuous stimulation during day 5. An attenuated cortisol response is observed after heterotypic acute stress exposure in larvae pre-exposed to prolonged vortex flow stimulation. 9p 30min: 9 pulses of 30 minutes; (t test: *p<0.05, **p<0.01 compared to control group; sample size is indicated in parenthesis).

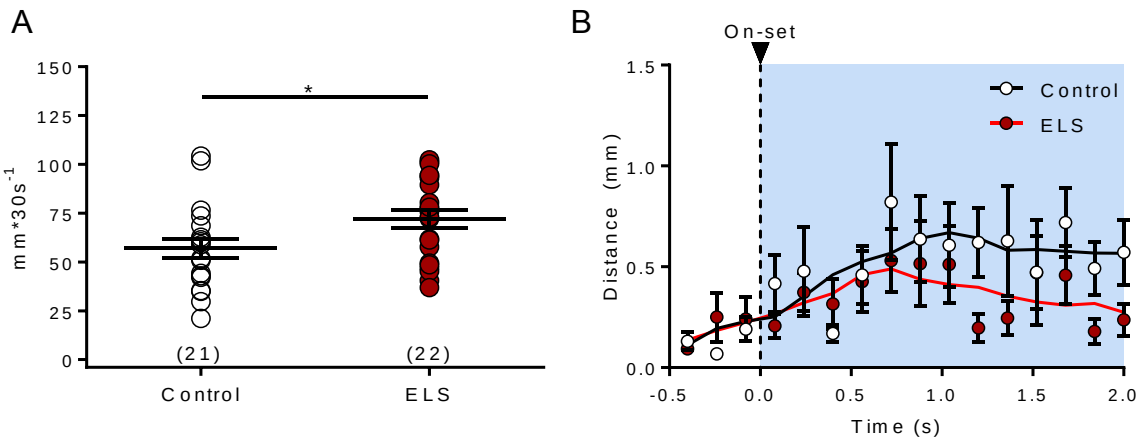

Figure 3.19. Prolonged vortex flow stimulation delivered at 5 dpf induces locomotor activity changes in 6 dpf larvae. A: Total distance swam at basal conditions is increased in 6 dpf previously exposed to prolonged vortex flow stimulation consisting of 9 continuous hours on day 5 (330 rpm) (t test: T = 2.240, p=0.0305, *p<0.05; sample sized indicated in parenthesis; ELS: early life stress). **B:** 6 dpf larvae pre-exposed to 9 hours of prolonged vortex flow stimulation on day 5 show a decreased locomotor activity as a response to an acute homotypic stimulation (Two-way ANOVA repeated measures: time: $F_{(15,150)}$=2.189, p=0.0089; treatment: $F_{(1,10)}$=6.622, p=0.0277; time x treatment: $F_{(15,150)}$=0.7557, p=0.7242; N=11 for both treatments; ELS: early life stress).

3.3.4 Prolonged exposure to vortex flow induces behavioral changes.

Prolonged vortex flow stimulation induced changes in cortisol response when applied in early developmental stages (Figure 3.16). To evaluate whether prolonged vortex flow stimulation alters behavioral outputs as well, larvae were exposed to continuous vortex flow stimulation on day 5 and locomotor activity and body orientation were measured on the following day either at basal conditions or as a response to an acute homotypic stimulation. Locomotor activity at basal conditions of 6 dpf larvae previously exposed to the prolonged vortex flow stimulation was enhanced (Figure 3.19A). Interestingly, when these larvae were exposed to an acute vortex flow stimulation (3 minutes, 330 rpm), they showed a reduced locomotor response at the stimulation onset (Figure 3.19B). Body angle orientation also changed after prolonged vortex flow stimulation. Larvae that were previously exposed to the prolonged vortex flow stimulation spent significantly more time than the untreated larvae re-orientating their body immediately after the onset of the stimulation (Figure 3.20A). Moreover, the frequency distribution of body angles during acute stimulation of a population of pre-treated larvae differed from that of a population of untreated larvae (Figure 3.20B); previously treated larvae showed a narrower range of body angle orientation than the untreated larvae, with a mean body angle of 62.3° and 42°, respectively (Figure 20B).

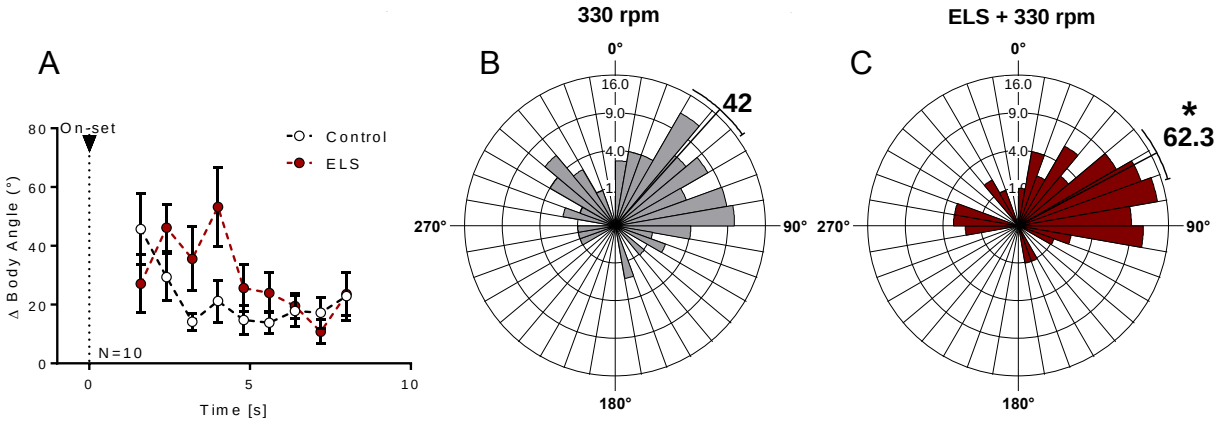

Figure 3.20. Prolonged vortex flow stimulation delivered at 5 dpf induces changes in body angle orientation in 6 dpf larvae. A: 6 dpf larvae pre-exposed to prolonged vortex flow on day 5 spend more time changing body angle orientation after acute vortex flow onset (Two-way ANOVA repeated measures: time: $F_{(8,72)}$=2.982, p=0.0122; treatment: $F_{(1,9)}$=6.507, p=0.0311; time x treatment: $F_{(8,72)}$=1.815, p=0.0882; N=10 for both treatments; ELS: early life stress). **B-C:** Circular representation of the frequency distribution of body angles showed by either un-treated larvae or larvae pre-exposed to prolonged vortex flow stimulation on day 5, respectively. Larvae were exposed to acute vortex flow stimulation (330 rpm) and body angles measures were taken 2 minutes after stimulation onset. Mean angle is represented with a line and the arcs extending to either side represent the 95% confidence limits. Note that pre-treated larvae with prolonged vortex flow stimulation show a narrower frequency distribution. Significant differences when compared to un-treated larvae are indicated by an asterisk (*) next to the mean angle (Watson-Williams F-test: Un-treated + 330 rpm vs ELS + 330 rpm: F = 6.127, p=0.014; N=90).

3.3.5 Prolonged vortex flow stimulation leads to decreased hypothalamic cell activity and stress-related peptide expression.

Exposure to prolonged vortex flow stimulation leads to altered behavioral performance and decreased endocrinological output (Figures 3.16-3.20). Since cortisol response depends on the activation of hypothalamic cells that culminate in secretion of stress-related peptides, I hypothesized that the decreased endocrinological output observed after prolonged exposure to vortex flow stimulation was mediated by a decreased activity of hypothalamic cells or to a decreased expression of stress-related peptides such as CRH, AVP, or OXT in hypothalamic cells. To evaluate this hypothesis, *in vivo* calcium activity of CRH-expressing neurons in the hypothalamus was measured. It was shown in section 3.3.3 that the cortisol response to a 250mM NaCl osmotic shock is decreased in larvae previously exposed to the prolonged vortex flow stimulation (Figure 3.18C). Since I am interested in robust changes in hypothalamic cells that lead to altered HPI axis activity, I selected osmotic shock as a robust stimulus to study the potential correlates of hypothalamic cell activity and reduced cortisol response after prolonged vortex flow stimulation. This stimulus was selected because habituation to a homotypic stressor may occur and lead to decreased cell activity, masking the robust effects in hypothalamic cells of the prolonged stimulation. Moreover, *in vivo* calcium imaging is facilitated by using a stressor that can be delivered while the larvae are fixed (Section 1.10, Figure 1.7). Based on this, calcium activity was recorded by Marcel Kegel before and after an osmotic shock (250mM NaCl) in 6 dpf larvae which were either untreated or previously exposed to prolonged vortex flow stimulation on day 5. Prolonged vortex flow stimulation led to reduced hypothalamic cell activity upon the

osmotic shock stimulation as measured by the area under the curve of the calcium events recorded (analyzed data was provided by Marcel Kegel) (Figure 3.21A). To test whether the expression of stress-related peptides was also affected by prolonged exposure to vortex flow stimulation, immunohistochemistry analysis was performed in 6 dpf larvae previously exposed to the prolonged stimulation protocol on day 5 and was compared with untreated larvae (imaging and immunohistochemistry analysis was performed by Dr. Ulrich Herget). The analysis revealed that the number of cells expressing CRH, AVP, and OXT was decreased after prolonged vortex flow stimulation when compared to control groups (Figure 3.21B-D).

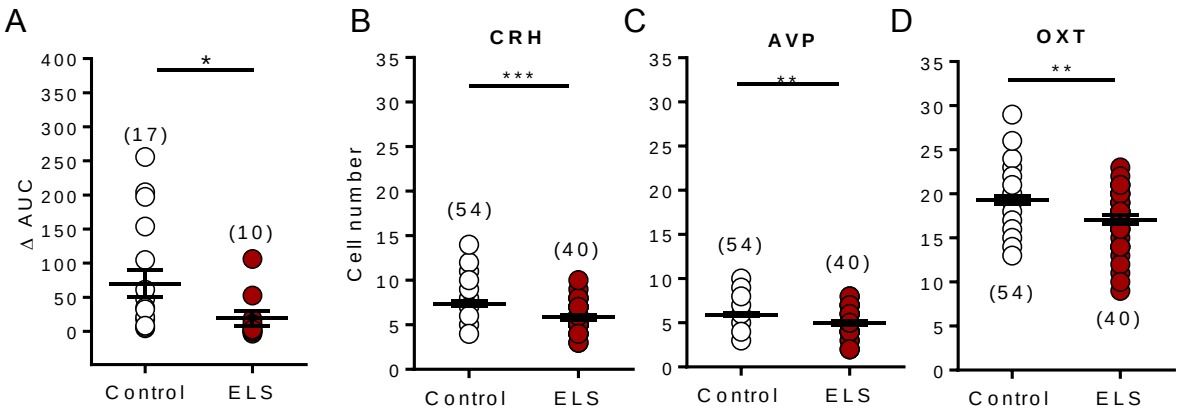

Figure 3.21. Prolonged vortex flow stimulation induces changes at the hypothalamic level. **A:** Calcium activity in hypothalamic cells of double transgenic *Tg(otpa3kb:GCaMP3.0)*^{hd22} x *Tg(crh:RFP)*^{hd21} larvae after acute osmotic shock (250 mM NaCl) is decreased in larvae pre-exposed to prolonged vortex flow stimulation (9h continuous stimulation, 330 rpm). The area under the curve (AUC) of the calcium events recorded from the calcium sensor GCaMP3.0 under a two-photon microscope after osmotic shock stimulation was calculated and compared between groups (data generated in collaboration with Marcel Kegel; Mann-Whithney test, U = 35, p=0.0109, *p<0.05; sample size is indicated in parenthesis; ELS: early life stress). **B-D:** Expression of stress related peptides (CRH, AVP, and OXT, respectively) is decreased in hypothalamic cells of larvae pre-exposed to prolonged vortex flow stimulation (data generated in collaboration with Dr. Ulrich Herget; Mann-Whithney test: ^{CRH}U = 606, p=0.0002; ^{AVP}U = 701.5, p=0.0027; t test ^{OXT}T = 3.217, p=0.0018; sample size is indicated in parenthesis; ELS: early life stress).

3.4 Transcriptomics of hypothalamic and non-hypothalamic cells after prolonged exposure to vortex flow stimulation.

3.4.1 Hypothalamic cell labeling and establishment of cell-dissociation protocol.

The zebrafish NPO is homologous to the mammalian PVN (Herget et al., 2014). It plays a key role as an integrative center of signals coming from upstream sensory centers in the brain and translates these signals into an endocrine response when needed. Therefore, understanding to what extent this region undergoes developmental programming after early life stress is of pivotal importance.

To study this in a tissue-specific manner, the transgenic zebrafish line *Tg(otpECR6-E1b:mmGFP)*^{hd12} was used (section 1.10, Figure 1.4). In this transgenic line, GFP is driven by a *cis*-regulatory NPO-specific enhancer element of the gene *otpa* (*otp*ECR6), labeling NPO cells involved in the stress response (Figure 1.4). GFP expression in these cells allows to isolate cell-specific populations using fluorescence activated cell sorting (FACS) for GFP+ and GFP- cells.

To accomplish this, four cell-dissociation protocols were compared to evaluate their efficiency in generating single cell suspensions and maintaining cell viability as high as possible (Table 1 and Figure 3.22). Two simple homogenization protocols were tested in wild type zebrafish larvae, either using a syringe and needle or a plastic pestle attached to an electric-motorized rotor. Each of these homogenization protocols was used with or without a commercially available cell-dissociation buffer solution (FACSmax), resulting in four different cell-dissociation protocols. Cell viability and single cell suspension of each of the dissociation protocols were assessed using flow cytometry. All cell-dissociation protocols generated single cell-suspensions; the highest percentage of single cell counts was found when the plastic pestle attached to the motorized rotor was used in the presence of the cell-dissociation buffer solution giving 90.3 % of single cell counts. This was followed closely with 88.5 % of single cell counts found when the larvae were homogenized using a syringe and a needle in the absence of the cell-dissociation buffer solution. The third best method regarding the generation of a single cell suspension was obtained with the syringe method in the presence of the cell-dissociation buffer solution, giving 80.1 % of single cell counts. Finally, when the motorized plastic pestle was used without the cell-dissociation buffer solution, a considerably lower single cell count of 62.4 % was found.

Table 1. Analysis of cell dissociation protocols

	Single cells (%)	Alive (%)
Syringe + FACSmax	80.1	96.2
Pestle + FACSmax	90.3	89.4
Syringe only	88.5	89.5
Pestle only	62.4	85

High levels of cell viability were found for all cell-dissociation protocols. The highest cell viability value was found when the syringe method was used in the presence of the cell-dissociation buffer solution; when this method was used, 96% of the cells were identified as viable as indicated by propidium iodide (PI) staining. This was followed by the motorized-pestle method with cell-dissociation buffer and the syringe method without cell-dissociation buffer, both showing 89 % of viable cells. Finally, the motorized-pestle method without the cell-dissociation buffer showed 85 % of viable cells. Based on these results, the syringe homogenization method in the presence of cell-dissociation buffer was selected as cell-dissociation protocol for subsequent experiments.

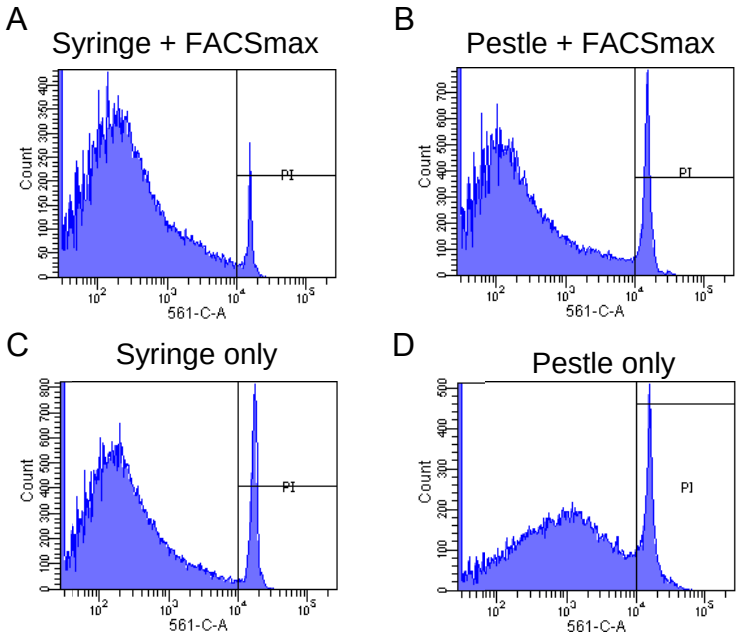

Figure 3.22. Comparison of cell dissociation protocols. A-D: four cell dissociation protocols were evaluated by measuring the total number of single cells generated and the cell viability using flow cytometry; cell dissociation using a syringe in the presence of dissociation buffer showed the higher cell viability rate as measured by PI staining.

3.4.2 Fluorescence activated cell sorting (FACS) of hypothalamic cells.

Once the cell-dissociation protocol was selected, GFP-labeled cells from *Tg(otpERC6-E1b:mmGFP)* larvae were sorted. Groups of 500 transgenic larvae were pooled and the cell dissociation protocol described above was performed. Approximately 60,000 GFP+ cells were sorted using FACS for every 500 larvae used. Figure 3.23 shows the gates used for cell sorting. The identity of the cells sorted as GFP+ after FACS was confirmed by two methods: 1) fluorescence microscopy and 2) real time qPCR to quantify the expression level of *oxt*, whose expression is strictly restricted to the hypothalamus. After cell-count of GFP+ cells under the fluorescent microscope, 92.5 % of the sorted cells were confirmed as GFP+ (Figure 3.24A-B). This was further evaluated by real time qPCR, where the analysis showed a significant enrichment of *oxt* relative gene expression in cells sorted as GFP+ when compared to the cells sorted as GFP-; o*xt* expression in GFP- cells was nearly absent (Figure 24C).

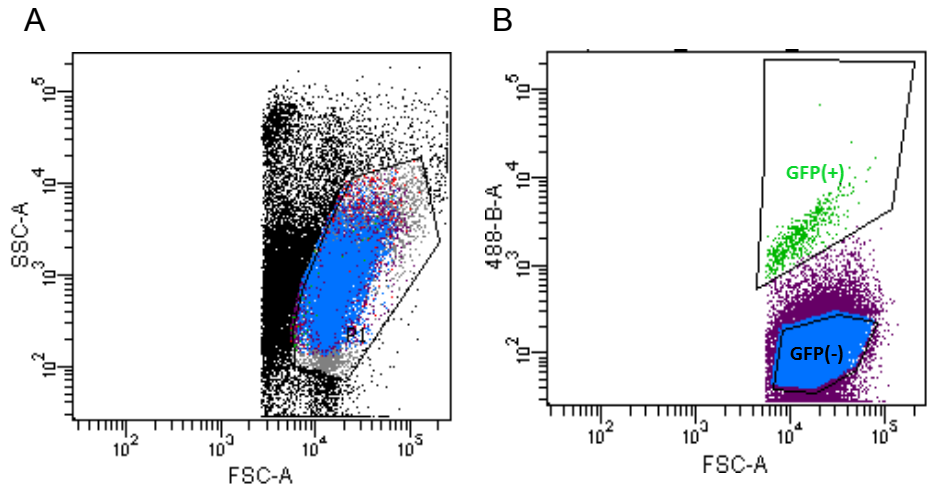

Figure 3.23. Settings used to isolate GFP+ and GFP- cells by fluorescence activated cell sorting (FACS). A: Cells were sorted depending on the cell size (forward scatter, FSC-A) and granularity (side scatter, SSC-A); gates were set to avoid cell debris and clumps of cells. **B:** Cells were sorted depending on their fluorescence and divided in GFP+ and GFP- cell populations; gates were set as to minimize cross contamination.

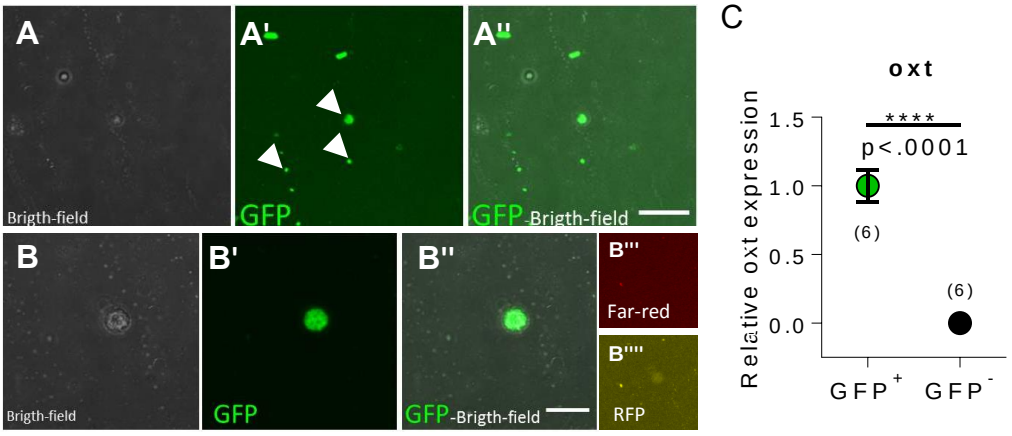

Figure 3.24. Validation of cell identity of isolated cells from transgenic line *Tg(otpERC6-E1b:mmGFP)*. A-A": single cells identified as GFP+ by fluorescence activated cell sorting (FACS) from transgenic larvae *Tg(otpERC6-E1b:mmGFP)* expressing GFP (92.5% of cells were GFP+) (scale bar: 30 µm). **B-B"":** magnified view of a single cell identified as GFP+ by FACS expressing GFP (scale bar: 10 µm). Fluorescent signal was detected only for green fluorescent protein (GFP). **C:** Relative expression of *oxt* was measured by qPCR in isolated cells identified as GFP+ and GFP-. Relative expression of *oxt* in cells identified as GFP- was nearly absent (t test: T = 8.582, p<0.0001, ****p<0.0001; sample size is indicated in parenthesis).

3.4.3 RNA isolation and cDNA library preparation from hypothalamic and non-hypothalamic cells after prolonged exposure to vortex flow stimulation.

Prolonged vortex flow stimulation during early life stages of zebrafish larvae induces changes at the behavioral, endocrinological, and cellular level. In order to identify the molecular correlates of early life exposure to vortex flow stimulation, I performed a transcriptomic analysis of hypothalamic and non-hypothalamic cells sorted from 6 dpf transgenic larvae *Tg(otpERC6-E1b:mmGFP)*, which were either unstimulated controls or exposed to 9 hours of continuous vortex flow stimulation during day 5. After sorting hypothalamic and non-hypothalamic cells using the protocol described in section 3.4.2, total RNA was isolated using a commercially available kit (Qiagen). Each treatment group was performed in triplicate (Table 2). Integrity of the isolated total RNA was evaluated by David Ibberson using a Bioanlayzer (Agilent 2100; Germany) (Figure 3.25). Concentration of total RNA is reported in table 3.

Table 2. Experimental groups and their corresponding sample identification.

Groups	Treatment	Samples No.
1	GFP(+) cells Control	1, 2, 9
2	GFP (-) cells Control	3, 4, 10
3	GFP (+) cells Prolonged vortex flow stimulation	5, 6, 11
4	GFP (-) cells Prolonged vortex flow stimulation	7, 8, 12

Table 3. Total RNA yield.

Sample	Total RNA (pg)	Sample	Total RNA (pg)
1	370	7	210
2	320	8	170
3	1760	9	625
4	1380	10	900
5	110	11	350
6	130	12	1875

Isolated total RNA was then used as template for cDNA library preparation; this was performed as described in section 7.2.10 in collaboration with Enric Llorens-Bobadilla, at the laboratory of Dr. Ana Martin-Villalba, Molecular Neurobiology Department of the German Cancer Research Center, Heidelberg, Germany. Figure 3.26 shows the quality control for each of the samples performed with a Bioanalyzer (Agilent, Germany).

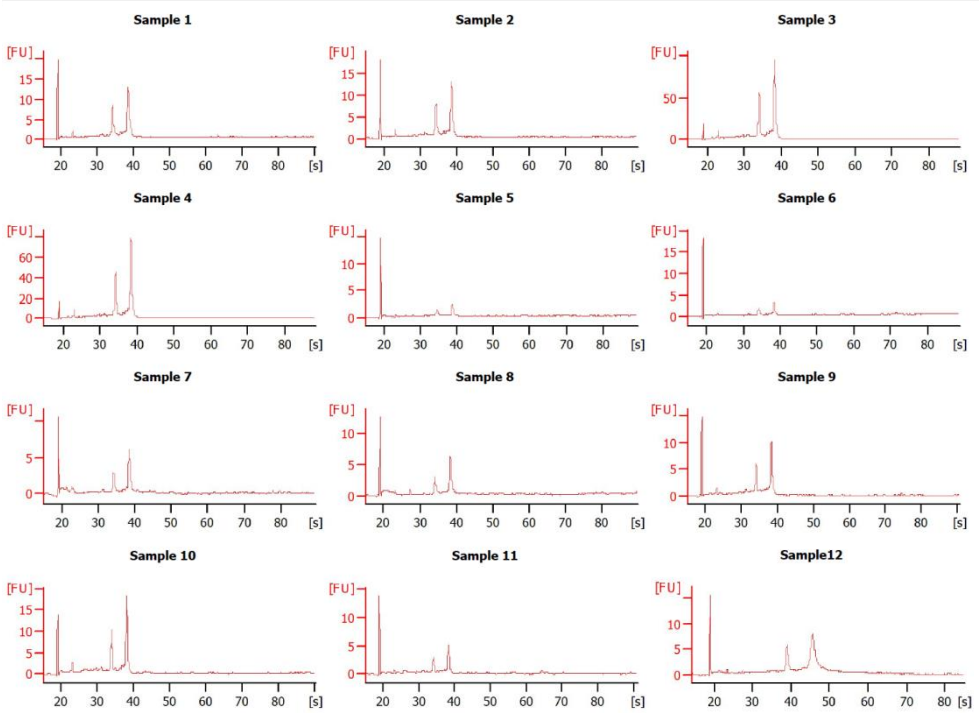

Figure 3.25. Quality control of the isolated total RNA from hypothalamic and non-hypothalamic cells. All samples of isolated RNA showed good integrity.

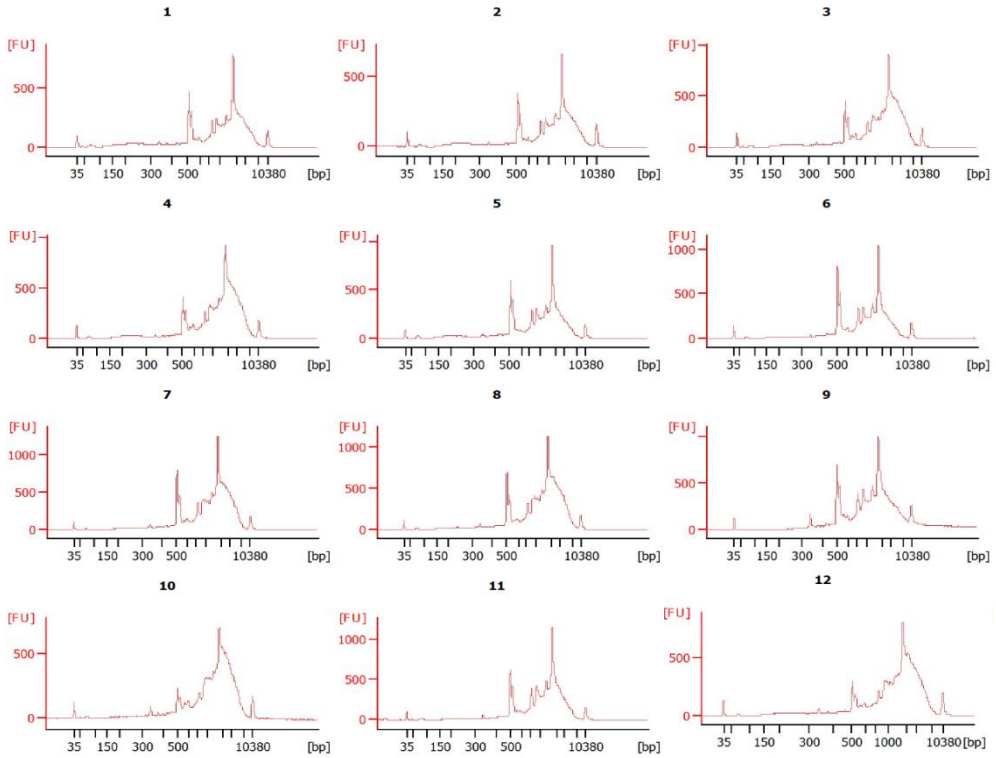

Figure 3.26. Quality control of cDNA generated from the total RNA isolated from hypothalamic and non-hypothalamic cells. All samples showed good integrity.

3.4.4 Transcriptome analysis of hypothalamic and non-hypothalamic cells after prolonged vortex flow stimulation.

Transcriptomic analysis using RNA-seq technology was performed in order to identify genes that are affected by early life exposure to prolonged vortex flow stimulation at a global and hypothalamus-specific level. High-throughput sequencing of the cDNA libraries generated for all treatment groups was performed by GATC Biotech (Konstanz, Germany). The generated raw reads ranged from 5.5 to 11.8 million pairs. More than 98% of raw reads for each sample were identified as clean reads after quality filtering (Table 4). The RNA-seq reads were aligned to the zebrafish genome using Bowtie and TopHat, showing a percentage of mapped reads ranging from 88.5 to 92.9% (Table 5). Cufflinks and Cuffmerge were used to identify, quantify, and annotate the transcripts from the RNA-seq alignment assembly. Finally, Cuffdiff was used to compare samples and evaluate the differential expression levels at the transcript and gene level. A total of 22,917 expressed genes were identified, from which 16,249 were known annotated genes. In this study, only known genes were considered for further analysis.

Table 4. Total amount of raw sequence data and quality control filtering of RNA-seq data.

Sample No.	Total Reads	Discarded Reads	Clean Reads (single)*	Clean Reads
1	9,700,846	1, 806 (0.0%)	156,524 (1.6%)	9,542,516 (98.4%)
2	11,709,050	1,678 (0.0%)	190,290 (1.6%)	11,517,082 (98.4%)
3	9,514,222	1,268 (0.0%)	120,420 (1.3%)	9,392,534 (98.7%)
4	7,928,094	702 (0.0%)	76,122 (1.0%)	7,851,270 (99.0%)
5	7,492,846	1,182 (0.0%)	100,188 (1.3%)	7,391,476 (98.6%)
6	5,489,102	1,200 (0.0%)	84,396 (1.5%)	5,403,506 (98.4%)
7	8,305,792	1,414 (0.0%)	93,840 (1.1%)	8,210,538 (98.9%)
8	8,994,456	1,102 (0.0%)	86,376 (1.0%)	8,906,978 (99.0%)
9	10,476,820	1,354 (0.0%)	95,262 (0.9%)	10,380,204 (99.1%)
10	11,756,554	1,128 (0.0%)	102,004 (0.9%)	11,653,422 (99.1%)
11	6,040,168	826 (0.0%)	57,338 (0.9%)	5,982,004 (99.0%)
12	8,714,652	1,208 (0.0%)	103,834 (1.2%)	8,609,610 (98.8%)

*Clean reads (single) are reads without mates and were not included in further analysis.

Table 5. Percentage reads mapped to the zebrafish genome (GRCz10) per sample.

Sample No.	Quality Control Passed Reads	Mapped Reads	% Mapped
1	9,542,516	8,651,254	90.66
2	11,517,082	10,454,060	90.77
3	9,392,534	8,394,164	89.37
4	7,851,270	7,292,452	92.88
5	7,391,476	6,773,551	91.64
6	5,403,506	4,943,405	91.49
7	8,210,538	7,409,487	90.24
8	8,906,978	7,880,694	88.48
9	10,380,204	9,669,547	93.15
10	11,653,422	10,787,378	92.57
11	5,982,004	5,544,448	92.69
12	8,609,610	7,889,058	91.63

Genes were considered as differentially expressed according to Cuffdiff parameters (Trapnell et al., 2013). After prolonged exposure to vortex flow stimulation, 1170 and 935 genes were identified as differentially expressed in hypothalamic and non-hypothalamic cells, respectively. From the 1170 genes expressed differentially in hypothalamic cells, 301 were also found to be differentially expressed in non-hypothalamic cells, leaving 869 genes whose differential expression was detected only in hypothalamic cells. In the same way, 634 genes were detected to be differentially expressed only in non-hypothalamic cells (Figure 3.27A).

From the 1170 genes differentially regulated in hypothalamic cells after prolonged vortex flow stimulation, 503 genes were upregulated and 667 downregulated. In the case of the 935 genes detected in non-hypothalamic cells as differentially expressed, 231 genes were upregulated and 705 downregulated (Figure 3.27B). Interestingly, from the 301 genes which were identified as differentially expressed in both hypothalamic and non-hypothalamic cells, there were some genes which showed opposite expression pattern depending on the cell type. From these genes, 12 were identified as downregulated in hypothalamic cells after prolonged vortex flow stimulation, but upregulated in non-hypothalamic cells. On the other hand, other 4 genes were identified as upregulated in hypothalamic cells after treatment, but downregulated in non-hypothalamic cells (Table 6).

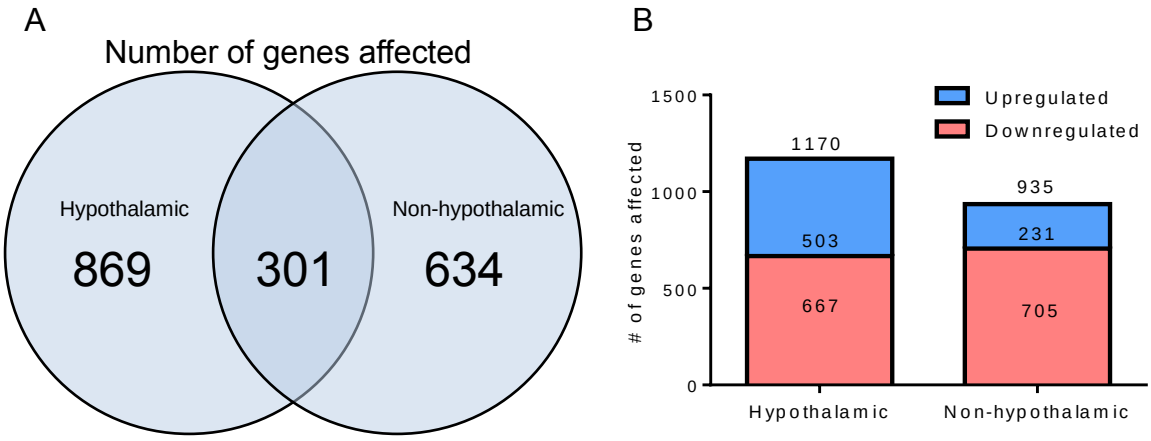

Figure 3.27. Number of genes differentially regulated in hypothalamic and non-hypothalamic cells after prolonged exposure to vortex flow stimulation. A: Venn diagram showing the number of genes affected after prolonged exposure to vortex flow stimulation in either hypothalamic cells or non-hypothalamic cells, or shared by both. **B:** Number of genes identified as up- or downregulated in hypothalamic and non-hypothalamic cells after prolonged exposure to vortex flow stimulation.

Table 6. Genes identified as regulated in opposite direction after prolonged exposure to vortex flow stimulation in hypothalamic cells when compared to non-hypothalamic cells.

Genes downregulated in hypothalamic cells and upregulated in non-hypothalamic cells			
Gene symbol	Gene name	Fold change	P-value
agxtb	Alanine-glyoxylate aminotransferase b	0.450	2.6E-02
ggt1b	Gamma-glutamyltransferase 1b	0.221	1.4E-03
grin1b	Glutamate receptor, ionotropic, N-methyl D-aspartate 1b	0.388	1.4E-03
mfsd4b	Major facilitator superfamily domain containing 4b	0.133	1.2E-02
mir124-2	microRNA 124-2	0.489	2.6E-02
mir182	microRNA 182	0.244	2.9E-02
si:ch211-139a5.9	Uncharacterized protein – FXYD family (ATP1G1/PLM/MAT8 domain)	0.308	1.4E-03
slc22a2	Solute carrier family 22 (organic cation transporter), member 2	0.315	1.4E-03
slc22a6l	Solute carrier family 22 (organic anion transporter), member 6, like	0.197	1.4E-03
slc22a7b.1	Solute carrier family 22 (organic anion transporter), member 7b, tandem duplicate 1	0.300	1.9E-02
slc5a8l	Solute carrier family 5 (iodide transporter), member 8, like	0.122	2.6E-03
tmem27	Transmembrane protein 27	0.236	1.4E-03
Genes upregulated in hypothalamic cells and downregulated in non-hypothalamic cells			
Gene symbol	Gene name	Fold change	P-value
caspb	Caspase b	2.41	4.6E-03
myl10	Myosin, light chain 10, regulatory	1.69	3.4E-02
myl13	Myosin light chain 13	1.98	4.6E-03
tnnt2e	Troponin T2e, cardiac	1.94	2.9E-02

Moreover, top up and downregulated genes in hypothalamic and non-hypothalamic cells after exposure to prolonged vortex flow stimulation were identified and are shown in tables 7 and 8, respectively.

3.4.5 Validation of RNA-seq data by real time qPCR.

To validate the gene expression profiles obtained by RNA-seq, real time qPCR was performed as an alternative method to measure relative gene expression. Two comparisons were made: 1) Control non-hypothalamic cells vs control hypothalamic cells (to assess *oxt* enrichment), and 2) control non-hypothalamic cells vs non-hypothalamic cells from larvae exposed to prolonged vortex flow stimulation (to assess treatment effects). The expression of *oxt* and selected genes identified by RNA-seq data among the top up and downregulated genes after prolonged vortex flow exposure was confirmed by real time qPCR. Expression profiles of all genes evaluated by real time qPCR were in agreement with RNA-seq data, showing a high degree of correlation (Table 9 and Figure 3.28).

Table 7. Top 15 genes identified as up and downregulated in hypothalamic cells after prolonged exposure to vortex flow stimulation.

Hypothalamic cells

Upregulated			Downregulated		
Gene	Fold change	P-value	Gene	Fold change	P-value
si:dkey-30j10.5	20.47	1.5E-03	*stc1l	0.002	3.7E-03
tnfa	8.51	1.5E-03	tcnl	0.053	1.5E-03
si:dkey-29h14.10	7.86	2.1E-02	slc26a6	0.085	3.5E-02
csf3a	7.20	1.5E-03	bx908782.1	0.090	1.5E-03
si:dkey-202i12.5	6.90	1.5E-03	*myhz2	0.096	1.5E-03
il4i1	6.49	1.5E-03	cnfn	0.100	3.7E-03
alpk1	6.02	1.2E-02	trpm1a	0.102	1.5E-03
itpripl2	5.87	3.7E-03	si:ch211-229d2.5	0.113	1.5E-03
il1b	5.78	1.5E-03	cyp4v8	0.114	9.5E-03
timp2b	5.73	1.5E-03	slc22a4	0.115	1.5E-03
slc2a3b	5.27	2.2E-02	lye	0.120	1.5E-03
tmtc4	5.12	3.7E-03	*mep1a.2	0.121	1.5E-03
tnfrsf18	5.08	1.5E-03	slc5a8l	0.122	2.7E-03
hapln2	5.04	2.1E-02	col10a1a	0.126	1.5E-03
ccl35.2	5.04	2.7E-03	slc23a1	0.129	5.4E-03

* Affected also in non-hypothalamic cells

Table 8. Top 15 genes identified as up and downregulated in non-hypothalamic cells after prolonged exposure to vortex flow stimulation.

Non-hypothalamic cells

Upregulated			Downregulated		
Gene	Fold change	P-value	Gene	Fold change	P-value
mfsd4b	6.48	2.2E-03	*stc1l	0.037	2.2E-03
si:dkey-90l23.1	6.03	2.2E-03	*mep1a.2	0.037	2.8E-02
rsad2	6.02	5.4E-03	Mogat2	0.116	3.4E-02
gpr84	5.26	3.9E-03	*myhz2	0.116	2.2E-03
slc13a1	5.19	2.2E-03	enpp7.1	0.120	2.2E-03
traf1	4.39	5.4E-03	fut9d	0.131	1.8E-02
si:ch211-13o20.3	4.09	1.1E-02	ch25hl1.1	0.134	2.5E-02
timd4	4.07	2.2E-03	si:dkey-22i16.7	0.136	2.2E-03
thbs3b	4.05	2.4E-02	myhz1.2	0.139	1.3E-02
slc2a6	4.00	2.2E-03	slc6a19a.2	0.141	2.2E-03
arg1	3.82	1.9E-02	cyp2y3	0.142	2.2E-03
slc6a18	3.80	2.2E-03	slc26a3.2	0.150	2.2E-03
epg5	3.80	4.2E-02	fabp6	0.151	2.2E-03
slc22a6l	3.71	2.2E-03	cd36	0.157	2.2E-03
mdp1	3.69	3.9E-03	asah2	0.159	2.2E-03

* Affected also in hypothalamic cells

Table 9. Validation of RNA-seq data by real time qPCR

Comparisons between RNA-seq and qPCR results

Comparison	Gene symbol	Log(Fold change)	
		RNA seq	qPCR
Control non-hypothalamic cells vs Control hypothalamic cells	oxt	↓ -10.36	↓ -10.68
Control non-hypothalamic cells vs Early Stress non-hypothalamic cells	mfsd4b	↑ 2.70	↑ 4.07
	rsad2	↑ 2.59	↑ 1.96
	stc1l	↓ -4.76	↓ 0.20
	mep1a.2	↓ -4.74	↓ -1.17
	nr3c1	-0.02	0.25

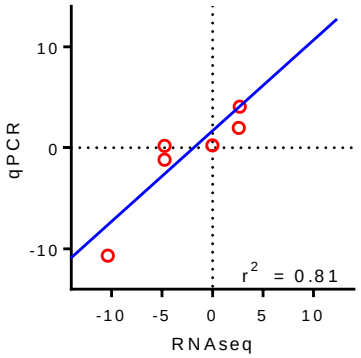

Figure 3.28. RNA-seq data and qPCR results are in agreement. Expression of *oxt* in control hypothalamic and non-hypothalamic cells and other 5 genes included in the top differentially expressed genes in non-hypothalamic cells after prolonged exposure to vortex flow stimulation (table 9) was analyzed by qPCR. The results were correspondingly compared to the RNA-seq data. Correlation analysis shows a high degree of agreement (Pearson analysis, p=0.0138).

3.4.6 Gene ontology enrichment analysis of hypothalamic and non-hypothalamic cells after prolonged exposure to vortex flow stimulation.

Gene ontology enrichment analysis was performed to elucidate overrepresented signaling and metabolic canonical pathways after molecular changes induced by prolonged exposure to vortex flow stimulation. To evaluate this, the Ingenuity Pathway Analysis (IPA) software, based on the Ingenuity Knowledge Base (Qiagen), was used. Differential expression data obtained from Cuffdiff was used as input data and an IPA's core analysis was generated for each of the two data sets: hypothalamic and non-hypothalamic cells.

Tables 10 and 11 show the top 15 overrepresented canonical pathways which are enriched (either up or downregulated) after prolonged exposure to vortex flow stimulation in hypothalamic and non-hypothalamic cells, respectively. Among the top-ranked pathway categories that are enriched in hypothalamic cells are lipid metabolism, cellular immune response, neurotransmitters and nervous system signaling, cardiovascular signaling, intracellular and second messenger signaling, and cellular stress and injury. In non-hypothalamic cells, the canonical pathway of eukaryotic initiation factor 2 signaling was ranked as the most significant enriched pathway; it was followed by the pathways categories of cellular growth, proliferation and development, neurotransmitters and nervous system signaling, lipid metabolism and nuclear receptor signaling, cardiovascular signaling, disease-specific pathways (Mitochondrial dysfunction and Maturity onset diabetes young signaling, MODY), glycolysis, electron transfer, and gluconeogenesis.

To evaluate the activation state after the treatment (activated or inhibited), IPA software calculates the z-score. This is calculated based on the expression pattern of the genes in the data set that are involved in a particular pathway and the one reported in the Ingenuity Knowledge Base. Pathways with positive z-scores are considered as activated. However, only pathways with z-scores ≥ 2 are considered as statistically significant. On the other hand, pathways with negative z-scores are considered as inhibited and only z-scores ≤ -2 are considered statistically significant. In hypothalamic cells, there is predicted activation of the canonical pathways identified as "Leukocyte Extravasation Signaling", "Production of Nitric Oxide and Reactive Oxygen Species in Macrophages", "Fcγ Receptor-mediated Phagocytosis in Macrophages and Monocytes", "Tec Kinase Signaling", and "Regulation of Actin-based Motility by Rho". In the case

of non-hypothalamic cells, the canonical pathway identified as “eif2 signaling” was predicted to be inhibited while the pathway identified as “RhoGDI signaling” was predicted to be activated.

3.4.7 Upstream regulator analysis

The IPA software was used to identify candidate molecules which may be involved upstream of the molecular changes found in hypothalamic and non-hypothalamic cells after prolonged vortex flow stimulation. Tables 12 and 13 summarize the top 20 upstream regulators which were predicted to be involved in hypothalamic and non-hypothalamic cells, respectively. Common molecules in the top 20 predicted upstream regulators in both hypothalamic and non-hypothalamic cells after stimulation include: tumor necrosis factor (TNF), transforming growth factor beta 1 (TGFB1), peroxisome proliferator-activated receptor alpha (PPARA), interleukin 1 beta (IL1B), nuclear receptor subfamily 1 group H member 4 (NR1H4), insulin, peroxisome proliferator-activated receptor gamma (PPARG), amyloid beta precursor protein (APP), leptin (LEP), and preproinsulin (Ins1). Predicted upstream regulators found in the top 20 regulators only in hypothalamic cells include: Interferon gamma (IFGN), glucocorticoid receptor (NR3C1), interleukin 4 (IL4), CREB binding protein (CREBBP), estrogen receptor 2 (ESR2), Nuclear factor κ–β (NFκβ), Colony stimulating factor 1 (CSF2), CCAAT/enhancer binding protein alpha (CEBPA), low density lipoprotein (LDL), and CD40 ligand (CD40LG). Predicted upstream regulators found only in the top 20 regulators of non-hypothalamic cells include: Myelocytomatosis oncogene (MYC), Tumor protein p53 (TP53), hepatocyte nuclear factor 4 alpha (HNF4α), RNA polymerase II, epidermal growth factor (EGF), microtubule associated protein Tau (MAPT), huntingtin (HTT), Harvey rat sarcoma viral oncogene homolog (HRAS), pancreatic and duodenal homebox 1 (PDX1), and presenilin 1 (PSEN1). Interestingly, the predicted upstream regulators TGB1 and insulin show an opposite direction of regulation in hypothalamic cells and non-hypothalamic cells; TGB1 was predicted to be activated after prolonged vortex flows stimulation in hypothalamic cells (z-score: 2.827), while in non-hypothalamic cells a tendency to be inhibited was found (z-score: -0.541). In the case of insulin, it was predicted to be activated after prolonged vortex flow treatment in hypothalamic cells (z-score: 2.070), while in non-hypothalamic cells there was a tendency to be inhibited (z-score: -0.305).

Table 10. Top 15 canonical pathways enriched in hypothalamic cells after exposure to prolonged vortex flow stimulation.

Hypothalamic cells

Ingenuity Canonical Pathway	Pathway Category	-log(p-value)	Ratio	z-score
FXR/RXR Activation	Lipid metabolism, Nuclear receptor signaling	12.69	28/126	NA
Leukocyte Extravasation Signaling	Cellular immune response	11.13	33/198	2.294
Phototransduction Pathway	Neurotransmitters and other nervous system signaling	10.69	17/53	NA
Production of Nitric Oxide and Reactive Oxygen Species in Macrophages	Cellular immune response	10.17	30/180	2.502
Axonal Guidance Signaling	Neurotransmitters and other nervous system signaling	8.75	47/434	NA
Atherosclerosis Signaling	Cardiovascular signaling	8.15	22/124	NA
Ephrin Receptor Signaling	Neurotransmitters and other nervous system signaling, Organismal growth and development	7.87	26/174	1.964
Protein Kinase A Signaling	Intracellular and second messenger signaling	7.47	41/386	0.354
Fcγ Receptor-mediated Phagocytosis in Macrophages and Monocytes	Cellular immune response	7.39	18/93	2.357
Type II Diabetes Mellitus Signaling	Cellular stress and injury	7.25	20/116	1.387
Signaling by Rho Family GTPases	Intracellular and second messenger signaling	6.86	29/234	1.460
Tec Kinase Signaling	Intracellular and second messenger signaling	6.27	22/157	2.840
Relaxin Signaling	Growth factor signaling, Organismal growth and development	6.15	20/135	0.333
Regulation of Actin-based Motility by Rho	Neurotransmitters and other nervous system signaling	6.05	16/91	2.324
Thrombin Signaling	Cardiovascular signaling	5.94	24/190	0.943

Table 11. Top 15 canonical pathways enriched in non-hypothalamic cells after exposure to prolonged vortex flow stimulation.

Non-hypothalamic cells

Ingenuity Canonical Pathway	Pathway Category	-log(p-value)	Ratio	z-score
EIF2 Signaling	Cellular growth, proliferation and development, cellular stress and injury, intracellular and second messenger signaling.	34.12	54/184	-4.914
Regulation of eIF4 and p70S6k Signaling	Cellular growth, proliferation and development, cellular stress and injury, intracellular and second messenger signaling.	12.11	26/146	NA
Phototransduction Pathway	Neurotransmitters and other nervous system signaling	11.37	16/53	NA
mTOR Signaling	Cellular growth, proliferation and development	11.08	28/187	0.378
FXR/RXR Activation	Lipid metabolism, nuclear receptor signaling	9.34	21/126	NA
Atherosclerosis Signaling	Cardiovascular signaling	7.14	18/124	NA
Mitochondrial Dysfunction	Disease-specific pathway	6.93	21/171	NA
Glycolysis I	Glycolysis	6.19	8/25	NA
Oxidative Phosphorylation	Electron transfer	5.75	15/109	NA
Maturity Onset Diabetes of Young (MODY) Signaling	Disease-specific pathway	5.61	7/21	NA
Gluconeogenesis I	Gluconeogenesis	5.04	7/25	NA
Tight Junction Signaling	Apoptosis, Cell cycle regulation	4.63	17/167	NA
Axonal Guidance Signaling	Neurotransmitters and other nervous system signaling	4.62	31/434	NA
LXR/RXR Activation	Nuclear receptor signaling	4.53	14/121	-1.941
RhoGDI Signaling	Intracellular and second messenger signaling.	4.43	17/173	2.111

Table 12. Molecules predicted as upstream regulators of the molecular changes found in hypothalamic cells after prolonged exposure to vortex flow stimulation.

Hypothalamic cells					
Upstream regulator	Name	Molecule type	P-value of overlap	Predicted activation state	z-score
TNF	Tumor necrosis factor	cytokine	6.76E-22	Activated	5.703
IFNG	Interferon gamma	cytokine	5.22E-21	Activated	6.148
TGFB1	Transforming growth factor beta 1	growth factor	6.46E-21	Activated	2.827
PPARA	Peroxisome proliferator-activated receptor alpha	ligand-dependent nuclear receptor	4.04E-17		-0.400
IL1B	Interleukin 1 beta	cytokine	4.23E-16	Activated	3.545
NR3C1	Nuclear receptor subfamily 3 group C member 1	ligand-dependent nuclear receptor	1.10E-12		-1.005
IL4	Interleukin 4	cytokine	3.71E-12		1.677
CREBBP	CREB binding protein	transcription regulator	2.33E-11		0.149
NR1H4	Nuclear receptor subfamily 1 group H member 4	ligand-dependent nuclear receptor	3.37E-11		-0.697
ESR2	Estrogen receptor 2	ligand-dependent nuclear receptor	5.01E-11		-1.396
Insulin	Insulin	group	5.03E-11	Activated	2.070
NFkB (complex)	Nuclear factor κ–β	complex	7.45E-11	Activated	2.837
PPARG	Peroxisome proliferator-activated receptor gamma	ligand-dependent nuclear receptor	1.41E-10	Inhibited	-2.254
CSF2	Colony stimulating factor 1	cytokine	2.30E-10	Activated	3.344
APP	Amyloid beta precursor protein	other	3.30E-10	Activated	2.719
LEP	Leptin	growth factor	3.35E-10		1.679
CEBPA	CCAAT/enhancer binding protein alpha	transcription regulator	3.36E-10		-0.059
Ins1	Insulin I; preproinsulin	other	3.88E-10		0.107
LDL	Low density lipoprotein	complex	4.38E-10		0.456
CD40LG	CD40 ligand	cytokine	7.89E-10	Activated	3.322

3.4.8 Disease and function analysis

Based on the differential expression analysis from the RNA-seq data set obtained after prolonged vortex flow stimulation for hypothalamic and non-hypothalamic cells, the IPA software was used to evaluate the enriched canonical pathways and to predict candidate upstream regulators (section 3.4.5 and 3.4.6). Moreover, I used the IPA software to predict relevant biological functions and diseases which may be activated or inhibited based on the gene expression changes observed in the experimental data set. Tables 14 to 17 show the top diseases or function annotations that are predicted to be decreased or increased in hypothalamic and non-hypothalamic cells after prolonged vortex flow stimulation.

Table 13. Molecules predicted as upstream regulators of the molecular changes found in non-hypothalamic cells after prolonged exposure to vortex flow stimulation.

Non-hypothalamic cells					
Upstream regulator	Name	Molecule type	P-value of overlap	Predicted activation state	z-score
MYC	Myelocytomatosis oncogene	transcription regulator	1.52E-28	Inhibited	-5.015
TP53	Tumor protein p53	transcription regulator	1.52E-19		-1.585
PPARA	Peroxisome proliferator-activated receptor alpha	ligand-dependent nuclear receptor	5.16E-19		-0.746
TGFB1	Transforming growth factor beta 1	growth factor	3.88E-16		-0.541
HNF4A	Hepatocyte nuclear factor 4 alpha	transcription regulator	5.54E-16	Inhibited	-3.911
RNA polymerase II	RNA polymerase II	complex	2.23E-14		
Ins1	Insulin I; preproinsulin	other	2.32E-14	Inhibited	-2.107
LEP	Leptin	growth factor	2.70E-14		0.768
APP	Amyloid beta precursor protein	other	6.22E-14		1.264
TNF	Tumor necrosis factor	cytokine	1.85E-13	Activated	2.911
Insulin	Insulin	group	8.08E-13		-0.305
EGF	Epidermal growth factor	growth factor	7.72E-12		-1.685
IL1B	Interleukin 1 beta	cytokine	1.01E-11		0.603
MAPT	Microtubule associated protein Tau	other	1.42E-11		
HTT	Huntingtin	transcription regulator	2.76E-11		-1.844
HRAS	Harvey rat sarcoma viral oncogene homolog	enzyme	1.46E-10		0.059
PPARG	Peroxisome proliferator-activated receptor gamma	ligand-dependent nuclear receptor	3.88E-10	Inhibited	-2.380
NR1H4	Nuclear receptor subfamily 1 group H member 4	ligand-dependent nuclear receptor	1.11E-09		-02.37
PDX1	Pancreatic and duodenal homeobox 1	transcription regulator	1.50E-09		0.131
PSEN1	Presenilin 1	transcription regulator	1.78E-09		0.928

In hypothalamic cells, function annotations in the category of “molecular transport”, “small molecule biochemistry”, and “Lipid metabolism” are the most prevalent in the list; other categories such as “infectious diseases”, “development”, and “carbohydrate metabolism” were also predicted to be decreased in hypothalamic cells after treatment.

On the other hand, among the most prevalent categories predicted to be increased in hypothalamic cells after prolonged vortex flow stimulation are “cellular movement”, “cellular function and maintenance”, and “cell to cell signaling and interaction”. Categories such as “immune cell trafficking”, “inflammatory response”, “organismal survival”, “cell death and survival”, and “hematological system development and function” also appeared among the top list.

In the case of non-hypothalamic cells, the function annotation with decreased activity ranked as the most significant was “nucleic acid metabolism”; this was followed by function annotation categories such as “lipid metabolism”, “small molecule

biochemistry", "molecular transport", "organismal survival", "endocrine system development and function", "cardiovascular system development and function", "energy production", "infectious diseases", and "cellular assembly and organization". Among the categories which were predicted to have increased activity are "cell death and survival", "cancer", "organismal injury and abnormalities", "tumor morphology", "inflammatory disease", "metabolic disease", "gene expression", and "cardiovascular disease".

Table 14. Top predicted categories of function annotations with a decreased activation state in hypothalamic cells after exposure to prolonged vortex flow stimulation.

Hypothalamic cells – Decreased activation state				
Category	Disease or Functions Annotation	P-value	z-score	No. of molecules
Molecular Transport	transport of molecule	5.40E-33	-4.317	216
Lipid Metabolism, Small Molecule Biochemistry	fatty acid metabolism	3.25E-19	-2.401	91
Lipid Metabolism, Molecular Transport, Small Molecule Biochemistry	transport of lipid	1.63E-18	-2.449	50
Molecular Transport	secretion of molecule	8.83E-18	-2.366	84
Infectious Diseases	infection of Mammalia	2.75E-14	-3.532	55
Cellular Development, Cellular Growth and Proliferation, Embryonic Development, Organ Development, Organismal Development, Tissue Development, Visual System Development and Function	formation of retinal cells	2.03E-13	-2.724	21
Lipid Metabolism, Molecular Transport, Small Molecule Biochemistry	transport of steroid	6.08E-13	-2.708	32
Lipid Metabolism, Molecular Transport, Small Molecule Biochemistry	secretion of lipid	1.62E-11	-3.381	34
Embryonic Development, Organ Development, Organismal Development, Tissue Development, Visual System Development and Function	development of retina	8.75E-11	-2.462	23
Lipid Metabolism, Molecular Transport, Small Molecule Biochemistry	absorption of lipid	3.03E-10	-2.356	16
Lipid Metabolism, Molecular Transport, Small Molecule Biochemistry	flux of lipid	4.23E-10	-2.422	25
Lipid Metabolism, Molecular Transport, Small Molecule Biochemistry	transport of sterol	5.81E-10	-2.021	25
Lipid Metabolism, Molecular Transport, Small Molecule Biochemistry	efflux of lipid	7.44E-10	-2.290	24
Molecular Transport	export of molecule	9.32E-10	-3.056	42
Lipid Metabolism, Molecular Transport, Small Molecule Biochemistry	transport of cholesterol	1.41E-09	-2.346	24
Lipid Metabolism, Molecular Transport, Small Molecule Biochemistry	efflux of cholesterol	1.62E-09	-2.070	22
Molecular Transport	transport of ion	2.91E-09	-2.787	59
Carbohydrate Metabolism, Molecular Transport	transport of carbohydrate	4.57E-09	-2.050	31
Lipid Metabolism, Molecular Transport, Small Molecule Biochemistry	uptake of cholesterol	4.95E-09	-2.610	14
Infectious Diseases	Bacterial Infections	1.07E-08	-3.379	51

Table 15. Top predicted categories of function annotations with an increased activation state in hypothalamic cells after exposure to prolonged vortex flow stimulation.

Hypothalamic cells – Increased activation state				
Category	Disease or Functions Annotation	P-value	z-score	No. of molecules
Cellular Movement	cell movement	3.01E-26	2.652	243
Cellular Movement	migration of blood cells	6.92E-26	2.251	133
Cellular Movement, Immune Cell Trafficking	leukocyte migration	1.91E-25	2.226	132
Cellular Movement	migration of cells	1.64E-24	2.739	221
Cellular Function and Maintenance	cellular homeostasis	1.23E-21	2.617	187
Cellular Movement	homing of cells	2.53E-21	2.199	93
Cellular Movement	homing of blood cells	2.32E-20	2.388	70
Inflammatory Response	inflammatory response	2.13E-19	2.357	110
Cellular Movement, Hematological System Development and Function, Immune Cell Trafficking	homing of leukocytes	2.90E-19	2.275	68
Cell-To-Cell Signaling and Interaction	adhesion of blood cells	9.51E-19	2.312	67
Organismal Survival	morbidity or mortality	8.29E-18	2.046	240
Cellular Movement, Hematological System Development and Function, Immune Cell Trafficking, Inflammatory Response	chemotaxis of myeloid cells	1.33E-16	2.191	54
Cellular Function and Maintenance, Inflammatory Response	phagocytosis	6.39E-16	2.047	54
Inflammatory Response	immune response of cells	1.33E-15	2.302	82
Cell Death and Survival	cell death	3.42E-15	2.452	300
Hematological System Development and Function, Tissue Morphology	quantity of lymphocytes	1.16E-14	2.121	93
Hematological System Development and Function, Tissue Morphology	quantity of mononuclear leukocytes	1.96E-14	2.137	95
Cellular Function and Maintenance	engulfment of blood cells	2.24E-14	2.015	37
Cellular Function and Maintenance, Hematological System Development and Function	engulfment of myeloid cells	1.82E-13	2.132	32
Cell-To-Cell Signaling and Interaction, Inflammatory Response	immune response of leukocytes	1.88E-13	2.648	51

3.5 Functional characterization of optogenetic and genetically targeted ablation tools for manipulating HPI axis activity.

3.5.1 Optogenetic manipulation of pituitary corticotrophs increases stress-induced cortisol levels.

To manipulate endogenous cortisol levels in zebrafish larvae, Dr. Arturo Gutierrez-Triana, in our laboratory, generated the transgenic line *Tg(Pomc:bPAC-2A-tdTomato)*^{hd10} (*pomc*:bPAC) where expression of a blue light-photoactivated adenylyl cyclase from the soil bacterium *Beggiatoa* (bPAC) is driven by a fragment of the *pomc* promoter, resulting in bPAC expression in pituitary corticotroph cells (Ryu et al., 2010, Stierl et al., 2011, De Marco et al., 2013). This protein is expected to increase cAMP levels in corticotroph cells upon blue light stimulation, culminating in increased ACTH and cortisol secretion (Section 1.10, Figure 1.5A and C).

Table 16. Top predicted categories of function annotations with a decreased activation state in non-hypothalamic cells after exposure to prolonged vortex flow stimulation.

Non-hypothalamic cells – Decreased activation state				
Category	Disease or Functions Annotation	P-value	z-score	No. of molecules
Nucleic Acid Metabolism	metabolism of nucleic acid component or derivative	7.08E-09	-2.723	51
Nucleic Acid Metabolism, Small Molecule Biochemistry	metabolism of nucleotide	8.46E-09	-2.183	45
Lipid Metabolism, Molecular Transport, Small Molecule Biochemistry	transport of steroid	2.54E-08	-3.258	22
Organismal Survival	survival of organism	1.51E-07	-2.343	62
Endocrine System Development and Function, Small Molecule Biochemistry	metabolism of hormone	2.63E-07	-2.323	24
Nucleic Acid Metabolism, Small Molecule Biochemistry	synthesis of nucleotide	1.14E-06	-2.188	35
Endocrine System Development and Function, Small Molecule Biochemistry	synthesis of hormone	1.19E-05	-2.077	18
Cardiovascular System Development and Function, Cellular Movement	cell movement of endothelial cells	1.42E-05	-2.523	32
Energy Production, Lipid Metabolism, Small Molecule Biochemistry	oxidation of lipid	1.55E-05	-2.375	22
Lipid Metabolism, Molecular Transport, Small Molecule Biochemistry	efflux of cholesterol	1.66E-05	-2.443	14
Cardiovascular System Development and Function, Cellular Movement	migration of endothelial cells	1.79E-05	-2.609	30
Infectious Diseases	replication of virus	3.22E-05	-3.355	44
Lipid Metabolism, Molecular Transport, Small Molecule Biochemistry	flux of lipid	3.28E-05	-2.693	15
Lipid Metabolism, Molecular Transport, Small Molecule Biochemistry	transport of sterol	3.89E-05	-2.612	15
Cellular Assembly and Organization, Tissue Development	formation of filaments	4.03E-05	-2.746	34
Infectious Diseases	replication of RNA virus	4.92E-05	-2.620	40
Lipid Metabolism, Molecular Transport, Small Molecule Biochemistry	excretion of lipid	9.61E-05	-2.117	7
Lipid Metabolism, Small Molecule Biochemistry	conversion of lipid	1.05E-04	-2.309	16
Cardiovascular System Development and Function, Cellular Movement	movement of vascular endothelial cells	1.25E-04	-2.282	18

Table 17. Top predicted categories of function annotations with an increased activation state in non-hypothalamic cells after exposure to prolonged vortex flow stimulation.

Non-hypothalamic cells – Increased activation state				
Category	Disease or Functions Annotation	P-value	z-score	No. of molecules
Cell Death and Survival	cell death	1.64E-26	2.178	275
Cell Death and Survival	necrosis	3.17E-24	2.812	226
Cancer, Cell Death and Survival, Organismal Injury and Abnormalities, Tumor Morphology	cell death of tumor cells	5.34E-21	3.221	69
Cancer, Cell Death and Survival, Organismal Injury and Abnormalities, Tumor Morphology	cell death of cancer cells	5.06E-18	3.357	58
Cancer, Organismal Injury and Abnormalities	cancer	6.50E-10	3.053	586
Inflammatory Disease	chronic inflammatory disorder	7.75E-09	2.183	82
Metabolic Disease	glucose metabolism disorder	4.46E-08	2.504	100
Gene Expression	expression of mRNA	5.85E-07	2.723	27
Cardiovascular Disease, Organismal Injury and Abnormalities	fibrosis of heart	3.22E-05	2.184	19
Cancer, Hematological Disease, Immunological Disease, Organismal Injury and Abnormalities	leukemia	1.21E-04	2.290	114

To evaluate whether bPAC expression in pituitary corticotrophs culminates in increased cortisol levels upon blue light stimulation, 6 dpf larvae expressing bPAC (bPAC+) and their negative siblings (bPAC-) were collected for cortisol measurement at either basal conditions, or after 5 minutes of blue light stimulation onset consisting of a 3 minutes-squared pulse of blue light (2.8 $mW*cm^{-2}$). Cortisol levels at basal conditions in bPAC+ and bPAC- did not present significant differences (Figure 3.29A). On the other hand, bPAC+ larvae showed higher cortisol levels after blue light stimulation (Figure 3.29A). I then asked whether repeated exposure to blue light stimulation would induce a sustained hypercortisolic state in bPAC+ larvae. To evaluate this, bPAC+ and bPAC- larvae were exposed to four consecutive squared blue light pulses (2.8 mW*cm-2) with an inter-trial interval of 30 minutes. This inter-trial interval was selected because it assured comparable low cortisol levels in bPAC+ and bPAC- by the time of the onset of the subsequent blue light stimulations; by doing so, it was possible to compare the cortisol levels induced by the most recent blue light stimulation and not from previously elevated cortisol levels. Samples were collected 2 minutes after blue light offset in all cases. Figure 3.29B shows that, while bPAC+ larvae responded to each of the light pulses with higher cortisol levels, bPAC- larvae failed to do so after the first pulse, indicating that hypercortisolic states were induced in bPAC+ larvae after repeated blue light stimulation.

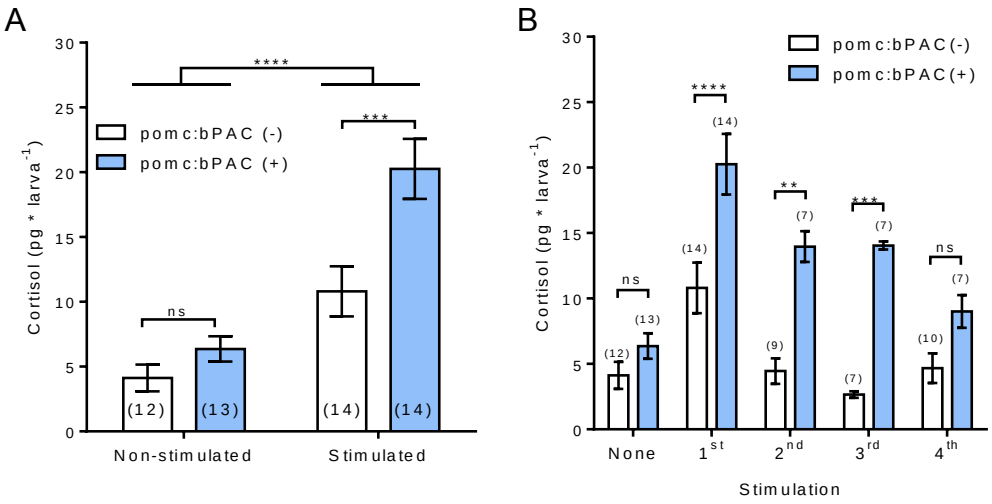

Figure 3.29. Optogenetic manipulation of pituitary corticotrophs increases HPI axis gain and leads to hypercortisolic states. A: exposure to a blue light pulse of 3 minutes leads to higher cortisol levels in pomc:bPAC(+) larvae as compared to their siblings pomc:bPAC(-). No significant differences were observed between genotypes at basal conditions (Two way ANOVA: treatment: $F(1,49)=35.17$, $p<0.0001$; genotype: $F(1,49)=11.37$, $p=0.0015$; treatment x

genotype: F(1,49)=4.327, p=0.0428; Sidak's post-test: genotype effect for each treatment, ***p<0.001; sample size indicated in parenthesis). **B:** a sequence of blue light pulses consisting of 3 minutes with an inter-trial interval of 30 minutes induce sustained hypercortisolic state in pomc:bPAC(+) but not in pomc:bPAC(-) larvae (Two way ANOVA: stimulation: F(4,90)=15.99, p<0.0001; genotype: F(1,90)=50.04, p<0.0001; stimulation x genotype: F(4,90)=3.036, p=0.0213; Sidak's post-test: genotype effect for each stimulation, *p<0.05, **p<0.01, ***p<0.001, ****p<0.0001).

3.5.2 Optogenetic manipulation of interrenal gland cells increases stress-induced cortisol levels.

To manipulate HPI axis activity at the level of the interrenal gland, Dr. Arturo Guiterrez-Triana, in our laboratory, generated the transgenic line *Tg(2kbStARp:bPAC-tdTomato)*^{hd19} (*StAR*:bPAC) where expression of bPAC is driven by a 2kb regulatory region of the *StAR* promoter, resulting in bPAC expression in the steroidogenic interrenal cells. Similar to the *pomc*:bPAC transgenic line, expression of bPAC in steroidogenic cells of the interrenal gland was expected to increase cortisol secretion upon blue light stimulation (Section 1.10, Figure 1.5B and C).

To evaluate whether blue light exposure increases overall cortisol levels in larvae expressing bPAC under the *StAR* promoter, 4 dpf *StAR*:bPAC+ larvae were exposed to a squared pulse of blue light (2.8 mW*cm-2) for 3 minutes and samples were collected for cortisol measurement 2 minutes after blue light stimulation offset. Transgenic line *Tg(2kbStARp:GFP)*, where GFP is driven by the same 2kb regulatory region of the *StAR* promoter used in the *StAR*:bPAC line, was used as control genotype and exposed to the same type of stimulation. Cortisol measures showed that at basal conditions both, *StAR*:bPAC+ and *StAR*:GFP+ larvae, presented similar cortisol levels which were not significantly different. However, after blue light stimulation, *StAR*:bPAC+ larvae showed higher cortisol levels than the *StAR*:GFP+ larvae (Figure 3.30).

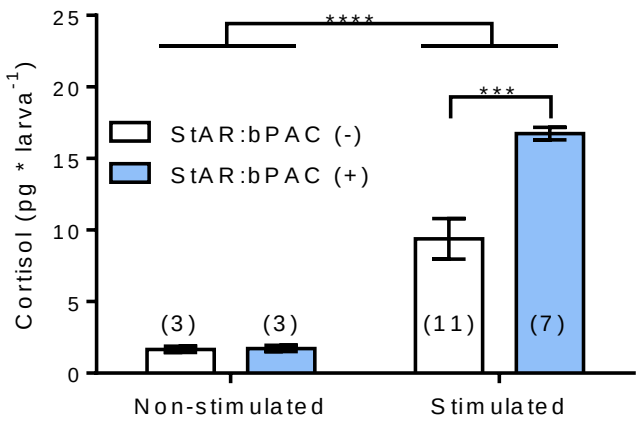

Figure 3.30. Optogenetic manipulation of interrenal gland cells increases HPI axis gain leading to higher exposure to endogenous cortisol. Exposure to a blue light pulse of 3 minutes leads to higher cortisol levels in *StAR*:bPAC larvae as compared to *StAR*:GFP. No significant differences were observed between genotypes at basal conditions (Two way ANOVA: treatment: $F(1,20)=60.16$, $p<0.0001$; genotype: $F(1,20)=5.325$, $p=0.0318$; treatment x genotype: $F(1,20)=5.154$, $p=0.0344$; Sidak's post-test: genotype effect for each treatment: ***$p<0.001$).

3.5.3 Genetically targeted ablation of hypothalamic cells reduces stress-induced cortisol levels.

The optogenetic tools described in previous sections (3.5.1 and 3.5.2) induced hypercortisolic states in freely swimming zebrafish larvae by manipulating pituitary corticotrophs or interrenal gland cells activity. In order to manipulate HPI axis activity in the opposite direction and generate hypocortisolic states in zebrafish larvae, Dr. Arturo Gutierrez-Triana generated in our laboratory a genetically targeted ablation tool targeted to the NPO region of the hypothalamus (Section 1.10, Figure 1.6). In the transgenic line *Tg(otpECR6-E1b:nfsB-GFP)*^{hd14} (*otp*ECR6:nfsB-GFP) the regulatory element *otp*ECR6 was used to drive expression of the *E. coli* nfsB as a GFP fusion protein. Metronidazole treatment in this transgenic line is expected to culminate in ablation of those cells expressing nfsB, and therefore in reduced HPI axis output (Section 1.10, Figure 1.6).

To evaluate whether NPO cell ablation results in impaired cortisol response, cortisol levels were measured in 6 dpf *otp*ECR6:nfsB-GFP and *otp*ECR6:GFP (control) larvae at basal condition or after exposure to acute vortex flow stimulation (3 minutes, 330 rpm). Larvae were previously incubated in either E2 medium or in E2 medium supplemented with Metronidazole (Met). Interestingly, neither genotype nor Met treatment had an effect in cortisol levels at basal conditions (Figure 31A). Acute vortex flow stimulation resulted in increased cortisol levels in both genotypes regardless of Met treatment (Figure 31B); however, Met treatment resulted in attenuation of cortisol response in both genotypes. Importantly, *otp*ECR6:nfsB-GFP larvae exposed to Met showed a significant reduction in cortisol response when compared to *ot*pECR6:GFP larvae treated with Met; in fact, cortisol response to the vortex flow stimulation differed between genotypes only when larvae were treated with Met (Figure 31B).

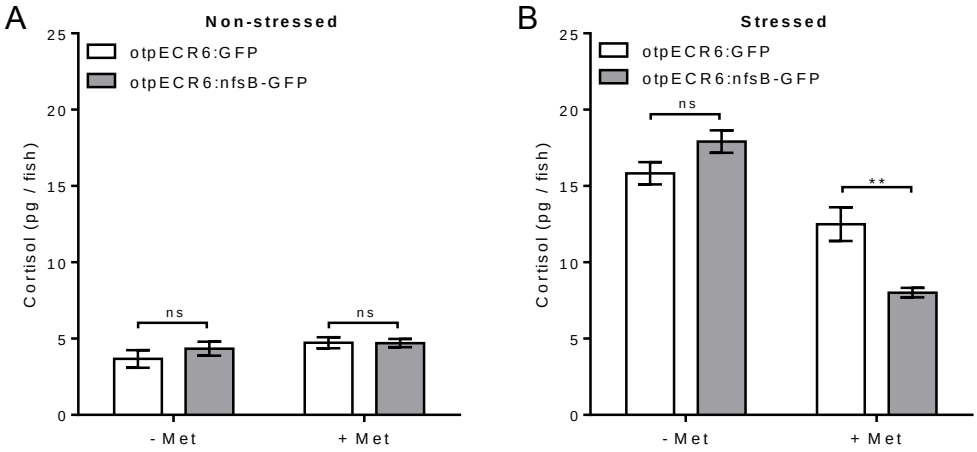

Figure 3.31. Targeted ablation of hypothalamic cells results in impaired cortisol response after metronidazole treatment. A: Cortisol levels at basal conditions of otpECR6:GFP and otpECR6:nfsb larvae with or without metronidazole (Met) treatment. No differences were observed between groups (Two way ANOVA: Met: $F(1,20)=2.689$, $p<0.1167$; genotype: $F(1,20)=0.5703$, $p=0.4589$; Met x genotype: $F(1,20)=0.6486$, $p=0.4301$; Sidak's post- test: genotype effect for each treatment: no significant difference, $p<0.05$). **B:** Cortisol levels after acute exposure to vortex flow stimulation of *otp*ECR6:GFP and *otp*ECR6:nfsb larvae with or without Met treatment. Note that cortisol levels were different depending on genotype only when Met treatment was present (Two way ANOVA: Met: $F(1,20)=73.11$, $p<0.0001$; genotype: $F(1,20)=2.412$, $p=0.1361$; Met x genotype: $F(1,20)=18.03$, $p=0.0004$; Sidak's post-test: genotype effect for each treatment, $^{**}p<0.01$).

3.5.4 Genetically targeted ablation of interrenal gland cells reduces basal and stress-induced cortisol levels.

To target cell ablation to steroidogenic cells of the interrenal gland, the transgenic line *Tg(2kbStARp:nfsB-GFP)*^{hd18} (*StAR*:nfsB-GFP) was generated. In this transgenic line, expression of the bacterial nfsB is driven by a 2kb regulatory fragment of the *StAR* promoter. Similar to the *otp*ECR6:nfsB-GFP line, ablation of steroidogenic cells of the interrenal gland was expected to decrease HPI axis output (Section 1.10, Figure 1.6).

To evaluate whether ablation of interrenal cells in *StAR*:nfsB-GFP larvae culminates in hypocortisolic states, cortisol levels were measured in 6 dpf *StAR*:nfsB-GFP and *StAR*:GFP (control) larvae at basal conditions or after exposure to acute vortex flow stimulation (3 minutes, 330 rpm). Previous to acute stimulation, larvae were incubated in either E2 medium or E2 supplemented with Met. At basal conditions, cortisol levels were different between genotypes only when incubated in Met, where *StAR*:nfsB-GFP larvae showed reduced cortisol levels (Figure 3.32A). After acute vortex flow stimulation, cortisol levels were increased in both, *StAR*:nfsB-GFP and *StAR*:GFP larvae

without any significant difference between genotypes when the Met treatment was absent (Figure 3.32B). On the other hand, Met treatment attenuated the cortisol response to acute vortex flow stimulation of *StAR*:GFP larvae and completely abolished the response in *StAR*:nfsB-GFP larvae.

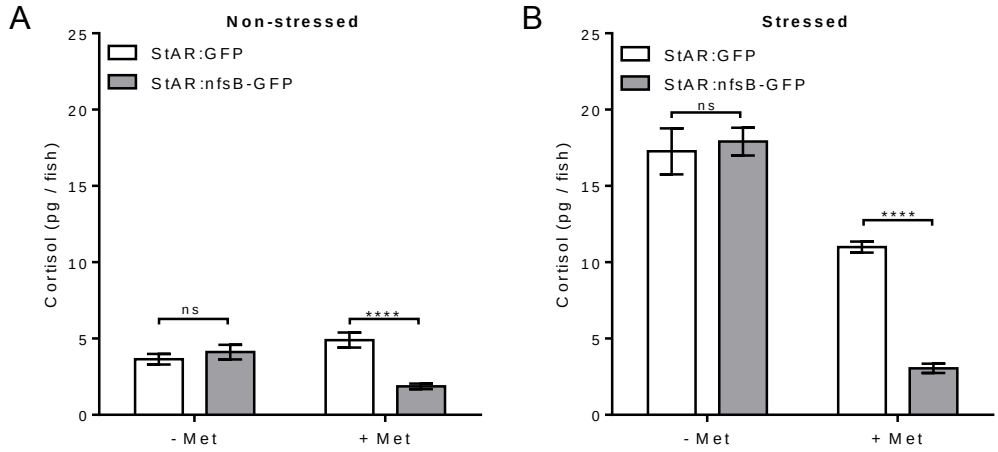

Figure 3.32. Targeted ablation of interrenal gland cells results in impaired cortisol response after metronidazole treatment. A: Cortisol levels at basal conditions of *StAR*:GFP and *StAR*:nfsb-GFP larvae with or without metronidazole (Met) treatment. Note that in the presence of Met only *StAR:*nfsb-GFP larvae showed reduced cortisol levels (Two way ANOVA: Met: $F(1,20)=1.562$, $p=0.2257$; genotype: $F(1,20)=10.52$, $p=0.0041$; Met x genotype: $F(1,20)=19.66$, $p=0.0003$; Sidak's post- test: effect of genotype for each treatment, ****$p<0.0001$). **B:** Cortisol levels after acute exposure to vortex flow stimulation (330 rpm, 3 minutes) of *StAR*:GFP and *StAR*:nfsb-GFP larvae with or without Met treatment. Note that cortisol levels were different depending on genotype only when Met treatment was present (Two way ANOVA: Met: $F(1,28)=134.8$, $p<0.0001$; genotype: $F(1,28)=16.10$, $p<0.0004$; Met x genotype: $F(1,28)=22.24$, $p<0.0001$; Sidak's post-test: effect of genotype for each treatment, ****$p<0.0001$).

4. DISCUSSION

4.1 Characterization of the vortex flow stimulation.

This work revealed that vortex flow stimulation can be used as an input signal to induce a stress response that culminates in increased cortisol levels and behavioral outputs changes in freely swimming zebrafish larvae. Although other studies have shown that different stressors are able to elicit a cortisol response in both larval and adult zebrafish, very few have reported a protocol capable of eliciting a strength-dependent cortisol response. This feature is essential to elucidate the mechanisms involved in early programming of the HPA axis activity. Predicted and moderate stress inoculation during early life may enhance stress resilience by increasing the stress coping fitness of the organism when it is exposed to similar conditions in later stages of life (Schmidt, 2010, Taylor, 2010, Khulan and Drake, 2012, Daskalakis et al., 2013). On the other hand, strong or prolonged adverse experience is linked to metabolic and brain disorders (Seckl and Meaney, 2004, Reynolds, 2013). Being able to generate a wide range of physiological states where different magnitudes of HPA axis activity can be induced is essential for studying the intensity-dependent effects of early life adverse experience underlying the programming mechanism leading to a more resilient or disease-prone organism.

The characterization of the stimulation protocol showed that the speed of the magnetic field inversion that can be controlled in the magnetic stirrer plate is linearly correlated to the mean speed to which a particle is exposed in the generated vortex flow; this allows the generation of a wide range of stress-induced states where the magnitude of the response can be manipulated by changing the strength of the input signal, an important aspect when analyzing subtle changes in HPA axis activity.

It is worth noting that, as expected, the speed to which a particle is exposed in the vortex flow depends on the distance to the center of the vortex: closer to the center, faster the flow. This represents an important feature of the stimulation protocol, since it allows free swimming larvae to actively direct themselves towards a preferred section of the dish, where the flow may be faster or slower This aspect of the stimulation protocol is essential for studying behavioral changes in adaptive coping strategies after early adverse experience.

An increased locomotor activity immediately after vortex flow stimulation onset was detected in 6 dpf larvae. Interestingly, this response was strength-dependent, being higher for higher strengths of vortex flow stimulation. Since the speed of the flow is faster at higher stimulation strengths, the larvae may respond with higher locomotor activity to cope with the perturbation. Other studies have shown that zebrafish larvae elicit an escape response by increasing their locomotor activity after sensing a water flow that may represent a predator threat (Kohashi and Oda, 2008, Olszewski et al., 2012). The magnitude of the escape response depends on the flow speed to which the larvae are exposed and it is mediated, at least in part, by the visual and the mechanosensory lateral line systems. This may be relevant for survival in their natural environment in order to evade predation while efficiently using energetic resources. However, further experiments need to be performed in order to elucidate whether the strength-dependent locomotor activity seen after vortex flow stimulation onset is elicited by the speed of the generated flow and mediated by its perception by the visual and lateral line systems.

Startle response to the onset of vibration stimulus of the stirrer may also contribute to the strength-dependent locomotor response observed. Startle response in zebrafish larvae consists of a "C-bend" of the body that is followed by a counter bend and a swimming bout (Kimmel et al., 1974). Features of this behavioral response, known as long-latency responses, have been shown to be dependent on the stimulus intensity (Eaton et al., 1977, Burgess and Granato, 2007, Kohashi and Oda, 2008). It is possible that the intensity-dependent locomotor activity (distance swam) seen immediately after the vortex flow stimulation onset is linked to a locomotor startle response elicited by the vibrational stimulus of the stirrer onset. This is also supported by the increase in change of body angle after onset of the stimulation (Figure 3.3A). Further characterization of the locomotor activity right after vortex flow onset is needed in order to elucidate the mechanisms mediating this response.

4.1.1 Change in body angle orientation and rheotaxis behavior

Analysis of the body orientation after vortex flow stimulation onset, together with the analysis of distance swam after stimulation onset, suggest that vortex flow stimulation elicit a directed locomotor activity. Zebrafish larvae may re-orientate their bodies to maximize the distance between their bodies and the vortex origin, and to

maintain a specific body orientation to cope with the water flow by showing rheotactic behavior.

Increased change in body angle was found immediately after mild vortex flow stimulation onset. Startle response to vibrational stimulus of the stirrer onset (section 4.1) may contribute to the increased change in body angle. This is further supported by the fact that change in body angle is only transiently increased after mild stimulation onset. Moreover, increase in change of body angle seems to be directed, since the larvae swim away from the vortex origin (Figure 3.3B) and remain away for the rest of the stimulation (data not shown). This may also contribute to the increased distance swam observed immediately after vortex flow stimulation onset (Figure 3.2C). This suggests that a complex and fast integration of cues occurs to rapidly detect the direction of the perturbation and avoid it, a typical escape behavior that has been widely described before (O'Malley et al., 1996, Budick and O'Malley, 2000).

Further analysis of behavioral response to vortex flow stimulation showed that the percentage of larvae facing against the vortex current, a typical positive rheotactic behavior, positively correlates with the strength of the stimulation and therefore with the speed of the flow (Figure 3.4A and 3.1F). This is congruent with other studies showing that the strength of rheotaxis behavior in other fish species increases depending on the flow speed (Montgomery et al., 1997, Baker and Montgomery, 1999, Kanter and Coombs, 2003). Interestingly, the lowest speed flow tested (130 rpm) did not increase percentage of larvae facing to the vortex current nor affected the body angle orientation after stimulation onset (Figure 3.4A and B). Other studies have also found that low speed flows fail to elicit a consistent rheotactic behavior, confirming the presence of a rheotaxis threshold (Montgomery et al., 1997). This may be due simply to the low drag forces, where zebrafish larvae do not experience difficulty to keep performing, at least in part, exploratory behavior maintaining low energetic costs (Bak-Coleman et al., 2013).

The frequency distribution of the body angles during vortex flow stimulation also changed depending on flow speed (Figure 3.4C-F). Higher vortex flow speeds decreased the change in body angle as well as the range of body angles during vortex flow stimulation (Figure 3.4B-F). It is possible that this behavioral output reduces energetic costs for larvae by aligning their body axes to the strong water flow while

maintaining a specific spatial location in the arena when the highest strength of the stimulation was used (530 rpm). On the other hand, mild strength stimulation (330 rpm) resulted in altered frequency distribution, but only a non-significant tendency of reduced change in body angle was observed. There are two possible explanations for the difference of body angle orientation induced by mild and high strength stimulations. One is that the performance of rheotactic behavior is flow speed-dependent. Since faster flows increase performance of rheotactic behavior, the body orientation acquired by the larvae exposed to the strongest strength of the stimulation (and maintaining this particular orientation) may be more beneficial for coping with the perturbation than the one induced by the mild speed flow. The second possible explanation relates to the actual hydrodynamics of the generated vortex flow. It is likely that the water flows in the arena are different depending on the strength of the magnetic field inversion that drives the magnetic stirrer. If this is the case, it is possible that in both cases, mild and high strengths of the vortex flow stimulation, zebrafish larvae acquire an optimal body axis position for those particular conditions. By doing so, larvae may cope more efficiently with the perturbation. A detailed characterization of the hydrodynamics of the generated vortex flows at different strengths is required to differentiate between these two possibilities.

4.1.2 Vortex flow stimulation increases whole-body cortisol levels.

Vortex flow stimulation induces a wide range of stress-induced cortisol levels depending on the strength and duration of the stimulation. Other studies have used swirling vortex flows successfully to increase cortisol levels in both larval and adult zebrafish (Alsop and Vijayan, 2008, Fuzzen et al., 2010). Alsop and Vjayan (2008) showed that 30 seconds of swirling vortex flows are sufficient to detect a cortisol increase five minutes after the stressor onset at different developmental stages (1 to 4 dpf); however, they did not report the strength of the stimulation used. Fuzzen et al. (2010) used swirling vortex flows to activate the HPI axis of adult zebrafish. The authors report a clear linear correlation between the magnitude of the cortisol response and the vortex speed which is congruent with the data of 6 dpf zebrafish larvae reported in the present study. Although there are some differences between the study of Fuzzen et al. (2010) and the present study, such as duration of the stimulation, time of collection after the stimulation onset, and number of individuals per container, it is clear that both adults and larval zebrafish show a strength-dependent cortisol response to swirling

vortex flows, supporting the feasibility of using this protocol to study the mechanisms underlying stress-related processes in very early stages of development.

Fuzzen et al. (2010) report this strength-dependent cortisol response to vortex flow with a fixed duration of the stimulation (20 minutes). In the present study, I further explored the interaction between the duration and the strength of the stimulation. Increasing the duration of the stimulation from 1 to 3 minutes led to higher cortisol levels only when high strength stimulation was used. When doubling the duration of the stimulation from 3 to 6 minutes, the cortisol response reached similar levels than those reached after 3 minutes of exposure to the vortex flow stimulation (Figure 3.6B). It is possible that the negative feedback already exerts its rapid effects after approximately three minutes of stimulation in order to limit the rise in cortisol levels (Evanson et al., 2010, Tasker and Herman, 2011). Based on the data obtained in the present study, we can hypothesize that the absolute levels of cortisol reached after vortex flow stimulation are dictated, at least in part, by the strength of the stimulation perceived during the first minutes. This response is then terminated by the negative feedback relatively quickly after stress onset, preventing cortisol levels to keep increasing, even if the duration of the stimulation keeps increasing. This is further supported by data shown in section 3.2.2 (Figure 3.13), where the glucocorticoid receptor antagonist mifepristone was used. In this experiment, the levels of cortisol reached after repeated vortex flow stimulation in the presence of the GR antagonist were higher than in the control groups in 4 and 8 dpf larvae, suggesting that the absolute cortisol levels reached after repeated vortex flow stimulation of fixed duration and strength are controlled, at least in part, by rapid GR signaling (negative feedback), limiting the release of cortisol (details of this experiment are further discussed in section 4.2.3).

Previous work in our laboratory and from others showed that the peak of stress-induced cortisol levels in larvae can be detected 5-15 minutes after stressor onset (Alsop and Vijayan, 2008, Steenbergen et al., 2011, De Marco et al., 2013, Yeh et al., 2013). After this time, cortisol levels decrease as a function of time between 10 and 30 minutes after stressor onset, indicating that a functional negative feedback is present in 6 dpf larvae (De Marco et al., 2013). However, to date, there is no evidence in literature about how fast the HPI axis negative feedback exerts its effects in zebrafish larvae. Additionally, no study has addressed whether the stress-induced cortisol peak is influenced by rapid negative feedback signaling in zebrafish larvae. Taking into account

the data here presented, I propose that the negative feedback mediated by GR is already present and functional in zebrafish larvae and it may exert its rapid effects already after 3-5 minutes after stressor exposure onset. Although further experiments need to be performed to explore this hypothesis, the data supports the suitability of the vortex flow stimulation protocol to address this and other questions to elucidate the mechanisms involved in stress-related processes related to the HPI axis development and function in zebrafish larvae.

Further analysis of the vortex flow stimulation effects revealed a clear correlation between the behavioral output and the cortisol levels after exposure to vortex flow stimulation in 6 dpf zebrafish larvae (Figure 3.7A-B). It was previously discussed that locomotor activity (distance swam) immediately after vortex flow stimulation onset increases as the strength of the stimulation augments. This same trend in strength-dependent response is true for vortex flow-induced cortisol levels, revealing a positive correlation between locomotor activity and cortisol levels. In the case of body orientation, a strength-dependent response was also observed: change in body angle decreases as vortex flow strength augments. This leads to a negative correlation between change in body angle and cortisol levels, where higher strengths of vortex flow stimulation lead to high cortisol levels and low change in body angle.

A direct causal relationship between these aspects is difficult to establish without further experiments; however, it is reasonable to speculate that energy requirements and availability are common factors that may link locomotor activity, orientation maintenance, and cortisol response. The role of cortisol in energy mobilization is well established in both mammals and teleost fish (Dallman et al., 1993, Vijayan et al., 1994). In humans, it is well known that physical activity increases cortisol levels depending on the intensity and duration of the exercise session (Davies and Few, 1973, Hill et al., 2008). Increased levels of cortisol during exercise exert vital physiological functions such as protein and lipid metabolism, and gluconeogenesis. These processes provide the energy necessary to cope with the challenging situation and allow the organism to adapt (McMurray and Hackney, 2000, Viru and Viru, 2004). It is intuitive to expect that increased physical activity increases energy requirements. Indeed, in zebrafish larvae it has been shown that exposure to water flows of different speeds increases oxygen consumption, suggesting that there is an increase in energy requirements to cope with the situation (Bagatto et al., 2001).

Hence, taking all together, it is possible to propose that after vortex flow stimulation, cortisol levels increase to facilitate energy mobilization that allow the performance of behavioral strategies to cope with the perturbation.

4.2 Activation of the HPI axis during early life stages of zebrafish larvae.

The activity of the HPI axis of zebrafish larvae through early development was characterized; this was evaluated by using vortex flow stimulation as the input signal and cortisol levels as the output measure. All three aspects evaluated (basal activity, acute response activation, and response to repeated exposure) revealed significant changes in HPI axis activity through development (4 to 8 dpf). This is the first time the interaction between the stimulus-strength, duration of the stimulation, developmental stage, and cortisol levels is characterized in developing zebrafish. Besides contributing to our understanding of the HPI axis ontogeny, this information is necessary to develop early life stress protocols to study developmental programming processes after early life adverse experience.

4.2.1 Basal HPI axis activity

Previous studies have reported the changes in basal cortisol levels in developing zebrafish larvae (Alsop and Vijayan, 2009, Alderman and Bernier, 2009, Alsop and Vijayan, 2008). A general trend of increasing basal cortisol levels after hatching is consistent throughout the studies. At very early stages of development, deposition of maternal cortisol has been detected; this decreases as the embryo develops until endogenous cortisol can be synthesize at around 2 – 3 dpf, when the embryos hatch (Alsop and Vijayan, 2008). Previous work in our laboratory (Dr. Chen-Min Yeh) has shown a validated protocol to measure and report cortisol levels (Yeh et al., 2013). However, to date, there is no consensus about the units of cortisol levels to be used, making the comparisons among studies complicated. Different raising conditions and experimental procedures to measure hormone levels add another level of variability difficult to tackle. Despite these complications, the general trend observed in the present study in basal cortisol levels through development is in agreement with previous studies. A consistent increase in cortisol levels was observed from 2 to 8 dpf larvae. Although from day 4 to day 7 no significant difference in cortisol levels was detected,

the general tendency of basal cortisol levels to increase through development reported in earlier studies was confirmed.

4.2.2 HPI axis activation through development

Taking advantage of the versatility of vortex flows as a stressor, I exposed developing larvae to different strengths of vortex flow stimulation using either 1, 3, or 6 minutes as exposure time and asked whether the strength-dependent cortisol response profiles change through development. This characterization was essential to achieve the goals of the present study. First, it provides information about the nominal values of endogenous cortisol reached by zebrafish larvae after acute exposure to an external stimulation at different developmental stages; this facilitates the identification of potential deviations in HPI axis activity after early adverse experience (section 3.3). Second, it expands our understanding about the ontogeny and activity of the HPI axis after acute stress exposure, facilitating subsequent studies about stress response dynamics and effects of early life stress.

One of the differences observed in cortisol profiles at different developmental stages was that 4 dpf larvae responded with the lowest absolute values of cortisol when exposed to vortex flow stimulation of different strengths. There are several potential explanations for this. One possibility is that 4 dpf larvae have a reduced capacity to synthesize and/or release cortisol from the interrenal glands. Previous studies have shown that the HPI axis of zebrafish larvae starts responding to external stimulus at 3-4 dpf, suggesting that this hormonal response is in its early stages of maturation at 4 dpf (Alsop and Vijayan, 2008, Alderman and Bernier, 2009). However, it is unlikely that the relatively low cortisol levels observed in 4 dpf larvae can be explained only by a reduced capacity for cortisol synthesis/release from interrenal glands, since high strength osmotic shock induced higher cortisol response (Figure 3.11B). Moreover, by using optogenetic tools to increase endogenous cortisol levels, I observed that cortisol levels can be increased to higher levels than the ones observed after vortex flow stimulation (data not shown). Studies in trout have shown that cortisol synthesis starts 1 week after hatching, but stress-induced cortisol increase does not occur until 2 weeks after hatching (Barry et al., 1995a). Additionally, ACTH stimulation of embryonic interrenal tissue coming from unhatched trouts led to increased cortisol levels in vitro (Barry et al., 1995b). In zebrafish larvae, it has been shown that the expression of the ACTH receptor is increased by 2 dpf (To et al., 2007); moreover, expression of

enzymes involved in the synthesis of cortisol such as the steroidogenic acute regulatory protein (StAR) and steroid 11-b hydroxylase, are also increased starting from 2 dpf (Alsop and Vijayan, 2008). This together suggests that unhatched zebrafish embryos may also be able to respond to increased ACTH levels with an increase in cortisol. Therefore, other authors have proposed that the reduced cortisol response to external stimuli seen in early stages immediately after hatching may be due to limiting factors mediating the activation of upstream sensory inputs and integration centers in the brain involved in triggering the hormonal cascade leading to a cortisol increase (Alsop and Vijayan, 2008). This may also represent the hypo-responsive period of the stress response axis which has been reported widely in mammals and lately in zebrafish larvae (Levine, 1994, Lupien et al., 2009, Steenbergen et al., 2011).

Other possibility to explain the reduced cortisol response at 4 dpf is that the organs involved in sensing the vortex flow stimulation are not completely developed at this stage. However, the lateral line (the system most likely to be involved in sensing the water flow perturbation induced by vortex flow stimulation) develops at early stages of development before hatching (Kimmel et al., 1995, Sarrazin et al., 2010). Hence, it is most likely that the lower cortisol levels observed in 4 dpf larvae may be mediated by a combination of reduced capacity to synthesize/release cortisol, limited activation of the brain regions responsible for eliciting an input signal to the HPI axis, and/or an enhanced negative feedback mediated by glucocorticoids. Further experiments need to be performed to elucidate whether the mechanisms mediating the reduced cortisol response are an active developmental strategy to avoid detrimental effects of overexposure to glucocorticoids. This may provide insights into new interventions against stress-related disorders.

Interestingly, at 6 dpf, high strengths of vortex flow stimulation induced the highest absolute values of cortisol when compared to 4 and 8 dpf. Cortisol levels induced by high strength stimulation decreased from 6 to 8 dpf. In fact, 8 dpf larvae showed a narrower range of cortisol levels as a response to different strengths of the vortex flow stimulation. Importantly, it is unlikely that this was due to a compromised nutritional state, since both fed and unfed larvae showed comparable cortisol responses (Figure 3.11C). Hence, this difference in strength-dependent cortisol response observed in 8 dpf larvae may be due to a maturation process where either one or a combination of three aspects may be involved: 1) maturation of the regulatory systems involved in HPI axis

activity, 2) maturation of the sensory systems involved in perception and integration of the vortex flow stimulation input, and/or 3) maturation and growth of elements that facilitate coping with vortex flow perturbations, such as swimming bladder, muscle development, etc. Based on the current data, it is reasonable to propose that from 6 to 8 dpf, a change in the HPI axis activation threshold occurs. This is supported by the fact that only the highest strength of vortex flow stimulation elicited higher cortisol levels in 8 dpf larvae exposed for 3 or 6 minutes to the stimulation. All other conditions elicited lower cortisol levels in a narrow range, presumably because the threshold to respond with higher cortisol levels was not met by those conditions. Whether this change in threshold is at the level of the sensory system or at the HPI axis level is unclear (aspects No. 1 and 2); however, data from pharmacological experiments, where the GR was blocked using the antagonist mifepristone, showed that in the presence of the antagonist, cortisol levels reached higher levels than controls (Figure 3.13C). Although this experiments were performed using repeated vortex flow stress, they suggest that the low cortisol levels observed after exposure to vortex flow of low to medium strengths (130, 230, 330 rpm) at 8 dpf may be mediated by GR signaling; hence, it is possible that the cortisol peak is regulated by rapid negative feedback exerted by the GR-signaling, suggesting that the regulatory systems of the HPI axis are mediating, at least partially, the low cortisol levels observed in 8 dpf larvae (aspect No. 1). It is important to keep in mind that this change in cortisol output in 8 dpf larvae can also be mediated by a change in the "meaning" of the vortex flow perturbation input for the larvae, i.e. how challenging the situation is for them at a particular developmental stage. The hydrodynamic perturbation may not induce the same physiological and behavioral adaptations to cope with the situation in zebrafish larvae at different developmental stages; mechanisms that facilitate the larvae to deal with the perturbation may be more developed at 8 dpf, leading to a reduced cortisol demand required to cope with the situation (aspect No. 3). This opens new avenues to study the mechanisms mediating the establishment of this threshold of HPI axis activity through early development providing a valuable model that offers a well-defined time window in which this process occurs.

Moreover, the peak in HPI axis activity observed at 6 dpf is not stressor specific. Cortisol profiles obtained from 4 to 8 dpf after osmotic shock of low and high strengths revealed a similar pattern (Figure 3.11A-B). Based on this data, a potential explanation

for these patterns of cortisol profiles is proposed: first, a still ongoing maturation of the larvae's capacity to synthesize/secrete cortisol is present before 6 dpf, resulting in limited levels of cortisol after stress exposure (even to high strength-stressors); second, increased maturation of HPI axis regulatory elements accompanied with an increased maturation of elements that facilitate the ability of the organism to cope with the perturbation results in a decreased cortisol demand to maintain homeostasis in 8 dpf larvae; this in turn sets a higher threshold of the HPI axis to elicit a response.

4.2.3 Activation of the HPI axis after repeated exposure to vortex flow stimulation

Analysis of repeated exposure to vortex flow stimulation revealed that the cortisol response to a second perturbation depends on the strength of the stimulation, the time of recovery between the two stimulations, and the developmental stage. A clear inhibition of the cortisol response to a second vortex flow stimulation was observed; this inhibition is likely to be mediated by the negative feedback exerted by GCs at any of the three levels of the HPI axis (Wendelaar Bonga, 1997). Supporting this is the pharmacological data showing that in the presence of the GR antagonist mifepristone, larvae of all developmental stages tested (4, 6 and 8 dpf) were able to respond again with increased cortisol levels to repeated vortex flow stimulation. Interestingly, since these actions take place in the order of minutes, it suggests that the inhibition of the cortisol response to a second perturbation is mediated by a rapid negative feedback that involves GR signaling instead of the slow transcriptional negative feedback widely studied (Wendelaar Bonga, 1997, Dallman et al., 1994). Previous studies have shown that the endocannabinoid system is involved in the rapid negative feedback mediated by GC at the level of hippocampus, amygdala, anterior pituitary, and hypothalamus (Tasker and Herman, 2011). Within 10 minutes, increased GC levels induce the release of endocannabinoids in the hypothalamus in a concentration-dependent manner (Hill et al., 2010); released endocannabinoids from the postsynaptic neurons in hypothalamic neurons travel through the synaptic cleft and bind the cannabinoid receptor (CB1) located at the presynaptic neuron, forming a retrograde signaling process; this inhibits the release of excitatory neurotransmitters, facilitating the termination of the stress response (Di et al., 2003, Evanson et al., 2010). Although this particular mechanism has not been studied in zebrafish or other teleost fish, it has been shown that the endocannabinoid system is present and functional in zebrafish larvae (Lam et al., 2006,

Akhtar et al., 2013, Krug and Clark, 2015). It is possible that endocannabinoid signaling mediated by GCs is involved in the inhibition of the cortisol response to a second perturbation that was observed when a high strength stimulation was presented 30 minutes after the first one in 4 and 6 dpf larvae.

The fact that 8 dpf larvae responded with increased cortisol levels to a second perturbation 30 minutes after the first one indicates a faster recovery time. This may be due to a faster clearance of the negative feedback mechanisms exerting the inhibition of subsequent cortisol responses or to an increased capacity or availability of cortisol to be released. It has been previously postulated that one of the main functions of the rapid negative feedback that terminates the stress response in the brain is to prevent the depletion of stress hormones so the organism is able to elicit subsequent responses to cope with potential threatening situations (Tasker and Herman, 2011). As discussed in section 4.2.2, 8 dpf show a more restricted cortisol response to a wide range of stimulation strengths, presumably due to a more mature regulatory system. This may function as a way to prevent depletion of stress hormones, allowing the organism to respond to repeated exposures to stress as observed in 8 dpf larvae in the present study. If this is the case, it would also explain, at least partially, why 6 dpf larvae failed to elicit a cortisol response to repeated vortex flow stimulations; as shown by Hill et al. (2010), the strength of the cortisol response determines the strength of the negative feedback, suggesting that there is a relationship between the cortisol levels reached after the first stimulation and the probability of a cortisol response to a second perturbation. At 6 dpf, larvae respond with the highest cortisol levels to a high strength vortex flow stimulation. This high cortisol levels may induce a stronger and long lasting negative feedback, which may explain why 6 dpf larvae failed to elicit a cortisol response to a second stimulation even after 60 minutes of recovery.

Interestingly, when 8 dpf larvae were exposed to a second perturbation 60 minutes after the first one, they showed a tendency (although not statistically significant) to respond with even higher cortisol levels than the ones reached after the first exposure. Sapolsky et al. (2000) proposed that under some circumstances the actions of GCs can be preparative, meaning that they do not act immediately after stress onset to help coping with that situation, but to modulate the organism's response to subsequent homeostasis-threatening situations. It is possible that the cortisol increase induced by vortex flow stimulation in 8 dpf larvae may facilitate subsequent stress responses to

help coping with the perturbation. However, this goes in opposite direction to what is widely known about the transcriptional effects of the GCs negative feedback, where stress-related molecules are downregulated culminating in a reduced stress response to immediate subsequent stressors (Dallman et al., 1994). Further experiments are required to address the expression level dynamics as a function of time of stress-related molecules after vortex flow stimulation; this would contribute to elucidate the reasons why 8 dpf larvae are more prone to respond with increased cortisol levels after 60 minutes of the first stimulation.

Importantly, it was also revealed that the stress response to repeated exposure to vortex flow in 8 dpf larvae depends on the strength of the stimulation. This is evident from the results of cortisol response to a repeated vortex flow stimulation of low strength, where larvae did not respond with increased cortisol levels after any of the recovery times tested. Since higher strengths did induce a cortisol response, it is likely that the lack of cortisol increase after low strength stimulation is due to an insufficient stimulus input to reach the HPI axis activation threshold. On the other hand, cortisol profiles of 4 and 6 dpf larvae after repeated vortex flow stimulation were comparable regardless of the strength of the stimulation used. It is difficult to speculate whether the mechanisms mediating the inhibition of cortisol response after repeated stimulation in 4 and 6 dpf are the same for the different strengths tested; however, the data from 8 dpf larvae suggest that the strength of the stimulation plays indeed a role on the stress response to repeated stimulations, supporting the possibility of the presence of similar mechanisms at 4 and 6 dpf. If this is the case, it is possible that 4 and 6 dpf larvae showed reduced cortisol response to a repeated stimulation of low strength due to insufficient sensory input to overcome the HPI axis activation threshold; on the other hand, the reduced cortisol response observed after repeated stimulation of high strength may be mediated by an enhanced negative feedback due to the high levels of cortisol reached after the first response, especially for 6 dpf larvae.

4.3 Development of an early life stress model using vortex flow stimulation

4.3.1 Prolonged vortex flow stimulation induces changes in HPI axis activity

As discussed in section 4.1, zebrafish larvae initially respond to acute vortex flow stimulation with increased locomotor activity (distance swam); however, here it is

shown that after 5 minutes of the stimulation onset, larvae decreased their locomotor activity and kept this behavior for the entire duration of the stimulation (Figure 3.14A-B). This was accompanied with a decreased of body angle change (Figure 3.14C-D), meaning that the larvae kept a specific body orientation throughout the prolonged vortex flow stimulation. This indicates that zebrafish larvae respond to the vortex flow stimulation with a biphasic locomotor behavior; first, they respond to the onset of the vortex flow stimulation with increased locomotor activity to maximize the distance between the vortex flow center and their bodies (Figure 3.2C, Figure 3.3B-E); second, they maintain that position in order to cope with the perturbation. This is consistent with previous studies reporting rheotaxis behavior is fish (Montgomery et al., 1997, Bak-Coleman et al., 2013). Maintaining this behavior implies increasing energy availability. This is supported by the fact that a sustained hypercortisolic state that lasted for at least 4 hours after the stimulation onset was observed in larvae exposed to prolonged vortex flow (Figure 3.15). As discussed in section 4.1.2, it is well known that GCs play a key role in mobilizing energy to facilitate performance of coping strategies in threatening situations (Sapolsky et al., 2000). Hence, it is reasonable to suggest that zebrafish larvae that are exposed to prolonged vortex flow stimulation respond with a sustained increase in cortisol levels that facilitate coping strategies to deal with the vortex flow perturbation. Interestingly, increased cortisol levels were not sustained for the entire duration of the prolonged vortex flow stimulation. After approximately 4 hours, cortisol levels decreased to basal levels. It has been proposed that if stressful situations persist after the "general alarm reaction" (release of stress-related chemicals in the blood), a "general adaptation syndrome" would occur in which the stress-related chemicals would go back to basal levels (Selye, 1936). This decrease in cortisol levels during prolonged vortex flow stimulation may be due to the slow negative feedback exerted by cortisol, where transcriptional regulation takes place at the three levels of the HPI axis, culminating in the termination of a stress response (Wendelaar Bonga, 1997). It is also possible that cortisol levels decreased to basal levels during prolonged vortex flows stimulation due to exhaustion of the endocrine system or to an habituation process (Hontela et al., 1992). This is supported by previous studies showing that interrenal tissue of fish exposed to chronic stress becomes less sensitive to ACTH, culminating in decreased cortisol secretion (Mommsen et al., 1999).

Cortisol response to an acute homotypic stressor was attenuated after prolonged vortex flow stimulation (Figure 3.16). Prolonged activation of the stress axis has been previously shown to induce attenuated stress responses in fish (Barton, 2002). One of the known mechanisms to mediate these changes in stress response is the transcriptional regulation of stress-related molecules such as CRH and ACTH, which culminate in reduced stress responses (Birnberg et al., 1983, Eberwine and Roberts, 1984, Imaki et al., 1991). Moreover, as discussed before, endocrine exhaustion or desensitization to CRH or ACTH may occur at the level of corticotrophs or interrenal glands, respectively (Hontela et al., 1992, Mommsen et al., 1999). Interestingly, the attenuated cortisol response to acute vortex flow observed on the following day of exposure to prolonged vortex flow stimulation was only present when the prolonged stimulation was delivered from 4 to 6 dpf; this indicates that the effects of prolonged vortex flow stimulation on cortisol response to subsequent homotypic stimulations depend on the developmental stage at which it is delivered, being inducible only in early stages of development.

Since prolonged vortex flow exposure induces hypercortisolic states, the changes in HPI axis activity after prolonged exposure to vortex flow stimulation may be mediated, at least in part, by overexposure to cortisol. Hence, any aspect leading to a reduced exposure to endogenous cortisol may be linked to a reduced vulnerability to changes in HPI axis activity. As shown in section 3.2, 8 dpf larvae show reduced levels of cortisol when exposed to acute vortex flow stimulation, a tendency which started to be detectable already at 7 dpf. Although in the present study the response to prolonged vortex flow stimulation was only measured in 5 dpf larvae, based on the data of acute response to vortex flow stimulation through development (Figure 3.11), it is reasonable to suggest that the meaning of the prolonged vortex flow stimulation is not the same for 7 dpf larvae than for younger stages; this may culminate in a reduced probability to induce changes in cortisol response to subsequent stressors.

Some potential explanations about why prolonged vortex flow stimulation induced changes in cortisol response when presented at 4, 5, and 6 dpf, but not when presented at 7 dpf are: 1) It is possible that the probability to induce changes in the cortisol response by early adverse experience is linked to the state of maturation of regulatory elements of the stress response, i.e. larvae younger than 8 dpf may be more susceptible to cortisol overexposure which would facilitate adaptive changes in HPI axis activity; 2) the maturation of the sensory system or integrating centers of sensory information may

also be linked to the probability of inducing HPI axis activity changes by exposing the larvae to prolonged vortex flow stimulation, i.e. older larvae may be more efficient in filtering and integrating sensory information, culminating in a more regulated cortisol response and avoiding overexposure to endogenous cortisol; 3) anatomical elements which facilitate coping with vortex flow perturbations may be more mature in later stages of development, reducing the cortisol demand to deal with the situation and maintain homeostasis. These three aspects are linked to the magnitude of the cortisol response at different developmental stages and therefore to the probability of overexposure to endogenous cortisol.

Other possible explanation for the attenuated cortisol response to acute vortex flow stimulation that was observed after prolonged vortex flow exposure may be related to a stress response habituation process. It is known that prolonged or repeated exposure to a homotypic stressor leads to a reduction in physiological response in comparison to the stress response elicited by acute exposure to the same type of stressor (Grissom and Bhatnagar, 2009). The fact that cortisol response to a heterotypic stressor (osmotic shock) was also attenuated (Figure 3.18C), suggests that the changes induced by prolonged vortex flow stimulation are not at the sensory system level but rather may be at the level of the integrating centers of sensory input or at the level of the HPI axis elements. When a habituation process occurs, it is sometimes possible that the habituation is generalized to heterotypic stimulations; however, it has been reported that for this criteria to be fulfilled, it is necessary that both types of stimulation are similar in modality (Grissom and Bhatnagar, 2009). The sensory systems involved in the perception and processing of the sensory input after osmotic stress or hydrodynamic flow stimulation present substantial differences (Fiol and Kultz, 2007, Montgomery et al., 1995). Hence, it is likely that the changes induced by prolonged vortex flow stimulation occur at the level of the integrating centers or at any of the HPI axis elements.

Changes at the level of hypothalamic cells in larvae previously exposed to the prolonged vortex flow stimulation were confirmed by measuring calcium activity of CRH cells during a heterotypic stressful event (osmotic shock) and by analyzing the number of cells expressing the stress-related peptides CRH, AVP, and OXT. The attenuated cortisol response observed after prolonged exposure to vortex flow stimulation is in line with the lower cell activity observed in hypothalamic cells and

reduced hypothalamic cell number expressing CRH, AVP, and OXT (Figure 3.21A-D) revealing a decreased HPI axis activity. Both decreased hypothalamic activity and decreased expression of these three peptides after chronic stress or early adverse experience have been reported previously and it is known that these processes are mediated, at least partially, by GCs (Erkut et al., 1998, Wismer Fries et al., 2005, Herman et al., 2008, Tasker and Herman, 2011). Since prolonged vortex flow stimulation induces sustained hypercortisolic states, overexposure to endogenous cortisol after prolonged stimulation may be linked to the reduced expression of the stress-related peptides in hypothalamic cells, and therefore also to the attenuated cortisol response to subsequent acute stimulations. Further experiments are needed to confirm this hypothesis. To achieve this, it is possible to deliver the prolonged vortex flow stimulation in the presence of a GR antagonist in order to inhibit GCs signaling and then ask whether the changes seen in cortisol response to acute stress and in hypothalamic cells are still detectable.

Altogether, these results showed that prolonged exposure to vortex flow stimulation induced sustained hypercortisolic states that culminated in reduced cortisol responses to subsequent acute stimulation of both homotypic and heterotypic nature. Importantly, the attenuated cortisol response was still detectable at 10 dpf. This was the case only when the prolonged stimulation consisted of 9 hours of continuous stimulation at 5 dpf, and not when the prolonged exposure was delivered in 9 pulses of 30 minute at the same developmental stage. This suggests that the effects of prolonged vortex flow stimulation depend on the format on which it is delivered. The reduced cortisol response observed at 6 dpf may be mediated by overexposure to endogenous cortisol, which presumably exerts its adaptive effects on hypothalamic cells through transcriptional mechanisms, culminating in reduced hypothalamic cell activity and reduced expression of stress-related peptides; this together may contribute to the attenuated cortisol response.

Hypocortisolemic stress response has been observed in patients with stress-related disorders such as post-traumatic stress disorder (PTSD), chronic fatigue syndrome (CFS), burn-out, and atypical depression (Fries et al., 2005). It has been proposed that an hyporeactive HPA axis might result from exposure to prolonged periods of stress accompanied with increased activity of the HPA axis and overexposure to GCs (Hellhammer and Wade, 1993). In rodents, chronic stress consisting of repeated restrain induces a shift from hyperactive HPA axis during the chronic stress period, to

hypoactive HPA axis 2 weeks after the offset of the chronic stress period (Fries et al., 2005). These adaptive changes may occur to protect the organism and reduce the impact of the potential deleterious effects of overexposure to GCs. It has been proposed that the change from hyper- to hypoactivity of the HPA axis may be mediated by 1) downregulation of receptors at different levels of the HPA axis that regulate the cascade of events after stress response activation, 2) reduced synthesis and/or depletion of stress-hormones at different levels of the HPA axis, and/or 3) increased negative feedback sensitivity to GCs (Hellhammer and Wade, 1993, Heim et al., 2000, Fries et al., 2005). Further experiments are needed to evaluate whether these mechanisms mediate the reduced cortisol response observed in 6 dpf larvae after prolonged exposure to vortex flow stimulation.

4.3.2 Prolonged vortex flow stimulation induces behavioral changes

Changes in cortisol profiles, hypothalamic cell activity, and expression of stress-related peptides after prolonged exposure to vortex flow stimulation were accompanied by changes in the behavioral output. Larvae exposed to the prolonged vortex flow stimulation showed increased basal locomotor activity. This is congruent with previous studies showing that swimming training during larval stages leads to increased swimming activity at basal conditions (Bagatto et al., 2001).

Although swimming activity was increased at basal conditions in larvae previously exposed to prolonged vortex flow stimulation, locomotor activity as a response to acute vortex flow stimulation onset was reduced. Figure 3.7 shows the relationship between the locomotor activity immediately after vortex flow stimulation onset and the peak of cortisol reached after the stimulation. Here, it was observed that prolonged vortex flow stimulation induced both a reduced locomotor activity after acute vortex flow stimulation onset and a reduced cortisol response, suggesting that this relationship is maintained; however, whether this is a causal relationship remains unclear.

Interestingly, the frequency distribution of the body angle orientation shown after acute vortex flow stimulation by larvae previously exposed to prolonged vortex flow stimulation was also different when compared to control larvae (Figure 3.20). Larvae previously exposed to the prolonged stimulation showed a narrower frequency distribution of body angle orientation. This suggests that more larvae were able to acquire a body angle orientation that presumably facilitates coping with the vortex flow

perturbation in a more efficient manner, potentially leading to a reduced cortisol demand. In this way, increased ability to acquire a particular body orientation to cope better with the vortex flows may be linked to the reduced cortisol response observed after prolonged vortex flow exposure.

4.4 Transcriptomics of hypothalamic and non-hypothalamic cells after prolonged exposure to vortex flow stimulation.

Transcriptomic analysis of whole body and tissue-specific hypothalamic cells coming from larvae previously exposed to prolonged vortex flow stimulation revealed substantial molecular changes when compared to control larvae. Molecular candidates likely to be involved in adaptive strategies after early adverse experience were identified. Moreover, gene ontology enrichment analysis showed that core pathways involved in lipid metabolism, immune response, and neurotransmitter and nervous system signaling were affected in hypothalamic cells. In the case of whole body cells, gene ontology enrichment analysis showed that pathways involved in cellular growth and proliferation, neurotransmitter and nervous system signaling, and glucose metabolism were affected. This is the first time a genome-wide transcriptome analysis is performed from tissue-specific cells from hypothalamus of developing larvae after early adverse experience. The results provide valuable insights into the potential mechanisms by which early adverse experience shapes the function of hypothalamic cells.

I optimized a cell isolation protocol for 6 dpf larvae using the transgenic line *Tg(otpECR6-E1b:mmGFP)* and fluorescent activated cell sorting (FACS). The cell dissociation protocol showed comparable results to previous studies which have reported cell isolation from zebrafish larvae (Manoli and Driever, 2012, Gallardo and Behra, 2013, Rougeot et al., 2014). This protocol successfully generated a single-cell suspension that allowed the isolation of around 60,000 cells identified as GFP+ coming from 500 zebrafish larvae. The transgenic line used in this study labels around 130-150 cells per larvae with GFP (personal communication Dr. Ulrich Herget); this indicates that for 500 larvae a total amount of cells ranging from 65-75 thousand cells should be present. The lower number of cells isolated may be due to several factors: 1) the dissociation protocol was not 100% efficient, since it generated 80% of single cells and 96% of viable cells; 2) there may be variations on the number of cells labeled with GFP; 3) false negative and false positive results while cell sorting may occur.

Importantly, the identity of the cells identified as GFP+ was confirmed successfully using fluorescence microscopy and levels of *oxt* expression by qPCR. GFP+ cells presented a much higher relative *oxt* expression than the one showed by cells identified as GFP-. Since expression of *oxt* is restricted to the hypothalamic region (Eaton et al., 2008, Herget et al., 2014), this confirms the identity of the isolated cells, supporting the feasibility of using these cells for further analysis. The RNA isolated from sorted cells and subsequent cDNA library preparation showed high quality (Figure 3.25 and 3.26). The generated raw reads from RNAseq ranged from 5.5 to 11.8 million pairs per sample, indicating that the data generated was suitable for further differential gene expression analysis of mid to high abundance gene transcripts; however, the number of generated reads may not be sufficient for identification of low abundant gene transcripts.

A direct comparison between the results from hypothalamic cells and non-hypothalamic cells should be done only after considering the implications of how the samples were obtained. While hypothalamic cells represent a tissue-specific sample, non-hypothalamic cells are a combination of all other cell types coming from whole body tissue (except hypothalamus). Hence, the differences observed in the differential gene expression analysis need to be interpreted with special care. For example, when a gene is identified as differentially expressed in hypothalamic cells, but not in non-hypothalamic cells, it does not necessarily mean that the gene is only differentially expressed in the hypothalamus; although in some cases these differences may be due to genes that are only expressed in the hypothalamic region, in other cases this may be due to a dilution effect resulting from the fact that non-hypothalamic cells samples consist of a combination of different cell types of diverse tissues. Therefore, results from non-hypothalamic cells samples should be considered as a robust indication at a global level about the effects of prolonged vortex flow exposure at early developmental stages. On the other hand, there are genes which were identified as differentially expressed in non-hypothalamic cells but not in hypothalamic cells; in these cases it can be proposed with more certainty that these differences may be due either to the lack of expression of those gene in the hypothalamic region or to the absence of an effect of the treatment in the hypothalamic region.

Of particular interest are those genes which were expressed in both hypothalamic and non-hypothalamic cells, but which showed opposite direction in their regulation.

Members of the solute carrier family 22 were downregulated in hypothalamic cells but upregulated in non-hypothalamic cells (s*lc22a2, sc22a6l, slc22a7b.1*); this group of proteins is involved in transporting endogenous substrates such as steroids, hormones and neurotransmitters across the cell membrane (Roth et al., 2012). Downregulation of these molecules at the hypothalamic level suggests that decreased transport of neurotransmitters may occur, leading to decreased cell activity. This was further supported by the function annotation analysis performed with the software IPA, where the category of "molecular transport" was ranked first on the list of categories with decreased activation state, showing 216 molecules involved and a z-score of -4.317. The decreased transport of molecules may underlie the lower calcium activity of hypothalamic cells observed after exposure to an osmotic shock in larvae which were previously exposed to the prolonged vortex flow stimulation.

The gene s*lc5a8l* was also found to be downregulated in hypothalamic cells but upregulated in non-hypothalamic cells. It has been reported that the protein encoded by this gene plays a key role in transporting l-lactate and ketone bodies across the cell membrane in neurons in order to maintain the energy requirements of the cell (Martin et al., 2006). In situations of intense neuronal activity, or when the energy demand is higher than the energy availability, glycogen in astrocytes is converted into lactate, which is then transported into the neurons to fulfill energy requirement (Falkowska et al., 2015). The prolonged vortex flow stimulation may induce a state in which energy homeostasis is compromised. Reduced expression of s*lc5a8l* in hypothalamic cells may be related to the reduced cell activity observed after prolonged vortex flow stimulation; it is possible that hypothalamic cells reduce their energy requirements after reducing its overall activity as indicated by calcium imaging and expression of other genes involved in neurotransmitter transport. On the other hand, the fact that s*lc5a8l* is upregulated in non-hypothalamic cells suggests that increased transport of lactate occurs potentially to supply cells with the energy required.

MicroRNA molecules miR-124-2 and miR-182 where identified as downregulated in hypothalamic cells but upregulated in non-hypothalamic cells. The molecule miR-124-2 is one of the most abundant microRNAs in the brain (Sun et al., 2015). It has been reported that miR124 targets anti-neuronal function of phosphatase SCP1, leading to reduced expression of the latter and therefore, to neurogenesis (Visvanathan et al., 2007). Moreover, it has been shown that reduced expression of miR-124 results in

changes of glutamate receptor composition, which leads to social dysfunction (Gascon et al., 2014). Gascon and colleagues showed that the mechanisms by which miR-124 homeostasis is disrupted involves the gene *Chmp2b* (charged multivesicular body protein 2B), which is a component of the endosomal sorting complex required for transport-III (ESCRT-III) involved in endosomal trafficking. They reported that in mice with increased activity of *Chmp2b*, decreased expression of miR-124 leads to increased levels of certain AMPAR (glutamate receptors) subunits (GLUA2, GLUA3, and GLUA4). Changes in these subunits mediate calcium permeability in the cell, leading to cell activity changes and consequently to dysfunctional behavior.

In the present study, several genes involved in glutamate signaling were differentially regulated. The glutamate ionotropic receptor NMDA type subunit 1 (g*rin1b*) was identified as downregulated in hypothalamic cells, but upregulated in non-hypothalamic cells. This gene encodes a subunit of the ionotropic glutamate receptor NMDA, which mediate the postsynaptic excitation after ligand binding allowing positively charged ions to flow through the cell membrane (Furukawa et al., 2005). The glutamate ionotropic receptor kainate 1a and 1b (g*rik1a*, g*rik1b*), and the glutamate ionotropic receptor AMPA type subunit 4b (g*ria4b*) were identified as downregulated only in hypothalamic cells. These genes encode glutamate receptor subunits which mediate excitatory neurotransmission and play key roles in synaptic function (Monyer et al., 1992, Seeburg et al., 2001, Lerma, 2003). Downregulation of these genes in hypothalamic cells suggest that the reduced hypothalamic cell activity observed in larvae previously exposed to the prolonged vortex flow stimulation (Figure 3.20A) may be due to a reduced input to the hypothalamus mediated by a reduction in glutamate signaling.

The molecular mechanisms mediating the effects of chronic or prolonged stress on glutamate receptor expression is largely unknown. However, it has been shown that the subtype composition, trafficking, and posttranslational regulation of the glutamate receptors are essential for synaptic plasticity (Kessels and Malinow, 2009, Lau and Zukin, 2007, Mabb and Ehlers, 2010). In particular, the ubiquitin pathway is involved in changes of synaptic transmission through posttranslational modification of the glutamate receptors and their interacting proteins (Mabb and Ehlers, 2010). In rodents, repeated stress reduced the number of glutamate receptors in PFC neurons through increased ubiquitin-proteasome-dependent degradation of *Gria1* and *Grin1*, a process

which relied on glucocorticoid receptor activation (Popoli et al., 2011, Yuen et al., 2012). Moreover, chronic exposure to corticosterone reduced expression of the glutamate receptor *Grin2b* and *Gria2/3* also in PFC neurons of rats (Gourley et al., 2009). In this way, chronic stress may alter membrane trafficking and/or synthesis and degradation of glutamate receptors, culminating in reduced glutamate transmission (Popoli et al., 2011). The main mechanism for downregulating transmembrane receptors, and hence downstream signaling, is by sorting the cell-surface proteins into multi-vesicular bodies (MVBs) through the ESCRT-I complex, a process that is regulated by ubiquitination (Raiborg and Stenmark, 2009, de Souza and Aravind, 2010). The MVBs then fuse with lysosomes and are degraded. In metazoan, the protein MVB12 (multivesicular body sorting factor of 12 kD) plays a key role for receptor endocytosis (Morita et al., 2007). This protein contains an UMA domain (UBAP-1-MVB12-associated) and a MABP domain (MVB12-associated β-prism). While the UMA domain recruits MVB12 to the ESCRT-I complex, the MABP domain has been suggested to be involved in the recognition of membranes and/or specific interaction with membrane components. It is likely that MABP domains act as adaptors that link other associated domains found in the same polypeptide to vesicular membranes (de Souza and Aravind, 2010).

In the present study, the molecule *si:dkey-30j10.5* was ranked first on the top upregulated molecules in hypothalamic cells after prolonged exposure to the vortex flow stimulation. This molecule showed a 20-fold difference in expression when compared with controls. After analyzing the protein sequence of *si:dkey-30j10.5* with Interproscan software, a MABP domain was identified. Interestingly, no other domain was identified in the same polypeptide. Further characterization of the protein needs to be performed in order to clarify its function. Nevertheless, it is likely that this protein is involved in the trafficking of MVBs and hence, in the downregulation of transmembrane proteins. This, together with downregulation of miR-124-2, may mediate the reduced expression of molecules involved in glutamate signaling and may contribute to the reduced activity of hypothalamic cells observed after prolonged exposure to vortex flow stimulation.

There were also genes identified as upregulated in hypothalamic cells but downregulated in non-hypothalamic cells. Among these genes is c*aspb*. This gene encodes the protein caspase b, which is the human ortholog of caspase 1 and is involved

in initiation of inflammatory responses and programmed cell death (Denes et al., 2012). This suggests that prolonged vortex flow stimulation induces an inflammatory response in hypothalamic cells; this is further supported by expression profiles in hypothalamic cells of other molecules involved in inflammatory response such as TNFα and IL1β, which were ranked 2nd and 9th on the top upregulated genes in hypothalamic cells (Table 7). Moreover, pathway enrichment analysis revealed that several canonical pathways involved in cellular immune response were enriched in hypothalamic cells from larvae that were exposed to prolonged vortex flow stimulation (Table 10). In the same way, among the predicted upstream regulators of the molecular changes found in hypothalamic cells after stimulation, several cytokines such as TNF, IFNG, IL1β, IL4, were predicted to be activated, suggesting an activation of the immune cellular response (Table 12). Additionally, functional annotation analysis of hypothalamic cells after prolonged vortex flow stimulation also revealed a predicted activation of inflammatory response (Table 15).

The molecule *si:dkey-29h14.10* was ranked 3rd among the upregulated genes in hypothalamic cells after prolonged exposure to the vortex flow stimulation. Analysis of the product of this gene with the Interproscan software revealed a caspase recruitment domain (CARD), suggesting that this molecule plays a role on programmed cell death and/or inflammatory response. Additionally, function annotation analysis revealed "cell death" as one of the top categories with increased activation in hypothalamic cells from larvae previously exposed to the prolonged vortex flow stimulation (Table 15). This, together with increased expression of caspase b, suggests that prolonged exposure to vortex flow stimulation increases apoptosis and/or inflammatory response, which may be linked to the decreased number of cells expressing CRH, AVP, and OXT that was observed in hypothalamic cells after prolonged exposure to vortex flow stimulation (Figure 3.21B-D). Moreover, this is in line with the hypoactivity of the HPI axis observed after prolonged exposure to vortex flow stimulation. GCs are essential players on the anti-inflammatory response (Coutinho and Chapman, 2011). Hence, hypocortisolic stress response may culminate in hyperactivity of inflammatory responses, due to the impaired inhibition of low GC levels (Heim et al., 2000, Fries et al., 2005). Further experiments need to be performed to evaluate apoptosis and inflammation in hypothalamic cells and confirm this hypothesis.

Interestingly, two genes encoding proteins from the myosin light chain family were upregulated in hypothalamic cells but downregulated in non-hypothalamic cells (*myl10* and *myl13*, table 6). Members of the myosin light chain family have been shown to interact with glutamate NMDA receptors and to be involved in the contractile and motile forces occurring during process such as synaptic plasticity and neuronal morphogenesis (Amparan et al., 2005). Moreover, annotation functional analysis revealed "Cellular movement" as the top function which showed an increased activation state in hypothalamic cells after prolonged exposure to vortex flow stimulation (Table 15). This suggests that vortex flow stimulation may induce changes in hypothalamic morphology, which could potentially lead to long lasting changes in its function.

Function annotation analysis of hypothalamic cells from larvae which were exposed to the prolonged vortex flow stimulation revealed a decreased activation of lipid metabolism. Dysfunction in brain lipid homeostasis may contribute to neurodegenerative diseases such as Alzheimer's disease, Huntington's disease, and Parkinson disease, among many others (Yadav and Tiwari, 2014). Among the lipid metabolism categories of function annotation analysis with a decreased activation state are "transport of cholesterol", "efflux of cholesterol", and "uptake of cholesterol" (Table 14). Cholesterol metabolism homeostasis has been shown to have a strong impact on neurodegeneration; modifications of cholesterol homeostasis may create favorable environments for the initiation or progression of neurodegenerative diseases (Anchisi et al., 2012). Moreover, there is evidence showing that lower levels of cholesterol in neurons may culminate in neurodegeneration (Anchisi et al., 2012). This suggests that prolonged vortex flow stimulation may induce detrimental effects on hypothalamic cells. In line with this, apolipoprotein E gene (*apoe*) was significantly downregulated in hypothalamic cells, but not in non-hypothalamic cells. The protein encoded by this gene is an essential regulator of cholesterol metabolism and the main carrier of cholesterol in the brain (Puglielli et al., 2003, Sato and Morishita, 2015). Moreover, *apoe* is one of the strongest genetic risk factor for sporadic Alzheimer's disease and it has been linked to post-traumatic stress disorder (PTSD), a condition closely related to HPA axis function (Ashford, 2004, Johnson et al., 2015). It has been shown that *Apoe* deficiency in transgenic mice ($Apoe^{-/-}$) culminates in dysregulation of the HPA axis (Raber et al., 2000). This together, suggests that prolonged vortex flow stimulation induces changes in lipid homeostasis in hypothalamic cells, which may have

further effects on hypothalamic neuronal function and therefore on stress response activity.

Moreover, decreased cholesterol metabolism may reduce steroidogenesis, which has been linked to detrimental health conditions such as PTSD, anxiety spectrum disorders, and depression (Pinna, 2013). Specifically, reduced levels of the hormone allopregnanolone have been related to these disorders, and administration of this hormone has been shown to reduce HPA axis activity and have anxiolytic and antidepressant effects (Rouge-Pont et al., 2002, Wirth, 2011). In the present study, the molecule *srd5a2* was downregulated in hypothalamic cells from larvae previously exposed to prolonged vortex flow stimulation. This gene encodes the enzyme 5α-reductase 2, which is involved in the first step of allopregnanolone biosynthesis by converting progesterone into 5α-dihydroprogesterone (Reddy, 2010). This further suggests that prolonged vortex flow stimulation induced detrimental states in hypothalamic cells which may culminate in dysregulation of the stress response reactivity.

The canonical pathway "FXR/RXR activation" was ranked first after enriched pathway analysis. The fernesoid X receptor (FXR) is activated by bile acids and their intermediates, and therefore functions as a bile acid sensor (Zhang and Edwards, 2008). This receptor is a member of the nuclear family of receptors and, together with the retinoid X receptor (RXR), plays a key role in a wide range of metabolic pathways linking bile acid levels with lipid and glucose metabolism (Zhang and Edwards, 2008). The hepato-biliary system regulates cortisol clearance (Vijayan and Leatherland, 1990). Since prolonged vortex flow stimulation induced a sustained hypercortisolic state during the stimulation at 5 dpf, it is possible that the hepato-biliary system activity was increased to process the increased cortisol levels. It has been shown that increased bile acids can penetrate the brain blood barrier and alter peptide expression in hypothalamic cells, resulting in attenuated CRH expression and repression of the HPA axis (McMillin et al., 2015, Piekarski et al., 2016). This together, suggests that prolonged vortex flow stimulation results in altered FXR/RXR signaling in hypothalamic cells which may culminate in metabolic changes and dysregulation of the HPA axis.

4.5 Functional characterization of optogenetic and genetically targeted ablation tools for manipulating HPI axis activity

Our laboratory has developed optogeneitc and genetically targeted ablation tools in order to manipulate HPI axis activity in freely swimming zebrafish larvae in a non-invasive manner. In the present study, I showed evidence of altered levels of endogenous cortisol in larvae that were manipulated at any of the three levels of the HPI axis. Expression of the protein bPAC specifically in pituitary corticotrophs resulted in enhanced cortisol levels after blue light exposure when compared to control larvae. It is important to note that exposure to blue light induced a cortisol response also in larvae which did not express bPAC; however, this cortisol response was of lower magnitude. Importantly, the cortisol levels reached after blue light stimulation in bPAC+ larvae are kept in a physiological range. Moreover, by amplifying only the GC response through enhanced corticotroph cell activity, no other upstream processes are altered. This facilitates the study of the effects of enhanced levels of ACTH and GC on upstream elements, such as the hypothalamus, in a more natural context.

Repeated exposure to blue light stimulation resulted in blunted cortisol response in bPAC- larvae after the first stimulation. This is in line with the results described in section 3.2.2, where repeated exposure to vortex flow stimulation in 6 dpf larvae failed to elicit a cortisol response of the same magnitude then the first one (inter-trial interval: 30 min). Previous work in our laboratory showed that the blunted cortisol response observed in bPAC- larvae was mediated by GR signaling, since incubation in the GR antagonist mifepristone resulted in a higher cortisol response, suggesting that the GC negative feedback is activated (De Marco et al., 2013). Interestingly, bPAC+ larvae did respond with increased cortisol levels to each of the blue light stimulations, indicating that optogeneitc manipulation of corticotroph cells can be used to induce sustained hypercortisolic states even if the HPI axis has been downregulated due to previously elevated GC levels. Similarly, amplified HPI axis activity in response to blue light was observed when bPAC expression was targeted to steroidogenic interrenal cells. However, further experiments are needed in order to evaluate whether repeated blue light exposure leads to sustained hypercortisolic states when bPAC is expressed in these cells.

Genetically targeted cell ablation of either hypothalamic NPO cells or steroidogenic interrenal cells resulted in reduced cortisol levels after Met treatment. Work in our

laboratory has confirmed the specific cell ablation for both transgenic lines by TUNEL and immunohistochemistry (Gutierrez-Triana et al., 2014, Gutierrez-Triana et al., 2015). Importantly, in the case of steroidogenic interrenal cell ablation, chromaffin cells were not affected; this represents an advantage when compared with traditional adrenalectomy methods, where the entire adrenal gland is surgically removed, resulting in extraction of both steroidogenic and chromaffin cells, which adds an extra variable to the experimental design.

Interestingly, there were some differences in cortisol profiles depending on what type of cells were ablated. Ablation of NPO cells did not affect cortisol levels at basal conditions. On the other hand, ablation of steroidogenic interrenal cells resulted in a significant reduction of cortisol levels at basal conditions. This is in line with several previous studies showing the association between the suprachiasmatic nucleus in the hypothalamus, the circadian clock in the adrenal glands, and basal cortisol levels, indicating that cortisol levels at basal conditions are not exclusively under the control of the NPO/PVN activity (Dickmeis, 2009, Chung et al., 2011).

Stress-induced cortisol levels were also different depending on which cell type was ablated. Although Met treatment induced a reduction in cortisol response also in larvae that did not express nfsB (no cell ablation), cortisol levels were lower in NPO-ablated larvae and completely blunted in larvae with ablated steroidogenic interrenal cells. Importantly, the reduced stress-induced cortisol levels induced by Met treatment in control larvae may be mediated by a reduced volume of the rostral pituitary *pomc* and interrenal *StAR* clusters, and not to a reduced cell number (Gutierrez-Triana et al., 2015). The fact that ablation of NPO cells was not sufficient to completely abolish stress-induced cortisol response is in line with several other studies showing that extra-pituitary and pituitary hormones (different from ACTH) may play a role in controlling plasma cortisol levels. This together suggests that other compensatory regulatory mechanisms may be involved in cortisol release after stress exposure (Mommsen et al., 1999).

5. CONCLUSION

In this thesis, I developed and characterized vortex flow stimulation as a suitable, non-invasive tool to activate the HPI axis in developing zebrafish in a strength-dependent manner, reducing handling effects, and avoiding unspecific effects of the stimulation. This type of stimulation can be readily delivered transiently in short bursts, facilitating the analysis of the effects of repeated activation of the HPI axis and the mechanisms underlying this process. Moreover, since it can be applied in freely swimming larvae, behavioral outputs that result from HPI axis activation can be studied.

Using this stimulation, I characterized the ontogeny of the HPI axis activity and revealed that the strength-dependent cortisol response changes substantially through development. Importantly, I identified a dynamic maturation process of the cortisol response occurring from 4 to 8 dpf, which potentially occurs at the level of HPI axis regulatory elements, sensory systems, and/or anatomical elements that facilitate stress coping strategies.

Prolonged exposure to vortex flow stimulation delivered to 5 dpf larvae as an early life stress paradigm induced an overall downregulation of the HPI axis activity at the endocrinological, behavioral, and cellular level. Transcriptomic analysis of hypothalamus-specific cell populations identified downregulation of glutamate signaling, molecular transport, and lipid metabolism as potential mechanisms to mediate the reduced activity of these cells. Additionally, increased expression of molecules involved in inflammatory response and programmed cell death may contribute to the reduced hypothalamic cell activity and therefore to the reduced cortisol response observed after prolonged exposure to vortex flow stimulation.

Finally, this thesis contributed to the development of optogenetic and targeted transgenic tools suitable to manipulate all three elements of the HPI axis in a non-invasive manner. Manipulation of these elements resulted in altered exposure to endogenous cortisol (hypo- or hypercortisolemia), providing a valuable platform to study the effects of rapid and non-rapid negative feedback mediated by GCs as well as the effects of both acute and prolonged exposure to GCs.

Altogether, this work provides evidence that zebrafish is a suitable model to study developmental programming of the HPI axis in a highly controlled fashion. By taking

advantage of the versatility of the zebrafish model and of the molecular tools available for its manipulation, further studies will be able to reveal detailed mechanisms underlying developmental programming of the HPI axis elements after early adverse experience. This knowledge is essential to understand the link between early life stress, dysregulation of the stress response, and subsequent development of stress-related disorders such as PTSD, anxiety, and depression. This will open new avenues for the development of more comprehensive treatments and preventive measures against these disorders.

6. OUTLOOK

Vortex flow stimulation is a valuable tool to activate zebrafish larvae HPI axis and induce changes in its activity. In the present study, in order to identify potential mechanisms involved in the adaptive processes occurring after early adverse experience, I focused on the analysis of molecular changes observed relatively shortly after prolonged exposure to vortex flow stimulation; this was done in this way under the assumption that all adaptive mechanisms which are activated during or shortly after the stimulation are necessary for regulating or maintaining homeostasis, i.e. if any of these mechanisms are disrupted, it would potentially lead to dysfunction. Hence, the molecular changes observed in hypothalamic and non-hypothalamic cells after prolonged exposure to vortex flow stimulation include both transient adaptive changes and potential long-lasting changes. Therefore, further complementary work will evaluate juvenile zebrafish which had been exposed to prolonged vortex flow stimulation in order to elucidate which of the molecular changes observed in the present study are transient adaptive processes and which present a more persistent change through development.

Moreover, future work will study what aspects of the stimulation are driving the molecular changes observed in hypothalamic and non-hypothalamic cells. Potential aspects of the prolonged vortex flow stimulation that may be driving the molecular changes observed in hypothalamic cells include: 1) Overexposure to endogenous GC; 2) increased excitatory input to hypothalamic cells coming from sensory integrational centers in the brain; 3) metabolic challenge due to increased energy demand and limited nutritional resources.

To elucidate whether the molecular changes observed in hypothalamic cells are mediated by overexposure to GCs or by increased excitatory input to hypothalamic cells, our laboratory has generated a plethora of molecular tools to manipulate all three levels of the HPI axis in zebrafish larvae. Optogenetic manipulation at the pituitary and interrenal gland level has been demonstrated effective for inducing hypercortisolic states in zebrafish larvae while minimizing sensory inputs which may otherwise culminate in activation of upstream integrational centers in the brain (section 3.5) (De Marco et al., 2013, Gutierrez-Triana et al., 2015). Moreover, our laboratory has developed molecular tools which allow the ablation of interrenal gland cells, culminating in blunted stress-induced cortisol release (Section 3.5) (Gutierrez-Triana et al., 2015). Altogether, these molecular and optogenetic tools will be essential for dissecting the role of overexposure to endogenous GCs and increased excitatory input to hypothalamic cells on the molecular changes observed after prolonged exposure to vortex flow stimulation.

Of particular interest is the study of the top differentially regulated molecules identified by transcriptome analysis of hypothalamic cells after prolonged exposure to vortex flow stimulation. These molecules represent strong candidates to be key players of the changes observed in HPI axis activity at the endocrinological and hypothalamic cell activity level and therefore also potential candidates to mediate developmental programming processes.

Overall, future experiments will address three questions: 1) what are the dynamics of the adaptive processes induced by early adverse experience, i.e. which processes are transient and which are long-lasting? 2) What are the mediators involved in the regulation of the differentially regulated molecules after early adverse experience? And 3) what is the role of these molecules in altered HPI axis activity?

7. MATERIALS AND METHODS

7.1 Materials

7.1.1 Buffers and solutions

Buffers and solutions	
Name	Composition
4 % Paraformaldehyd (PFA)	40 g PFA in 1 L PBS. Make aliquots and store at -20°C.
Anti-Cortisol monoclonal antibody	40 µg/mL Cortisol mAB in 1x PBS and store at -20°C. Dilute to 1.6 µg/mL with 1x PBS upon use.
Blocking buffer	0.1% BSA in PBS.
Citrate Buffer (205 mmol/L)	21.53 g Citric acid monohydrate in 300 mL milli-Q-H_2O. Adjust with NaOH to pH = 4.5 add milli-QH_2O to 500 mL and store at 4 °C.
Cortisol-HRP	1 mL of cortisol-HRP (see section 6.1.2) and add 1x PBS to reach a total volume of 20 mL. Store at 4°C.
Cortisol stock solution (50 µg/ml)	Dissolved 1 mg cortisol in 1 mL EtOH and add 19 mL 1x PBS. Store at -20°C in BSA blocked tubes.
Embryo-Medium 2 (E2), modified	5 mM NaCl, 0.25 mM KCl, 0.5 mM $MgSO_4$x7 H_2O, 0.15 mM KH_2PO_4, 0.05 mM Na_2HPO_4, 0.5 mM $CaCl_2$, 0.71 mM $NaHCO_3$ To make 1 L 0.5x E2:5 mL E2-A, 1 mL E2-B, 1 mL E2-C into 950 mL milli-Q-H_2O. pH was adjusted to 7.0. Make final volume to 1 L with milli-Q-H_2O.
E2-A	14.61 g NaCl, 0.933 g KCl, 6.163 g $MgSO_4$ × 7 H_2O, 1.02 g KH_2PO_4, 0.355 g Na_2HPO_4. Add milli-Q-H_2O to 250 mL. Make 5 mL aliquots, store at -20°C.
E2-B	3.675 g $CaCl_2$ and add milli-Q-H_2O to 50 mL make 1 mL aliquots, store at -20°C.
E2-C	2.99 g $NaHCO_3$ add milli-Q-H_2O to 50 mL make 1 mL aliquots, store at -20°C.
Egg water	3 g Red Sea Salt in 10 L ddH_2O.
Mifepristone (50 mM)	Disolve in DMSO and make aliquots. Store at -20°C.
PBS (20x)	160 g/L NaCl, 4 g/L KCl, 28.8 g/L Na_2HPO_4, 4.8 g/L KH_2PO_4.
PTU	0.03 % 1-phenyl-2-thiourea in egg water buffer.
Sample-Buffer	0.2% BSA in PBS.
Staining solution A (TMB; TBABH)	41 mM TMB and 8 mM TBABH in DMA. Store at 2-8°C and protected from light.
Staining solution B	3.14 µL 30% H_2O_2 (3.075 mM) in 10 ml Citrate-Buffer and store at 2-8°C, protected from light (up to 1 month).
Staining solution for ELISA	200 µL solution A, 8 mL solution B. Protect from ligth.
Stop solution	1M sulfuric acid.
Tricaine solution	4 g/L tricaine powder, 25 mL 1M Tris-HCL, pH 7
Wash buffer ELISA	1x PBS, 0.05 % Tween-20
Washing solution cell dissociation	7.5 µL DNase I (10 KU)in 1 mL PBS

7.1.2 Chemicals and other reagents

Chemicals and other reagents	
Name	Supplier
3,3',5,5'-Tetramethylbenzidine (TMB), ultra pure	Biomol GmbH
Albumin from bovine serum, ≥ 98%	Sigma-Aldrich Chemie GmbH
Citric acid monohydrate, p. a. ≥ 99.5%	Roth
Cortisol-HRP conjugate	EastCoast Bio, Inc.
DNase I from bovine pancreas 10KU	Sigma-Aldrich Chemie GmbH
DMSO	Sigma-Aldrich Chemie GmbH
Ethanol absolute, p.a. ≥99,8%	Sigma-Aldrich Chemie GmbH
Ethyl acetate, p. a. ≥99,5%	Fluka Chemie GmbH
FACSmax cell dissociation solution	Amsbio
Hydrogen peroxide, 30 %, p.a.	Merck KGaA
Magnesium sulfate heptahydrate, p.a., ≥99,5 %	Merck KGaA
Metronidazole	Sigma-Aldrich Chemie GmbH
Mifepristone, RU-486	Sigma-Aldrich Chemie GmbH
N,N-dimethylacetamide, p. a. ≥99,5%	Sigma-Aldrich Chemie GmbH
Propodium Iodide	Sigma-Aldrich Chemie GmbH
Sodium chloride, p. a. ≥99,5%	Merck KGaA
Tricaine, MS-222	Sigma-Aldrich Chemie GmbH
Sulfuric acid, p.a., 95- 97%	Fluka Chemie GmbH
Tetrabutylammonium borohydride, 98% (TBABH)	Sigma-Aldrich Chemie GmbH
Tween-20	Roth
α-Cortisol monoclonal antibody	EastCoast Bio, Inc.

7.1.3 Commercial kits

Commercial kits	
Name	Supplier
Agencourt AMPure XP	Beckman Coulter, Life Sciences
Cortisol Saliva ELISA kit	IBL International
Dnase PureLink Set	Life Technologies, Ambion
KAPA HiFi PCR kit	Kapa Biosystems
Nextera XT Index Kit	Ilumina
Nextera XT Sample Preparation Kit	Ilumina
MessageAmp II aRNA Amplification Kit	Life Technologies
Power SYBR Green RNA-to-CT 1-Step kit	Thermo Fisher Scientific
Power SYBR Green PCR Master Mix	Thermo Fisher Scientific
Rneasy Micro Kit	Qiagen
RNA 6000 Pico kit	Agilent Technologies

7.1.4 Consumables and equipment

Consumables and equipment		
Name	Supplier	Catalog / Model
7500 Real-time PCR System	Applied Biosystems	
Camcorder	Sony	HDR-CX240 HD Flash
Cell strainer 40µm	Sigma-Aldrich Chemie GmbH	Corning, CLS431750-50EA
Centrifuges	Heraeus Labofuge	400 R
	Eppendorf	5417R
ELISA plate reader	Thermo scientific	Multiskan Ascent
ELISA plates, Flat-bottom	VWR International GmbH	Immulon 2 HB, 735-0462
FACS tube with cell strainer	neoLab Migge GmbH	BD Falcon 352235
Fluorescence stereomicroscope	Leica	MZ16
Incubator	Rubarth Apparate GmbH	RuMed 3101
Light glass filters 550nm	Thorlabs	FGL550S
Magentic stirrer plate	Thermo scientific	Variomag Poly 15
Magnetic stir bar 6x3 mm	Fischer scientific	11888882
Microscope Laser scanning confocal	Leica	SP5
Orbital shaker	Heidolph	Polymax 2040
Pestles	VWR International GmbH	431-0094
Pestle motor	VWR International GmbH	431-0100
Petri dishes Ø=35mm		
pH-meter	Knick	766 Calimatic
Thermomixer	Eppendorf	Thermomixer compact 5350
Vacum concentrator	Eppendorf	Vacufuge 5301
Vacum pump	Vacuubrand GmbH	PC2004

7.1.5 Fish lines

Fish strains		
Strain	Description	Reference
AB/TL	Wild type.	
*otp*ECR6:GFP	NPO marker (hypothalamus).	Gutierrez-Triana et al. , 2014
otp:ECR6:nfsB-GFP	Nitroreductase-Metronidazole system for NPO cell ablation.	Gutierrez-Triana et al. , 2014
2kb*StAR*:bPAC	Optogenetic manipulation of steroidogenic interrenal cells.	Gutierrez-Triana et al., 2015
2kb*StAR*:nfsB-GFP	Nitroreductase-Metronidazole system for steroidogenic interrenal cell ablation.	Gutierrez-Triana et al., 2015
pomc:bPAC	Optogenetic manipulation of corticotrophs	De Marco et al., 2013

7.1.6 Riboprobes

Riboprobes				
Target	Plasmid	Enzyme	Polymerase	Reference
avp	zVasotocin	EcoRI	Sp6	Eaton et al. , 2008
crh	pCRII-CRH	NotI	Sp6	Löhr et al., 2009
oxt	zIsotocin	SalI	Sp6	Eaton and Glasgow, 2006

7.1.7 Primers for real time qPCR

Primers for qPCR		
Target	Sequence forward (F) and reverse (R)	Reference
Ef1 alpha	F - 5'-CTG GAG GCC AGC TCA AAC GT-3' R - 5'-ATC AAG AAG AGT AGT ACC GCT AGC ATT AC-3'	Yeh, 2015
mep1a.2	F - 5'-CAG AAG CTT TAC CAC TGA TGC-3' R - 5'-AAG CAA AGG CAA CTA TCA TCC-3'	GETPrime
mfsd4b	F - 5'-CTA TCT TTC TGC AGG CTC TG-3' R - 5'-CGG ATA TGA AAG GCT CTG C-3'	GETPrime
nr3c1	F - 5'-ACA GCT TCT TCC AGC CTC AG-3' R - 5'-CCG GTG TTC TCC TGT TTG AT-3'	GETPrime
oxt	F - 5'-CGG CCT GCT ACA TCT CAA AC-3' R - 5'-TGC CTT CAC CAC AGC AGA TA-3'	GETPrime
rsad2	F - 5'-GCT GAA AGA AGC AGG AAT GG-3' R - 5'-AAA CAC TGG AAG ACC TTC CAA-3'	Briolat et al. 2014
stc1l	F - 5'-CCA AGC CAC TTT CCC AAC AG-3' R - 5'-ACC CAC CAC GAG TCT CCA TTC-3'	Chou et al. 2015

7.1.8 Software

Software	
Name	Company/Institution
7500 Software v. 2.0.6	Applied Biosystems
Amira 5.3, 5.4, 5.6	FEI VSG
Ascent software 2.6	Thermo scientific
GETPrime	Swiss Federal Institute of Technology in Lausanne
Image J 1.48v	National Institute of Health, USA
InterProScan	EMBL-EBI
Ingenuity Pathway Analysis (IPA)	Qiagen
Leica LAS AF	Leica Microsystems
Oriana v 4.02	Kovach Computing Services
Prism 6	GraphPad Software Inc.

7.2 Experimental procedures

7.2.1 Fish maintenance

Maintenance and breeding of AB/TL wildtype zebrafish (Danio rerio) were performed under standard conditions at 28.5°C (Westerfield, 2000). All procedures were performed according to the guidelines of the German animal walfare law and approved by the local government. Zebrafish embryos were obtained by random mating between one male and one female which were set one day before in a container where the fish were separated by a plastic divider. The divider was removed on the following day at 9-10 a.m. Embryos were collected within 2-3 after the divider was removed and placed in petri dishes (Ø=100mm) with E2 medium for later sorting in small petri dishes (Ø=35 mm). Groups of 30 embryos were sorted in the small petri dishes containing 5 mL of E2. Zebrafish embryos were kept in an incubator (Rubarth Apparate GmbH, RuMed 3101) with a 12h/12h light/dark cycle at 28°C (lights on at 9 a.m.). At 3 dpf, chorions and other debris were removed with a pipette and E2 medium was replaced with fresh one. No feeding was provided in the petri dishes. These conditions were kept in experiments performed in 4-8 dpf larvae. For experiments in older stages, groups of 30 zebrafish larvae were transferred at 6 dpf at 3:00 p.m. to plastic cages (5 L) containing 400 mL of egg water. Larvae were fed using standard procedures and maintained at 28°C until the day of the experiment (10 dpf).

7.2.2 Exposure to stressors

7.2.2.1 Vortex flow stimulations

Acute exposure

Groups of 30 larvae were contained in small petri dishes with 5mL of E2 media. In order to avoid handling on the day of the experiments, a small magnetic stir bar (6 x 3mm; Fisher scientific) was placed in the petri dishes one day before the stimulation and immediately placed on top of a magnetic stirrer plate (Variomag Poly 15; Thermo scientific) inside an incubator (28°C). Control groups were managed in the same way, but placed on a second magnetic stirrer plate of the same model and specifications in order to avoid perturbations on the day of the experiment. On the day of the stimulation, larvae of the required age (4-8 dpf) contained on the small petri dishes were exposed to vortex flow stimulation of either 1, 3, or 6 minutes; the strength of the magnetic field

inversion was controlled on the magnetic stirrer plate and ranged from 130 to 530 rpm. Samples were either recorded for later behavioral analysis or immobilized with ice water and collected at the required time after stimulation onset for cortisol extraction. For experiments in 10 dpf larvae, plastic cages (5 L) containing the larvae were placed on top of the magnetic stirrer plate on the day of the stimulation; three magnetic stir bars (150 x 50 mm) were placed distributed along the plastic cage. Larvae were exposed to 3 minutes of vortex flow stimulation with a strength of 330 rpm. Samples were immobilized with ice water and collected for cortisol extraction 10 minutes after the stimulation onset. All experiments were performed between 11 a.m. and 2 p.m.

Repeated exposure (including mifepristone treatment)

For repeated vortex flow stimulation, all steps described in last section (7.2.2.1. acute exposure) were followed with some modifications. Larvae were exposed for 3 minutes to a vortex flow stimulation generated by 330 rpm of magnetic field inversion. Instead of sample collection after 10 minutes of acute stimulation onset, petri dishes containing the larvae of the desired age were left on the magnetic stirrer plate after acute vortex flow stimulation. A second stimulation of the same characteristics was delivered either 30 or 60 minutes after onset of the first stimulation. Samples were immobilized with ice water and collected for cortisol extraction 10 minutes after the second stimulation onset (40 or 70 minutes after first stimulation onset). All experiments were performed between 11 a.m. and 2 p.m.

Prolonged exposure

Prolonged exposure to vortex flow stimulation was carried out in small petri dishes (Ø=35 mm) containing 30 larvae each. The dishes containing the larvae were placed on top of a magnetic stirrer plate (Variomag Poly 15; Thermo scientific) and a magnetic stir bar (6 x 3mm; Fisher scientific) was placed on each of the dishes. Prolonged vortex flow stimulations were started at 11 a.m. and consisted of 9 pulses with an inter-trial interval of 60 minutes of either 5 or 30 minutes length, or 9 hours of continuous stimulation; strength of the stimulation was fixed at 330 rpm. Prolonged stimulations were delivered in 4-7 dpf larvae. Control larvae were placed on top of the magnetic stirrer plate and exposed to the magnetic field without a magnetic stir bar. At the end of the prolonged vortex flow stimulation, samples were prepared for the following day depending on further experiments to be performed.

7.2.2.2 Osmotic shock

Groups of 30 embryos were sorted in small petri dishes (Ø=35 mm) with 5 mL of E2 media. In order to minimize handling on the day of the experiments, E2 medium was adjusted to 4 mL one day before the experiment. On the day of the experiment, 1 mL of a 5X NaCl solution of concentration 50mM or 250mM was added to each experimental petri dish containing the larvae of the desired age. For control larvae, 1 mL of pre-warmth (28°C) E2 medium was added. Larvae were incubated for 10 minutes in the solution inside the incubator (28°C). Larvae were immobilized with ice water after the incubation time and collected for cortisol extraction. All experiments were performed between 11 a.m. and 2 p.m.

7.2.3 Cortisol measure

7.2.3.1 Cortisol extraction

Cortisol extraction was performed as described elsewhere (Yeh et al., 2013). Briefly, upon collection, samples were immobilized with ice water, frozen in an ethanol-dry ice bath after medium was removed, and stored at -20°C until cortisol extraction was performed. For extraction, samples were thawed on ice and 150 µL of milli-Q-H2O was added into each tube. Samples were homogenized with a motor pestle (VWR-International) for 20 seconds. After homogenization, 1 mL of ethyl acetate was added to each sample and they were vortexed at maximum speed for 30 seconds. Samples where then centrifuged at 3000x g at 4°C for 5 minutes for solvent and aqueous phase separation. The aqueous phase was frozen in an ethanol/dry ice bath and the solvent phase, which contained the extracted cortisol, was transferred into a new tube (1.5 mL). To evaporate the ethyl acetate, samples were placed in a vacuum concentrator (Eppendorf, Vacufuge 5301) for 30 minutes at 30°C. Cortisol was re-dissolved in 60 µL of sample buffer (0.2% BSA in PBS) and samples were frozen at -20°C for at least 6 hours before using them for cortisol ELISA. To prepare the samples for cortisol ELISA, the tubes were thawed at room temperature and then mixed at 1200 rpm and 37°C for 5 minutes in a thermomixer (Eppendorf). Samples were then spun down and directly used for cortisol ELISA.

7.2.3.2 Cortisol ELISA

Cortisol measurements were performed by ELISA as described elsewhere (Yeh et al., 2013). Briefly, 96-well plates (Immulon 2 HB, VWR International) were pre-coated with cortisol monoclonal antibody (1.6 μg mL^{-1}; EastCoast Bio, Inc.) overnight at 4°C. On the following day, unbound cortisol monoclonal antibody was washed three times with washing buffer (0.05% tween-20 in PBS). After drying by inverted tapping into a paper towel, 250 μL of blocking buffer (0.1% BSA in PBS) was added into each well and the plate was incubated for 30 minutes at room temperature in an orbital shaker. The plate was then washed three times with washing buffer and dried using the same method. Samples and standards were loaded to the corresponding wells (50 μL into each well); subsequently, 50 μL of conjugate cortisol-HRP (1:80 dilution from stock; EastCoast Bio, Inc.) was added into each well and the plate was covered and incubated at room temperature for 2 hours. After incubation, the plate was washed three times with washing buffer and dried as before. Each well then received 100 μL of TMB substrate (staining solution) prepared by mixing 200 μL of solution A and 8 mL of solution B not longer than 30 minutes before usage. The plate was incubated for 20 minutes and the reaction was stopped with 100 μL of 1M sulfuric acid (stop solution) in each well. Immediately after adding the stop solution, absorbance was read at 450 nm in a microplate reader (Multiskan Ascent, Thermo Scientific). The data were corrected for dilution factor, extraction efficiency, and recovery function.

7.2.4 Behavioral analysis – Video analysis

Behavioral analysis during or after vortex flow stimulation were performed in 5 or 6 dpf AB/TL wildtype larvae, depending on the experiment. Groups of 30 larvae contained in small petri dishes (Ø=35 mm) were placed on a magnetic stirrer plate inside an incubator (Rubarth Apparate GbmH, RuMed 3101) and recorded with a camcorder (Sony, HDR-CX240 HD) from above. Videos were analyzed using the software ImageJ 1.48v (National Institute of Health, USA) and the plugin MTrackJ (Meijering et al., 2012).

7.2.4.1 Distance swam

Total distance swam and speed were calculated by the software plugin MTrackJ after calibration with the measures of the arena and specification of the time length per

frame (0.08s frame^{-1}). For evaluating the trajectories and speed of anesthetized larvae during vortex flow stimulation of different strengths (130, 330, and 530 rpm), individual animals (6 dpf) were placed in a small petri dish containing 5 mL of E2 medium with 100 μL of Tricaine solution and a magnetic stir bar. Larvae were considered to be anesthetized when they failed to respond to tactile stimulation. Video recordings were obtained for each condition and 30 consecutive frames taken one minute after vortex flow stimulation onset were considered for analysis using the tracking tool of the plugin MTrackJ.

To evaluate total distance swam after acute vortex flow stimulation exposure in freely swimming larvae, groups of 30 larvae (6 dpf) contained in small petri dishes with 5 mL of E2 medium were exposed to 130, 330 or 530 rpm of vortex flow stimulation for three minutes. Video recordings were five minutes in length (starting one minute before stimulation onset and finishing one minute after stimulation offset). The plugin MTrackJ was used to track individual larvae and the total distance swam was calculated based on the tracking data after calibration. For some analysis, the mean of the total distance swam during the first 10 seconds after the stimulation onset was calculated and used for statistical comparisons. Similarly, the mean of the total distance swam during the first 10 seconds after the stimulation offset was calculated and used for further comparisons. To evaluate total distance swam during prolonged continuous exposure to vortex flow stimulation (9 hours of continuous vortex flow stimulation), groups of 30 larvae (5 dpf) were placed in small petri dishes and videos were recorded starting either before stimulation onset, 5 minutes after prolonged stimulation onset, or 8.5 hours after prolonged stimulation onset. Analysis was performed as described before for acute vortex flow stimulations with one modification: the mean of the total distance swam during a period of time of 30 seconds was used for comparisons.

7.2.4.2 Distance to vortex origin

Distance to vortex origin was calculated by the software plugin MTrackJ after calibration with the measures of the arena and establishment of the magnetic stir bar as the reference point.

7.2.4.3 Body angle orientation

Body angle orientation was measured by analyzing the recorded videos with the software ImageJ 1.48v (videos used for measuring distance swam, described above). Body axis angle was measured by drawing a line along the larva's axis from the tail to the head (point between the larva's eyes); then, a second line from the head of the larvae to the origin of the vortex flow (center of the dish) was drawn. The value of the angle was automatically stored by the software and the orientation of the larvae, i.e. facing towards or against the water flow, was manually documented. The measures were performed in two ways: 1) to evaluate frequency distribution of body angle orientation at a specific time point, three measures (10 seconds apart) were taken starting at two minutes after the onset of the stimulation. 2) To evaluate change in body angle as a function of time, the identity of individual larvae was considered and the angle orientation was measured every 10 frames for a total period of time of five seconds. Change in body angle was measured before, during, and after two minutes of the onset of vortex flow stimulation.

7.2.5 Whole-mount fluorescence in situ hybridization

To evaluate the cell number expressing CRH, AVP, and/or OXT in the NPO region of zebrafish larvae, whole mount fluorescence in situ hybridization was performed by Ulrich Herget in our laboratory as described elsewhere (Wolf and Ryu, 2013); probes for *crh*, *avp*, and *oxt* are reported in (Herget et al., 2014). Larvae were imaged in 80% glycerol in PBS using a Nikon 20x glycerol objective and a Leica SP5 confocal laser scanning microscope. Acquisition and analysis of confocal images for later cell counting was performed as reported in (Herget et al., 2014).

7.2.6 Calcium Imaging

For quantification of hypothalamic cell activity, the transgenic lines *Tg(crh:RFP)hd21* and *Tg(otpa3kb:GCaMP3.0)hd22* were used; these transgenic lines were established by Dr. Colette vom Berg-Maurer as described in (Vom Berg-Maurer et al., 2016). Double-transgenic larvae were either exposed to prolonged vortex flow stimulation, or untreated at day 5 and on the following day were used for cell activity measurements. In order to measure hypothalamic cell activity upon stress response activation, larvae were exposed to osmotic shock (250 mM NaCl) and calcium imaging

was measured *in vivo*. Calcium imaging was performed by Marcel Kegel in our laboratory using a custom-built two-photon microscope. Imaging acquisition, osmotic shock stimulation, and analysis of calcium events in hypothalamic cells were performed as described in (Vom Berg-Maurer et al., 2016). For this thesis, the area under the curve of calcium events elicited by responsive CRH cells after osmotic shock stimulation was calculated and plotted for comparison between larvae exposed to prolonged vortex flow stimulation at 5 dpf and untreated larvae.

7.2.7 Cell dissociation protocol

For cell isolation experiments, the transgenic line otpECR6:GFP (*Tg(otpECR6-E1b:mmGFP)hd12*) was used (Gutierrez-Triana et al., 2014). *otp*ECR6:GFP fish were incrossed and their progenies collected and maintained in standard conditions. At 2-3 dpf, embryos were selected for the presence of GFP expression in the NPO region using a fluorescent dissecting microscope (Leica, MZ16). Groups of 100 *otp*ECR6:GFP (+) and (-) larvae were placed in petri dishes (Ø=100 mm) containing 35 mL of E2 medium and kept at 28°C in an incubator (Rubarth Apparate GmbH, RuMed 3101). On the day of the experiment, groups of 100 larvae were sacrificed with ice water and collected in 1.5 mL tubes placed on ice. All samples were collected at 9 a.m. Medium was removed from the tubes and larvae were washed one time with PBS. Either 600 μL of cell dissociation solution (FACSmax, Amsbio), or of PBS, was added to each tube together with 5 μL of 10 KU/mL DNaseI (Sigma Aldrich Chemie GmbH). Tubes were placed on a water bath at 28°C to facilitate cell dissociation. Samples were homogenized either by using a syringe and needle or a plastic pestle with a motor (VWR International, 431-0100). In the case of syringe-needle homogenization, three sizes of needles were used to progressively homogenize the sample going from the largest to the smallest size (needle Ø= 0.6, 0.5, and 0.4 mm). The same size of a needle was used until no clumps were observed. Both homogenization protocols (syringe-needle and motor pestle) were performed in a period of time no longer than 30 minutes, alternating one-two minutes of homogenization and five minutes of resting periods on the water bath. When the homogenization was finished, samples were placed on ice and one volume (600 μL) of washing solution (7.5 μL DNase I (10 KU) in 1 mL PBS) was added to each sample. The content of each tube belonging to the same experimental group was then passed through a 40 μm cell strainer (Sigma Aldrich Chemie GmbH; Corning) and collected in

one single 50 mL tube. Samples were then centrifuged at 4500 rpm and 4°C for 5 minutes (Heraeus Labofuge 400R) and the supernatant was removed. Cell pellet coming from 500 dissociated larvae was re-suspended in 4 mL of a 1:1 solution of PBS and FACSmax (resuspension solution); propodium iodide was added in order to evaluate cell viability. The cell suspension was then passed through a 35 μm cell strainer and collected in a 5 mL FACS tube (neoLab Migge GmbH; BD Falcon). Samples were kept on ice until entered into the FACS machine (no longer than 20 minutes).

7.2.8 FACS

In order to separate GFP+ and GFP- cells, cell suspensions coming from the cell dissociation protocol were passed through a fluorescent activated cell sorter (BD FACSAria Illu). Cell sorting was performed at room temperature and the cell sorter laser was set at a wavelength of 488 nm at 200 mW. Sorted cells were directly collected either in lysis buffer for RNA extraction (Qiagen, RNeasy MicroKit) and stored at -80°C, or in PBS for confirmation of GFP expression by fluorescence microscopy. The settings for cell sorting were empirically determined by using a cell suspension coming from wildtype larvae. Cells were sorted depending on cell size (forward scatter, FSC-A) and granularity (side scatter, SSC-A) in order to avoid cell debris and clumps of cells. Single cells were then sorted depending on their fluorescence and categorized as GFP+ and GFP-; the gates for GFP+ and GFP- cell populations were carefully set as to assure minimum probability of cross contamination. Confirmation of the quality (cell debris vs single cells; percentage of GFP-expressing cells) and identity of cells sorted as GFP+ or GFP- was evaluated by fluorescence microscopy and qPCR (*oxt* expression), respectively.

7.2.9 RNA extraction

Isolation of total RNA was performed using the RNeasy Micro Kit (Qiagen) according to the manufacturer instructions. Quantitation and quality control of isolated RNA was evaluated by running a chip (Agilent Technologies, RNA6000 Pico Kit) on a bioanalyzer (Agilent 2100).

7.2.10 RNAseq libraries preparation

Libraries for RNAseq were prepared using Smart-seq2 technology as described elsewhere (Picelli et al., 2014, Llorens-Bobadilla et al., 2015); libraries were prepared by Enirc Llorens-Bobadilla at the Molecular Neurobiology Department of the German Cancer Research Center, Heidelberg, Germany. Briefly, 100 ng of total RNA were subjected to reverse transcription using an oligo(dT) primer and a locked nucleic acid (LNA)-containing template-switching oligonucleotide (Exiqon). The generated full-length cDNAs were amplified using 15 cycles of PCR with KAPA HiFi DNA polymerase (KAPA biosystems). The amplified cDNAs were purified using two rounds of AMPure XP SPRI purification at 0.8X (Beckman Coulter Inc.). Quantification of cDNAs was performed by using Qubit and cDNA integrity was controlled by running a High Sensitivity Bioanalyzer chip (Agilent). A total of 500 pg of cDNA from each sample was converted into uniquely barcoded libraries for Ilumina sequencing according to the Nextera XT Sample Preparation protocol (Ilumina) with minor modifications. Briefly, the tegmentation step was extended to 8 minutes and a double cleanup with 0.8X AMPure XP SPRI beads was performed after 9 cycles of PCR amplification. Multiplexing was performed with 5 ng of each sample. The multiplex was finally cleaned and concentrated using 1X SPRI beads, measured again by Qubit, and run on a bioanalyzer chip to evaluate the final molarity prior to sequencing.

7.2.11 RNA-seq and expression analysis

RNA sequencing was performed by GATC Biotech AG (Constance, Germany) using a Genome Sequencer Ilumina HiSeq2500. Briefly, RNAseq reads were aligned to zebrafish genome (GRCz10) using Bowtie (Langmead et al., 2009). TopHat (Trapnell et al., 2009) was used to identify the potential exon-exon splice junctions of the initial alignment; identification and quantification of the transcripts from the RNA-seq alignment-assembly was performed using Cufflinks (Trapnell et al., 2013). Subsequently, Cuffmerge (Trapnell et al., 2013) was used to merge the identified transcript pieces to full length transcripts and annotate the transcripts based on the given annotations. Finally, differential expression levels at the transcript and gene level were determined using Cuffdiff (Trapnell et al., 2013).

7.2.12 qPCR

Real time qPCR for validation of RNAseq data was performed from the generated cDNA libraries (section 6.2.10) using Power SYBR Green PCR Master Mix (Thermo Fisher Scientific) according to the manufacturer instructions. In the case of real time qPCR for confirmation of GFP(+) cell identity, total RNA was extracted from sorted cells as described in section 6.2.9 and one round of amplification using the MessageAmp II aRNA amplification kit (Life Technologies) was performed. Amplified RNA was then used as template for real time qPCR using the Power SYBR Green RNA-to-Ct 1 Step Kit (Thermo Fisher Scientific) according to the manufacturer instructions. Section 7.1.7 shows the list of primers used for real time qPCR. The sequences of the primers were obtained either from literature or from GETPrime (Swiss Federal Institute of Technology in Lausanne). All primers were tested for efficiency by running serial dilutions of samples. Efficiency was calculated with the formula:

$$E = 10^{\wedge}(-1/slope)-1$$

Where *E* is efficiency and *slope* is calculated from plotting template concentration (log) vs Ct values. Only primers with 90-110% efficiency were considered for further experiments. Real time qPCR was carried out in a 7500 Real Time PCR system (Applied Biosystems) and data was analyzed using the $2^{-\Delta\Delta Ct}$ method in order to calculate relative gene expression (Schmittgen and Livak, 2008).

7.2.13 Gene ontology analysis

Gene ontology, network, and pathway analysis were performed using the Ingenuity Pathway Analysis (IPA) software (Qiagen). Molecule identifiers from RNA-seq data from zebrafish larvae were converted into their human orthologs using BioMart (Smedley et al., 2015) and used as input to performer a core analysis using IPA software. The input data contained the Ensembl gene IDs, fragments per kilo base per million (FPKM), log ratio (log2(fold change)), and adjusted *p*-value (q-value) for each gene of the experimental groups that were compared. From 16,249 annotated genes identified after RNA-seq, IPA mapped 13,272. The criteria for gene selection for further pathway analysis were set as follows: adjusted p-value below 0.05, log ratio larger than 0.5, and FPKM larger than 1. Up- and downregulated genes were analyzed simultaneously. IPA software performs Fisher's exact tests for each network/interaction and it gives a *p*-value which is then converted into a score (-log10(*p*-value)). Top

enriched canonical pathways, upstream regulators, and function annotations were selected based on IPA's score.

7.2.14 Optogenetic manipulation

The transgenic lines pomc:bPAC (*Tg(Pomc:bPAC-2A-tdTomato)hd10*) and *StAR*:bPAC (*Tg2kbStARp:bPAC-tdTomato)hd19*) were generated as described elsewhere (De Marco et al., 2013, Gutierrez-Triana et al., 2015). Transgenic pomc:bPAC and *StAR*:bPAC fish were crossed with wild type fish and embryos were collected in groups of 30 in small petri dishes (Ø= 35 mm) with 5 mL of E2 media. To avoid unspecific activation of bPAC during development, small petri dishes containing the transgenic embryos were placed in custom-made containers covered by 550 nm long-pass filters (Thorlabs). The containers where then placed in an incubator (28°C) with a 12:12 light/dark cycle. For the transgenic line pomc:bPAC, larvae were screened for the presence of dtTomato expression in the pituitary at 4 or 5 dpf using a florescence dissecting microscope (MZ6, Leica). In the case of *StAR*:bPAC, larvae were screened for the presence of dtTomato expression in the interrenal gland at 3 dpf. Optogenetic manipulations were performed in 6 dpf pomc:bPAC or 4 dpf *StAR*:bPAC larvae using a custom-made LED ring placed at a fixed distance above a small petri dish containing the larvae. The incident angle of the LEDs allowed for homogenous illumination of the petri dish. LEDs were controlled with custom-made drivers, pulse generators and a TTL control box (USB-IO box, Noldus). Larvae were exposed to a single or multiple stimulations consisting of three minutes of blue light with an intensity of 2.8 $mW*cm^{-2}$. For multiple stimulations, pomc:bPAC larvae were exposed to four light stimulations with an inter-trial interval of 30 minutes. Each light pulse consisted of 100 ms flashes at 5Hz. Samples were immobilized with ice cold water and collected for cortisol extraction two minutes after the light stimulation offset.

7.2.15 Genetically targeted cell ablation

The transgenic lines *otp*ECR6:nfsB-GFP (*Tg(otpECR6-E1b:nfsb-GFP)hd14*) and *StAR*:nfsB-GFP (*Tg(2kbStARp:nfsb-GFP)hd18*) were generated as described elsewhere (Gutierrez-Triana et al., 2014, Gutierrez-Triana et al., 2015). Transgenic *otp*ECR6:nfsB-GFP and *StAR*:nfsB-GFP fish were incrossed and embryos were collected in groups of 80 in petri dishes (Ø= 100 mm) with 25-30 mL of E2 media. Conditional cell ablation

was performed as reported (Curado et al., 2007). At 3 dpf, embryos were screened for GFP expression in the NPO region for *otp*ECR6:nfsB-GFP embryos, or in the interrenal gland for *StAR*:nfsB-GFP embryos. GFP+ and GFP- embryos were transferred in groups of 30 to small petri dishes (Ø= 35 mm) containing either 5 mL of E2 or 5 mL of E2 + MTZ (10 mM). Embryos were maintained in this solution for 48 h (with medium exchange at 24 h) at 28°C, under dark conditions. At 5 dpf, medium was exchanged to fresh E2 medium for all experimental groups and larvae were kept at 28°C under normal 12:12 light/dark conditions for 24 h. GFP+ and GFP- larvae with or without exposure to MTZ treatment on the previous days, were then exposed to acute vortex flow stimulation as described in 6.2.2.1. Larvae were immobilized with ice cold water and collected for cortisol extraction after 10 minutes of vortex flow stimulation onset.

7.2.16 Statistical analysis

All group data are presented as mean ± standard error of the mean (S.E.M). Two-group comparisons were made using a Student's t-test; null hypothesis was rejected at the *$p<0.05$, **$p<0.01$, ***$p<0.001$, or ****$p<0.0001$ level. Multiple group comparisons were performed using One-way or Two-way ANOVA, followed by Turkey's or Sidak's post-test, respectively, for multiple comparisons between individual groups; null hypothesis was rejected at the $p<0.05$ level. When the data did not meet the assumptions of One-way ANOVA, the non-parametric Kruskal-Wallis test was performed, followed by a Dunn's multiple comparison post-test; null hypothesis was rejected at the $p<0.05$ level. To evaluate correlations, the Pearson's rank correlation coefficient was used. Fisher's test was used for comparing circular data; the null hypothesis was rejected at the $p<0.05$ level.

8. REFERNECES

AKHTAR, M. T., ALI, S., RASHIDI, H., VAN DER KOOY, F., VERPOORTE, R. & RICHARDSON, M. K. 2013. Developmental effects of cannabinoids on zebrafish larvae. *Zebrafish,* 10**,** 283-93.

ALBECK, D. S., MCKITTRICK, C. R., BLANCHARD, D. C., BLANCHARD, R. J., NIKULINA, J., MCEWEN, B. S. & SAKAI, R. R. 1997. Chronic social stress alters levels of corticotropin-releasing factor and arginine vasopressin mRNA in rat brain. *J Neurosci,* 17**,** 4895-903.

ALDERMAN, S. L. & BERNIER, N. J. 2009. Ontogeny of the corticotropin-releasing factor system in zebrafish. *Gen Comp Endocrinol,* 164**,** 61-9.

ALON, T., ZHOU, L., PEREZ, C. A., GARFIELD, A. S., FRIEDMAN, J. M. & HEISLER, L. K. 2009. Transgenic mice expressing green fluorescent protein under the control of the corticotropin-releasing hormone promoter. *Endocrinology,* 150**,** 5626-32.

ALSOP, D. & VIJAYAN, M. M. 2008. Development of the corticosteroid stress axis and receptor expression in zebrafish. *Am J Physiol Regul Integr Comp Physiol,* 294**,** R711-9.

ALSOP, D. & VIJAYAN, M. M. 2009. Molecular programming of the corticosteroid stress axis during zebrafish development. *Comp Biochem Physiol A Mol Integr Physiol,* 153**,** 49-54.

AMPARAN, D., AVRAM, D., THOMAS, C. G., LINDAHL, M. G., YANG, J., BAJAJ, G. & ISHMAEL, J. E. 2005. Direct interaction of myosin regulatory light chain with the NMDA receptor. *J Neurochem,* 92**,** 349-61.

ANCHISI, L., DESSI, S., PANI, A. & MANDAS, A. 2012. Cholesterol homeostasis: a key to prevent or slow down neurodegeneration. *Front Physiol,* 3**,** 486.

ARNOLD, G. P. 1974. Rheotropism in fishes. *Biol. Rev. Camb. Philos. Soc.,* 49**,** 515-576.

ARONSSON, M., FUXE, K., DONG, Y., AGNATI, L. F., OKRET, S. & GUSTAFSSON, J. A. 1988. Localization of glucocorticoid receptor mRNA in the male rat brain by in situ hybridization. *Proc Natl Acad Sci U S A,* 85**,** 9331-5.

ASHFORD, J. W. 2004. APOE genotype effects on Alzheimer's disease onset and epidemiology. *J Mol Neurosci,* 23**,** 157-65.

AUPERIN, B. & GESLIN, M. 2008. Plasma cortisol response to stress in juvenile rainbow trout is influenced by their life history during early development and by egg cortisol content. *Gen Comp Endocrinol,* 158**,** 234-9.

BAGATTO, B., PELSTER, B. & BURGGREN, W. W. 2001. Growth and metabolism of larval zebrafish: effects of swim training. *J Exp Biol,* 204**,** 4335-43.

BAINS, J. S., WAMSTEEKER CUSULIN, J. I. & INOUE, W. 2015. Stress-related synaptic plasticity in the hypothalamus. *Nat Rev Neurosci,* 16**,** 377-88.

BAK-COLEMAN, J., COURT, A., PALEY, D. A. & COOMBS, S. 2013. The spatiotemporal dynamics of rheotactic behavior depends on flow speed and available sensory information. *J Exp Biol,* 216**,** 4011-24.

BAKER, C. F., MONTGOMERY, J. C. & DENNIS, T. E. 2002. The sensory basis of olfactory search behavior in banded kokopu (Galaxias fasciatus). *J Comp Physiol A Neuroethol Sens Neural Behav Physiol,* 188**,** 553-60.

BAKER, F. C. & MONTGOMERY, C. J. 1999. The sensory basis of rheotaxis in the blind Mexican cave fish, Astyanax fasciatus. *Journal of Comparative Physiology A,* 184**,** 519-527.

BALE, T. L. 2015. Epigenetic and transgenerational reprogramming of brain development. *Nat Rev Neurosci,* 16**,** 332-44.

BARRY, T. P., MALISON, J. A., HELD, J. A. & PARRISH, J. J. 1995a. Ontogeny of the cortisol stress response in larval rainbow trout. *Gen Comp Endocrinol,* 97**,** 57-65.

BARRY, T. P., OCHIAI, M. & MALISON, J. A. 1995b. In vitro effects of ACTH on interrenal corticosteroidogenesis during early larval development in rainbow trout. *Gen Comp Endocrinol,* 99**,** 382-7.

BARTON, B. A. 2002. Stress in fishes: a diversity of responses with particular reference to changes in circulating corticosteroids. *Integr Comp Biol,* 42**,** 517-25.

BEATO, M. & SANCHEZ-PACHECO, A. 1996. Interaction of steroid hormone receptors with the transcription initiation complex. *Endocr Rev,* 17**,** 587-609.

BIRNBERG, N. C., LISSITZKY, J. C., HINMAN, M. & HERBERT, E. 1983. Glucocorticoids regulate proopiomelanocortin gene expression in vivo at the levels of transcription and secretion. *Proc Natl Acad Sci U S A,* 80**,** 6982-6.

BRIOLAT, V., JOUNEAU, L., CARVALHO, R., PALHA, N., LANGEVIN, C., HERBOMEL, P., SCHWARTZ, O., SPAINK, H. P., LEVRAUD, J. P. & BOUDINOT, P. 2014. Contrasted innate responses to two viruses in zebrafish: insights into the ancestral repertoire of vertebrate IFN-stimulated genes. *J Immunol,* 192**,** 4328-41.

BROWN, A. S., VINOGRADOV, S., KREMEN, W. S., POOLE, J. H., DEICKEN, R. F., PENNER, J. D., MCKEAGUE, I. W., KOCHETKOVA, A., KERN, D. & SCHAEFER, C. A. 2009. Prenatal exposure to maternal infection and executive dysfunction in adult schizophrenia. *Am J Psychiatry,* 166**,** 683-90.

BUDICK, S. A. & O'MALLEY, D. M. 2000. Locomotor repertoire of the larval zebrafish: swimming, turning and prey capture. *J Exp Biol,* 203**,** 2565-79.

BUIJS, R. M., VAN EDEN, C. G., GONCHARUK, V. D. & KALSBEEK, A. 2003. The biological clock tunes the organs of the body: timing by hormones and the autonomic nervous system. *J Endocrinol,* 177**,** 17-26.

BURGESS, H. A. & GRANATO, M. 2007. Sensorimotor gating in larval zebrafish. *J Neurosci,* 27**,** 4984-94.

BURNE, T., SCOTT, E., VAN SWINDEREN, B., HILLIARD, M., REINHARD, J., CLAUDIANOS, C., EYLES, D. & MCGRATH, J. 2011. Big ideas for small brains: what can psychiatry learn from worms, flies, bees and fish? *Mol Psychiatry,* 16**,** 7-16.

CALLAGHAN, B. L. & RICHARDSON, R. 2011. Maternal separation results in early emergence of adult-like fear and extinction learning in infant rats. *Behav Neurosci,* 125**,** 20-8.

CHAMPAGNE, F. A., WEAVER, I. C., DIORIO, J., DYMOV, S., SZYF, M. & MEANEY, M. J. 2006. Maternal care associated with methylation of the estrogen receptor-alpha1b promoter and estrogen receptor-alpha expression in the medial preoptic area of female offspring. *Endocrinology,* 147**,** 2909-15.

CHARMANDARI, E., TSIGOS, C. & CHROUSOS, G. 2005. Endocrinology of the stress response. *Annu Rev Physiol,* 67**,** 259-84.

CHEN, J., EVANS, A. N., LIU, Y., HONDA, M., SAAVEDRA, J. M. & AGUILERA, G. 2012. Maternal deprivation in rats is associated with corticotrophin-releasing hormone (CRH) promoter hypomethylation and enhances CRH transcriptional responses to stress in adulthood. *J Neuroendocrinol,* 24**,** 1055-64.

CHOLERIS, E., PFAFF, D. W. & KAVALIERS, M. 2013. *Oxytocin, Vasopressin and Related Peptides in the Regulation of Behavior,* New York, Cambridge University Press.

CHOU, M. Y., LIN, C. H., CHAO, P. L., HUNG, J. C., CRUZ, S. A. & HWANG, P. P. 2015. Stanniocalcin-1 controls ion regulation functions of ion-transporting epithelium other than calcium balance. *Int J Biol Sci,* 11**,** 122-32.

CHUNG, S., SON, G. H. & KIM, K. 2011. Circadian rhythm of adrenal glucocorticoid: its regulation and clinical implications. *Biochim Biophys Acta,* 1812**,** 581-91.

CICCHETTI, D. C., DONALD J. 2013. *Developmental Psychopathology, Developmental Neuroscience*.

COOTE, J. H. 1995. Cardiovascular function of the paraventricular nucleus of the hypothalamus. *Biol Signals,* 4**,** 142-9.

COTTRELL, E. C. & SECKL, J. R. 2009. Prenatal stress, glucocorticoids and the programming of adult disease. *Front Behav Neurosci,* 3**,** 19.

COUTINHO, A. E. & CHAPMAN, K. E. 2011. The anti-inflammatory and immunosuppressive effects of glucocorticoids, recent developments and mechanistic insights. *Mol Cell Endocrinol.*

CULLINAN, W. E. 2000. GABA(A) receptor subunit expression within hypophysiotropic CRH neurons: a dual hybridization histochemical study. *J Comp Neurol,* 419**,** 344-51.

CULLINAN, W. E., HERMAN, J. P., BATTAGLIA, D. F., AKIL, H. & WATSON, S. J. 1995. Pattern and time course of immediate early gene expression in rat brain following acute stress. *Neuroscience,* 64**,** 477-505.

CURADO, S., ANDERSON, R. M., JUNGBLUT, B., MUMM, J., SCHROETER, E. & STAINIER, D. Y. 2007. Conditional targeted cell ablation in zebrafish: a new tool for regeneration studies. *Dev Dyn,* 236**,** 1025-35.

DALLMAN, M. F., AKANA, S. F., LEVIN, N., WALKER, C. D., BRADBURY, M. J., SUEMARU, S. & SCRIBNER, K. S. 1994. Corticosteroids and the control of function in the hypothalamo-pituitary-adrenal (HPA) axis. *Ann N Y Acad Sci,* 746**,** 22-31; discussion 31-2, 64-7.

DALLMAN, M. F., STRACK, A. M., AKANA, S. F., BRADBURY, M. J., HANSON, E. S., SCRIBNER, K. A. & SMITH, M. 1993. Feast and famine: critical role of glucocorticoids with insulin in daily energy flow. *Front Neuroendocrinol,* 14**,** 303-47.

DASKALAKIS, N. P., BAGOT, R. C., PARKER, K. J., VINKERS, C. H. & DE KLOET, E. R. 2013. The three-hit concept of vulnerability and resilience: toward understanding adaptation to early-life adversity outcome. *Psychoneuroendocrinology,* 38**,** 1858-73.

DATSON, N. A., MORSINK, M. C., MEIJER, O. C. & DE KLOET, E. R. 2008. Central corticosteroid actions: Search for gene targets. *Eur J Pharmacol,* 583**,** 272-89.

DAVIES, C. T. & FEW, J. D. 1973. Effects of exercise on adrenocortical function. *J Appl Physiol,* 35**,** 887-91.

DAVIS, L. G., ARENTZEN, R., REID, J. M., MANNING, R. W., WOLFSON, B., LAWRENCE, K. L. & BALDINO, F., JR. 1986. Glucocorticoid sensitivity of vasopressin mRNA levels in the paraventricular nucleus of the rat. *Proc Natl Acad Sci U S A,* 83**,** 1145-9.

DE KLOET, E. R., JOELS, M. & HOLSBOER, F. 2005. Stress and the brain: from adaptation to disease. *Nat Rev Neurosci,* 6**,** 463-75.

DE KLOET, E. R., VREUGDENHIL, E., OITZL, M. S. & JOELS, M. 1998. Brain corticosteroid receptor balance in health and disease. *Endocr Rev,* 19**,** 269-301.

DE MARCO, R. J., GRONEBERG, A. H., YEH, C. M., CASTILLO RAMIREZ, L. A. & RYU, S. 2013. Optogenetic elevation of endogenous glucocorticoid level in larval zebrafish. *Front Neural Circuits,* 7.

DE SOUZA, R. F. & ARAVIND, L. 2010. UMA and MABP domains throw light on receptor endocytosis and selection of endosomal cargoes. *Bioinformatics,* 26**,** 1477-80.

DENES, A., LOPEZ-CASTEJON, G. & BROUGH, D. 2012. Caspase-1: is IL-1 just the tip of the ICEberg? *Cell Death Dis,* 3**,** e338.

DI, S., MALCHER-LOPES, R., HALMOS, K. C. & TASKER, J. G. 2003. Nongenomic glucocorticoid inhibition via endocannabinoid release in the hypothalamus: a fast feedback mechanism. *J Neurosci,* 23**,** 4850-7.

DI, S., MAXSON, M. M., FRANCO, A. & TASKER, J. G. 2009. Glucocorticoids regulate glutamate and GABA synapse-specific retrograde transmission via divergent nongenomic signaling pathways. *J Neurosci,* 29**,** 393-401.

DICKMEIS, T. 2009. Glucocorticoids and the circadian clock. *J Endocrinol,* 200**,** 3-22.

EATON, J. L., HOLMQVIST, B. & GLASGOW, E. 2008. Ontogeny of vasotocin-expressing cells in zebrafish: selective requirement for the transcriptional regulators orthopedia and single-minded 1 in the preoptic area. *Dev Dyn,* 237**,** 995-1005.

EATON, R. C., BOMBARDIERI, R. A. & MEYER, D. L. 1977. The Mauthner-initiated startle response in teleost fish. *J Exp Biol,* 66**,** 65-81.

EBERWINE, J. 1999. Glucocorticoid and Mineralocorticoid Receptors as Transcription Factors. *In:* SIEGEL, G. J., AGRANOFF, B. W., ALBERS, R. W., FISHER, S. K. & UHLER, M. D. (eds.) *Basic Neurochemistry: Molecular, Cellular and Medical Aspects.* 6th ed. Philadelphia: Lippincott-Raven.

EBERWINE, J. H. & ROBERTS, J. L. 1984. Glucocorticoid regulation of pro-opiomelanocortin gene transcription in the rat pituitary. *Journal of Biological Chemistry,* 259**,** 2166-2170.

ENGESZER, R. E., PATTERSON, L. B., RAO, A. A. & PARICHY, D. M. 2007. Zebrafish in the wild: a review of natural history and new notes from the field. *Zebrafish,* 4**,** 21-40.

ERKUT, Z. A., POOL, C. & SWAAB, D. F. 1998. Glucocorticoids suppress corticotropin-releasing hormone and vasopressin expression in human hypothalamic neurons. *J Clin Endocrinol Metab,* 83**,** 2066-73.

EVANSON, N. K., TASKER, J. G., HILL, M. N., HILLARD, C. J. & HERMAN, J. P. 2010. Fast feedback inhibition of the HPA axis by glucocorticoids is mediated by endocannabinoid signaling. *Endocrinology,* 151**,** 4811-9.

FALKOWSKA, A., GUTOWSKA, I., GOSCHORSKA, M., NOWACKI, P., CHLUBEK, D. & BARANOWSKA-BOSIACKA, I. 2015. Energy Metabolism of the Brain, Including the Cooperation between Astrocytes and Neurons, Especially in the Context of Glycogen Metabolism. *Int J Mol Sci,* 16**,** 25959-81.

FERGUSON, A. V., LATCHFORD, K. J. & SAMSON, W. K. 2008. The Paraventricular Nucleus of the Hypothalamus A Potential Target for Integrative Treatment of Autonomic Dysfunction. *Expert Opin Ther Targets,* 12**,** 717-27.

FIOL, D. F. & KULTZ, D. 2007. Osmotic stress sensing and signaling in fishes. *Febs j,* 274**,** 5790-8.

FLEISCHER, N., DONALD, R. A. & BUTCHER, R. W. 1969. Involvement of adenosine 3',5'-monophosphate in release of ACTH. *Am J Physiol,* 217**,** 1287-91.

FRIES, E., HESSE, J., HELLHAMMER, J. & HELLHAMMER, D. H. 2005. A new view on hypocortisolism. *Psychoneuroendocrinology,* 30**,** 1010-6.

FURUKAWA, H., SINGH, S. K., MANCUSSO, R. & GOUAUX, E. 2005. Subunit arrangement and function in NMDA receptors. *Nature,* 438**,** 185-92.

FUXE, K., WIKSTROM, A. C., OKRET, S., AGNATI, L. F., HARFSTRAND, A., YU, Z. Y., GRANHOLM, L., ZOLI, M., VALE, W. & GUSTAFSSON, J. A. 1985. Mapping of glucocorticoid receptor immunoreactive neurons in the rat tel- and diencephalon using a monoclonal antibody against rat liver glucocorticoid receptor. *Endocrinology,* 117**,** 1803-12.

FUZZEN, M. L., VAN DER KRAAK, G. & BERNIER, N. J. 2010. Stirring up new ideas about the regulation of the hypothalamic-pituitary-interrenal axis in zebrafish (Danio rerio). *Zebrafish,* 7**,** 349-58.

GALLARDO, V. E. & BEHRA, M. 2013. Fluorescent activated cell sorting (FACS) combined with gene expression microarrays for transcription enrichment profiling of zebrafish lateral line cells. *Methods,* 62**,** 226-31.

GALLO-PAYET, N. & PAYET, M. D. 2003. Mechanism of action of ACTH: beyond cAMP. *Microsc Res Tech,* 61**,** 275-87.

GARDINER, J. M. & ATEMA, J. 2007. Sharks need the lateral line to locate odor sources: rheotaxis and eddy chemotaxis. *J Exp Biol,* 210**,** 1925-34.

GASCON, E., LYNCH, K., RUAN, H., ALMEIDA, S., VERHEYDEN, J. M., SEELEY, W. W., DICKSON, D. W., PETRUCELLI, L., SUN, D., JIAO, J., ZHOU, H., JAKOVCEVSKI, M., AKBARIAN, S., YAO, W. D. & GAO, F. B. 2014. Alterations in microRNA-124 and AMPA receptors contribute to social behavioral deficits in frontotemporal dementia. *Nat Med,* 20**,** 1444-51.

GEE, D. G. & CASEY, B. J. 2015. The Impact of Developmental Timing for Stress and Recovery. *Neurobiol Stress,* 1**,** 184-194.

GLASGOW, E., MURASE, T., ZHANG, B., VERBALIS, J. G. & GAINER, H. 2000. Gene expression in the rat supraoptic nucleus induced by chronic hyperosmolality versus hyposmolality. *Am J Physiol Regul Integr Comp Physiol,* 279**,** R1239-50.

GOINES, P. E., CROEN, L. A., BRAUNSCHWEIG, D., YOSHIDA, C. K., GRETHER, J., HANSEN, R., KHARRAZI, M., ASHWOOD, P. & VAN DE WATER, J. 2011. Increased midgestational IFN-gamma, IL-4 and IL-5 in women bearing a child with autism: A case-control study. *Mol Autism,* 2**,** 13.

GOURLEY, S. L., KEDVES, A. T., OLAUSSON, P. & TAYLOR, J. R. 2009. A history of corticosterone exposure regulates fear extinction and cortical NR2B, GluR2/3, and BDNF. *Neuropsychopharmacology,* 34**,** 707-16.

GRISSOM, N. & BHATNAGAR, S. 2009. Habituation to repeated stress: get used to it. *Neurobiol Learn Mem,* 92**,** 215-24.

GROENEWEG, F. L., KARST, H., DE KLOET, E. R. & JOELS, M. 2011. Rapid non-genomic effects of corticosteroids and their role in the central stress response. *J Endocrinol,* 209**,** 153-67.

GUTIERREZ-TRIANA, J. A., HERGET, U., CASTILLO-RAMIREZ, L. A., LUTZ, M., YEH, C. M., DE MARCO, R. J. & RYU, S. 2015. Manipulation of Interrenal Cell Function in Developing Zebrafish Using Genetically Targeted Ablation and an Optogenetic Tool. *Endocrinology,* 156**,** 3394-401.

GUTIERREZ-TRIANA, J. A., HERGET, U., LICHTNER, P., CASTILLO-RAMÍREZ, L. A. & RYU, S. 2014. A vertebrate-conserved cis-regulatory module for targeted expression in the main hypothalamic regulatory region for the stress response. *BMC Developmental Biology,* 14**,** 41.

HARTIG, E. I., ZHU, S., KING, B. L. & COFFMAN, J. A. 2016. Cortisol-treated zebrafish embryos develop into pro-inflammatory adults with aberrant immune gene regulation. *Biol Open,* 5**,** 1134-41.

HEIM, C., EHLERT, U. & HELLHAMMER, D. H. 2000. The potential role of hypocortisolism in the pathophysiology of stress-related bodily disorders. *Psychoneuroendocrinology,* 25**,** 1-35.

HELLBACH, S., GARTNER, P., DEICKE, J., FISCHER, D., HASSAN, A. H. & ALMEIDA, O. F. 1998. Inherent glucocorticoid response potential of isolated hypothalamic neuroendocrine neurons. *Faseb j,* 12**,** 199-207.

HELLHAMMER, D. H. & WADE, S. 1993. Endocrine correlates of stress vulnerability. *Psychother Psychosom,* 60**,** 8-17.

HERGET, U. 2015. *The molecular neuroanatomy, chemoarchitecture and projectome of the hypothalamic center regulating the stress response in larval zebrafish* Doctoral thesis, Heidelberg University.

HERGET, U., WOLF, A., WULLIMANN, M. F. & RYU, S. 2014. Molecular neuroanatomy and chemoarchitecture of the neurosecretory preoptic-hypothalamic area in zebrafish larvae. *J Comp Neurol,* 522**,** 1542-64.

HERMAN, J. P. 1995. In situ hybridization analysis of vasopressin gene transcription in the paraventricular and supraoptic nuclei of the rat: regulation by stress and glucocorticoids. *J Comp Neurol,* 363**,** 15-27.

HERMAN, J. P., ADAMS, D. & PREWITT, C. 1995. Regulatory changes in neuroendocrine stress-integrative circuitry produced by a variable stress paradigm. *Neuroendocrinology,* 61**,** 180-90.

HERMAN, J. P. & CULLINAN, W. E. 1997. Neurocircuitry of stress: central control of the hypothalamo-pituitary-adrenocortical axis. *Trends Neurosci,* 20**,** 78-84.

HERMAN, J. P., FLAK, J. & JANKORD, R. 2008. Chronic stress plasticity in the hypothalamic paraventricular nucleus. *Prog Brain Res,* 170**,** 353-64.

HERMAN, J. P., SCHAFER, M. K., THOMPSON, R. C. & WATSON, S. J. 1992. Rapid regulation of corticotropin-releasing hormone gene transcription in vivo. *Mol Endocrinol,* 6**,** 1061-9.

HILL, E. E., ZACK, E., BATTAGLINI, C., VIRU, M., VIRU, A. & HACKNEY, A. C. 2008. Exercise and circulating cortisol levels: the intensity threshold effect. *J Endocrinol Invest,* 31**,** 587-91.

HILL, M. N., KARATSOREOS, I. N., HILLARD, C. J. & MCEWEN, B. S. 2010. Rapid elevations in limbic endocannabinoid content by glucocorticoid hormones in vivo. *Psychoneuroendocrinology,* 35**,** 1333-8.

HONTELA, A., RASMUSSEN, J. B., AUDET, C. & CHEVALIER, G. 1992. Impaired cortisol stress response in fish from environments polluted by PAHs, PCBs, and mercury. *Arch Environ Contam Toxicol,* 22**,** 278-83.

HU, S. B., TANNAHILL, L. A., BISWAS, S. & LIGHTMAN, S. L. 1992. Release of corticotrophin-releasing factor-41, arginine vasopressin and oxytocin from rat fetal hypothalamic cells in culture: response to activation of intracellular second messengers and to corticosteroids. *J Endocrinol,* 132**,** 57-65.

IMAKI, T., NAHAN, J. L., RIVIER, C., SAWCHENKO, P. E. & VALE, W. 1991. Differential regulation of corticotropin-releasing factor mRNA in rat brain regions by glucocorticoids and stress. *J Neurosci,* 11**,** 585-99.

ITOI, K., TALUKDER, A. H., FUSE, T., KANEKO, T., OZAWA, R., SATO, T., SUGAYA, T., UCHIDA, K., YAMAZAKI, M., ABE, M., NATSUME, R. & SAKIMURA, K. 2014. Visualization of corticotropin-releasing factor neurons by fluorescent proteins in the mouse brain and characterization of labeled neurons in the paraventricular nucleus of the hypothalamus. *Endocrinology,* 155**,** 4054-60.

IVY, A. S., REX, C. S., CHEN, Y., DUBE, C., MARAS, P. M., GRIGORIADIS, D. E., GALL, C. M., LYNCH, G. & BARAM, T. Z. 2010. Hippocampal dysfunction and cognitive impairments provoked by chronic early-life stress involve excessive activation of CRH receptors. *J Neurosci,* 30**,** 13005-15.

JAWAHAR, M. C., MURGATROYD, C., HARRISON, E. L. & BAUNE, B. T. 2015. Epigenetic alterations following early postnatal stress: a review on novel aetiological mechanisms of common psychiatric disorders. *Clin Epigenetics,* 7**,** 122.

JEZOVA, D., SKULTETYOVA, I., TOKAREV, D. I., BAKOS, P. & VIGAS, M. 1995. Vasopressin and oxytocin in stress. *Ann N Y Acad Sci,* 771**,** 192-203.

JOELS, M., PU, Z., WIEGERT, O., OITZL, M. S. & KRUGERS, H. J. 2006. Learning under stress: how does it work? *Trends Cogn Sci,* 10**,** 152-8.

JOHNSON, E. O., KAMILARIS, T. C., CHROUSOS, G. P. & GOLD, P. W. 1992. Mechanisms of stress: a dynamic overview of hormonal and behavioral homeostasis. *Neurosci Biobehav Rev,* 16**,** 115-30.

JOHNSON, L. A., ZULOAGA, D. G., BIDIMAN, E., MARZULLA, T., WEBER, S., WAHBEH, H. & RABER, J. 2015. ApoE2 Exaggerates PTSD-Related Behavioral, Cognitive, and Neuroendocrine Alterations. *Neuropsychopharmacology,* 40**,** 2443-53.

KADMIEL, M. & CIDLOWSKI, J. A. 2013. Glucocorticoid receptor signaling in health and disease. *Trends Pharmacol Sci,* 34**,** 518-30.

KALRA, S. P., DUBE, M. G., PU, S., XU, B., HORVATH, T. L. & KALRA, P. S. 1999. Interacting appetite-regulating pathways in the hypothalamic regulation of body weight. *Endocr Rev,* 20**,** 68-100.

KANTER, M. J. & COOMBS, S. 2003. Rheotaxis and prey detection in uniform currents by Lake Michigan mottled sculpin (Cottus bairdi). *J Exp Biol,* 206**,** 59-70.

KARST, H., BERGER, S., ERDMANN, G., SCHUTZ, G. & JOELS, M. 2010. Metaplasticity of amygdalar responses to the stress hormone corticosterone. *Proc Natl Acad Sci U S A,* 107**,** 14449-54.

KARST, H., BERGER, S., TURIAULT, M., TRONCHE, F., SCHUTZ, G. & JOELS, M. 2005. Mineralocorticoid receptors are indispensable for nongenomic modulation of hippocampal glutamate transmission by corticosterone. *Proc Natl Acad Sci U S A,* 102**,** 19204-7.

KESSELS, H. W. & MALINOW, R. 2009. Synaptic AMPA receptor plasticity and behavior. *Neuron,* 61**,** 340-50.

KHAN, A. M. & WATTS, A. G. 2004. Intravenous 2-deoxy-D-glucose injection rapidly elevates levels of the phosphorylated forms of p44/42 mitogen-activated protein kinases (extracellularly regulated kinases 1/2) in rat hypothalamic parvicellular paraventricular neurons. *Endocrinology,* 145**,** 351-9.

KHULAN, B. & DRAKE, A. J. 2012. Glucocorticoids as mediators of developmental programming effects. *Best Pract Res Clin Endocrinol Metab,* 26**,** 689-700.

KIM, J. K., SUMMER, S. N., WOOD, W. M. & SCHRIER, R. W. 2001. Role of glucocorticoid hormones in arginine vasopressin gene regulation. *Biochem Biophys Res Commun,* 289**,** 1252-6.

KIMMEL, C. B., BALLARD, W. W., KIMMEL, S. R., ULLMANN, B. & SCHILLING, T. F. 1995. Stages of embryonic development of the zebrafish. *Dev Dyn,* 203**,** 253-310.

KIMMEL, C. B., PATTERSON, J. & KIMMEL, R. O. 1974. The development and behavioral characteristics of the startle response in the zebra fish. *Dev Psychobiol,* 7**,** 47-60.

KING, M. S. & BAERTSCHI, A. J. 1990. The role of intracellular messengers in adrenocorticotropin secretion in vitro. *Experientia,* 46**,** 26-40.

KISS, A. & AGUILERA, G. 1993. Regulation of the hypothalamic pituitary adrenal axis during chronic stress: responses to repeated intraperitoneal hypertonic saline injection. *Brain Res,* 630**,** 262-70.

KOHASHI, T. & ODA, Y. 2008. Initiation of Mauthner- or non-Mauthner-mediated fast escape evoked by different modes of sensory input. *J Neurosci,* 28**,** 10641-53.

KOROSI, A., SHANABROUGH, M., MCCLELLAND, S., LIU, Z. W., BOROK, E., GAO, X. B., HORVATH, T. L. & BARAM, T. Z. 2010. Early-life experience reduces excitation to stress-responsive hypothalamic neurons and reprograms the expression of corticotropin-releasing hormone. *J Neurosci,* 30**,** 703-13.

KOVACS, K., KISS, J. Z. & MAKARA, G. B. 1986. Glucocorticoid implants around the hypothalamic paraventricular nucleus prevent the increase of corticotropin-releasing factor and arginine vasopressin immunostaining induced by adrenalectomy. *Neuroendocrinology,* 44**,** 229-34.

KOVACS, K. J., FOLDES, A. & SAWCHENKO, P. E. 2000. Glucocorticoid negative feedback selectively targets vasopressin transcription in parvocellular neurosecretory neurons. *J Neurosci,* 20**,** 3843-52.

KOVACS, K. J. & MEZEY, E. 1987. Dexamethasone inhibits corticotropin-releasing factor gene expression in the rat paraventricular nucleus. *Neuroendocrinology,* 46**,** 365-8.

KOVACS, K. J. & SAWCHENKO, P. E. 1996. Sequence of stress-induced alterations in indices of synaptic and transcriptional activation in parvocellular neurosecretory neurons. *J Neurosci,* 16**,** 262-73.

KRUG, R. G., 2ND & CLARK, K. J. 2015. Elucidating cannabinoid biology in zebrafish (Danio rerio). *Gene,* 570**,** 168-79.

KUWAHARA, S., ARIMA, H., BANNO, R., SATO, I., KONDO, N. & OISO, Y. 2003. Regulation of vasopressin gene expression by cAMP and glucocorticoids in parvocellular neurons of the paraventricular nucleus in rat hypothalamic organotypic cultures. *J Neurosci,* 23**,** 10231-7.

LAM, C. S., RASTEGAR, S. & STRAHLE, U. 2006. Distribution of cannabinoid receptor 1 in the CNS of zebrafish. *Neuroscience,* 138**,** 83-95.

LANDGRAF, R., KESSLER, M. S., BUNCK, M., MURGATROYD, C., SPENGLER, D., ZIMBELMANN, M., NUSSBAUMER, M., CZIBERE, L., TURCK, C. W., SINGEWALD, N., RUJESCU, D. & FRANK, E. 2007. Candidate genes of anxiety-related behavior in HAB/LAB rats and mice: focus on vasopressin and glyoxalase-I. *Neurosci Biobehav Rev,* 31**,** 89-102.

LANGMEAD, B., TRAPNELL, C., POP, M. & SALZBERG, S. L. 2009. Ultrafast and memory-efficient alignment of short DNA sequences to the human genome. *Genome Biol,* 10**,** R25.

LAU, C. G. & ZUKIN, R. S. 2007. NMDA receptor trafficking in synaptic plasticity and neuropsychiatric disorders. *Nat Rev Neurosci,* 8**,** 413-26.

LEE, J. H., KIM, H. J., KIM, J. G., RYU, V., KIM, B. T., KANG, D. W. & JAHNG, J. W. 2007. Depressive behaviors and decreased expression of serotonin reuptake transporter in rats that experienced neonatal maternal separation. *Neurosci Res,* 58**,** 32-9.

LERMA, J. 2003. Roles and rules of kainate receptors in synaptic transmission. *Nat Rev Neurosci,* 4**,** 481-95.

LEVINE, S. 1994. The ontogeny of the hypothalamic-pituitary-adrenal axis. The influence of maternal factors. *Ann N Y Acad Sci,* 746**,** 275-88; discussion 289-93.

LIPOSITS, Z., UHT, R. M., HARRISON, R. W., GIBBS, F. P., PAULL, W. K. & BOHN, M. C. 1987. Ultrastructural localization of glucocorticoid receptor (GR) in hypothalamic paraventricular neurons synthesizing corticotropin releasing factor (CRF). *Histochemistry,* 87**,** 407-12.

LIU, N. A., HUANG, H., YANG, Z., HERZOG, W., HAMMERSCHMIDT, M., LIN, S. & MELMED, S. 2003. Pituitary corticotroph ontogeny and regulation in transgenic zebrafish. *Mol Endocrinol,* 17**,** 959-66.

LLORENS-BOBADILLA, E., ZHAO, S., BASER, A., SAIZ-CASTRO, G., ZWADLO, K. & MARTIN-VILLALBA, A. 2015. Single-Cell Transcriptomics Reveals a Population of Dormant Neural Stem Cells that Become Activated upon Brain Injury. *Cell Stem Cell,* 17**,** 329-40.

LUPIEN, S. J., MCEWEN, B. S., GUNNAR, M. R. & HEIM, C. 2009. Effects of stress throughout the lifespan on the brain, behaviour and cognition. *Nat Rev Neurosci,* 10**,** 434-445.

LÖHR, H. & HAMMERSCHMIDT, M. 2011. Zebrafish in endocrine systems: recent advances and implications for human disease. *Annu Rev Physiol,* 73**,** 183-211.

LÖHR, H., RYU, S. & DRIEVER, W. 2009. Zebrafish diencephalic A11-related dopaminergic neurons share a conserved transcriptional network with neuroendocrine cell lineages. *Development,* 136**,** 1007-17.

MA, X. M. & AGUILERA, G. 1999. Differential regulation of corticotropin-releasing hormone and vasopressin transcription by glucocorticoids. *Endocrinology,* 140**,** 5642-50.

MABB, A. M. & EHLERS, M. D. 2010. Ubiquitination in postsynaptic function and plasticity. *Annu Rev Cell Dev Biol,* 26**,** 179-210.

MACRI, S. & WURBEL, H. 2006. Developmental plasticity of HPA and fear responses in rats: a critical review of the maternal mediation hypothesis. *Horm Behav,* 50**,** 667-80.

MAKINO, S., SMITH, M. A. & GOLD, P. W. 1995. Increased expression of corticotropin-releasing hormone and vasopressin messenger ribonucleic acid (mRNA) in the hypothalamic paraventricular nucleus during repeated stress: association with reduction in glucocorticoid receptor mRNA levels. *Endocrinology,* 136**,** 3299-309.

MANOLI, M. & DRIEVER, W. 2012. Fluorescence-activated cell sorting (FACS) of fluorescently tagged cells from zebrafish larvae for RNA isolation. *Cold Spring Harb Protoc,* 2012.

MARTIN, E. I., RESSLER, K. J., JASNOW, A. M., DABROWSKA, J., HAZRA, R., RAINNIE, D. G., NEMEROFF, C. B. & OWENS, M. J. 2010. A novel transgenic mouse for gene-targeting within cells that express corticotropin-releasing factor. *Biol Psychiatry,* 67**,** 1212-6.

MARTIN, P. M., GOPAL, E., ANANTH, S., ZHUANG, L., ITAGAKI, S., PRASAD, B. M., SMITH, S. B., PRASAD, P. D. & GANAPATHY, V. 2006. Identity of SMCT1 (SLC5A8) as a neuron-specific Na+-coupled transporter for active uptake of L-lactate and ketone bodies in the brain. *J Neurochem,* 98**,** 279-88.

MCCLELLAND, S., KOROSI, A., COPE, J., IVY, A. & BARAM, T. Z. 2011. Emerging roles of epigenetic mechanisms in the enduring effects of early-life stress and experience on learning and memory. *Neurobiol Learn Mem,* 96**,** 79-88.

MCGOWAN, P. O., SASAKI, A., D'ALESSIO, A. C., DYMOV, S., LABONTE, B., SZYF, M., TURECKI, G. & MEANEY, M. J. 2009. Epigenetic regulation of the glucocorticoid receptor in human brain associates with childhood abuse. *Nat Neurosci,* 12**,** 342-8.

MCMILLIN, M., FRAMPTON, G., QUINN, M., DIVAN, A., GRANT, S., PATEL, N., NEWELL-ROGERS, K. & DEMORROW, S. 2015. Suppression of the HPA Axis During Cholestasis Can Be Attributed to Hypothalamic Bile Acid Signaling. *Mol Endocrinol,* 29**,** 1720-30.

MCMURRAY, R. G. & HACKNEY, A. C. 2000. Endocrine responses to exercise and training. *In:* GARRETT W. E., K. D. T. (ed.) *Exercise and sport science.* Philadelphia: Lippincott Williams & Wilkins.

MEIJERING, E., DZYUBACHYK, O. & SMAL, I. 2012. Methods for cell and particle tracking. *Methods Enzymol,* 504**,** 183-200.

MOISIADIS, V. G. & MATTHEWS, S. G. 2014. Glucocorticoids and fetal programming part 1: Outcomes. *Nat Rev Endocrinol,* 10**,** 391-402.

MOMMSEN, T., VIJAYAN, M. & MOON, T. 1999. Cortisol in teleosts: dynamics, mechanisms of action, and metabolic regulation. *Reviews in Fish Biology and Fisheries,* 9**,** 211-268.

MONTGOMERY, J., COOMBS, S. & HALSTEAD, M. 1995. Biology of the mechanosensory lateral line in fishes. *Reviews in Fish Biology and Fisheries,* 5**,** 399-416.

MONTGOMERY, J. C., BAKER, C. F. & CARTON, A. G. 1997. The lateral line can mediate rheotaxis in fish. *Nature,* 389**,** 960-963.

MONYER, H., SPRENGEL, R., SCHOEPFER, R., HERB, A., HIGUCHI, M., LOMELI, H., BURNASHEV, N., SAKMANN, B. & SEEBURG, P. H. 1992. Heteromeric NMDA receptors: molecular and functional distinction of subtypes. *Science,* 256**,** 1217-21.

MORICEAU, S. & SULLIVAN, R. M. 2006. Maternal presence serves as a switch between learning fear and attraction in infancy. *Nat Neurosci,* 9**,** 1004-6.

MORITA, E., SANDRIN, V., ALAM, S. L., ECKERT, D. M., GYGI, S. P. & SUNDQUIST, W. I. 2007. Identification of human MVB12 proteins as ESCRT-I subunits that function in HIV budding. *Cell Host Microbe,* 2**,** 41-53.

MUELLER, B. R. & BALE, T. L. 2008. Sex-specific programming of offspring emotionality after stress early in pregnancy. *J Neurosci,* 28**,** 9055-65.

MURGATROYD, C., PATCHEV, A. V., WU, Y., MICALE, V., BOCKMUHL, Y., FISCHER, D., HOLSBOER, F., WOTJAK, C. T., ALMEIDA, O. F. & SPENGLER, D. 2009. Dynamic DNA methylation programs persistent adverse effects of early-life stress. *Nat Neurosci,* 12**,** 1559-66.

MURGATROYD, C. & SPENGLER, D. 2011. Epigenetic programming of the HPA axis: early life decides. *Stress,* 14**,** 581-9.

NEDERHOF, E. & SCHMIDT, M. V. 2012. Mismatch or cumulative stress: toward an integrated hypothesis of programming effects. *Physiol Behav,* 106**,** 691-700.

NESAN, D. & VIJAYAN, M. M. 2012. Embryo exposure to elevated cortisol level leads to cardiac performance dysfunction in zebrafish. *Mol Cell Endocrinol,* 363**,** 85-91.

NEWTON, R. & HOLDEN, N. S. 2007. Separating transrepression and transactivation: a distressing divorce for the glucocorticoid receptor? *Mol Pharmacol,* 72**,** 799-809.

O'MALLEY, D. M., KAO, Y. H. & FETCHO, J. R. 1996. Imaging the functional organization of zebrafish hindbrain segments during escape behaviors. *Neuron,* 17**,** 1145-55.

OLSZEWSKI, J., HAEHNEL, M., TAGUCHI, M. & LIAO, J. C. 2012. Zebrafish larvae exhibit rheotaxis and can escape a continuous suction source using their lateral line. *PLoS One,* 7**,** e36661.

PALKOVITS, M. 1999. Interconnections between the neuroendocrine hypothalamus and the central autonomic system. Geoffrey Harris Memorial Lecture, Kitakyushu, Japan, October 1998. *Front Neuroendocrinol,* 20**,** 270-95.

PICELLI, S., FARIDANI, O. R., BJORKLUND, A. K., WINBERG, G., SAGASSER, S. & SANDBERG, R. 2014. Full-length RNA-seq from single cells using Smart-seq2. *Nat Protoc,* 9**,** 171-81.

PIEKARSKI, A., DECUYPERE, E., BUYSE, J. & DRIDI, S. 2016. Chenodeoxycholic acid reduces feed intake and modulates the expression of hypothalamic neuropeptides and hepatic lipogenic genes in broiler chickens. *Gen Comp Endocrinol,* 229**,** 74-83.

PINNA, G. 2013. Targeting neurosteroidogenesis as therapy for PTSD. *Front Pharmacol,* 4.

POGODA, H. M. & HAMMERSCHMIDT, M. 2007. Molecular genetics of pituitary development in zebrafish. *Semin Cell Dev Biol,* 18**,** 543-58.

POPOLI, M., YAN, Z., MCEWEN, B. S. & SANACORA, G. 2011. The stressed synapse: the impact of stress and glucocorticoids on glutamate transmission. *Nat Rev Neurosci,* 13**,** 22-37.

PUGLIELLI, L., TANZI, R. E. & KOVACS, D. M. 2003. Alzheimer's disease: the cholesterol connection. *Nat Neurosci,* 6**,** 345-51.

RABER, J., AKANA, S. F., BHATNAGAR, S., DALLMAN, M. F., WONG, D. & MUCKE, L. 2000. Hypothalamic-pituitary-adrenal dysfunction in Apoe(-/-) mice: possible role in behavioral and metabolic alterations. *J Neurosci,* 20**,** 2064-71.

RAIBORG, C. & STENMARK, H. 2009. The ESCRT machinery in endosomal sorting of ubiquitylated membrane proteins. *Nature,* 458**,** 445-52.

REDDY, D. S. 2010. Neurosteroids: endogenous role in the human brain and therapeutic potentials. *Prog Brain Res,* 186**,** 113-37.

REUL, J. M. & DE KLOET, E. R. 1985. Two receptor systems for corticosterone in rat brain: microdistribution and differential occupation. *Endocrinology,* 117**,** 2505-11.

REYNOLDS, R. M. 2013. Glucocorticoid excess and the developmental origins of disease: two decades of testing the hypothesis--2012 Curt Richter Award Winner. *Psychoneuroendocrinology,* 38**,** 1-11.

ROOZENDAAL, B., HERNANDEZ, A., CABRERA, S. M., HAGEWOUD, R., MALVAEZ, M., STEFANKO, D. P., HAETTIG, J. & WOOD, M. A. 2010. Membrane-associated glucocorticoid activity is necessary for modulation of long-term memory via chromatin modification. *J Neurosci,* 30**,** 5037-46.

ROTH, M., OBAIDAT, A. & HAGENBUCH, B. 2012. OATPs, OATs and OCTs: the organic anion and cation transporters of the SLCO and SLC22A gene superfamilies. *Br J Pharmacol,* 165**,** 1260-87.

ROTH, T. L., LUBIN, F. D., FUNK, A. J. & SWEATT, J. D. 2009. Lasting epigenetic influence of early-life adversity on the BDNF gene. *Biol Psychiatry,* 65**,** 760-9.

ROUGE-PONT, F., MAYO, W., MARINELLI, M., GINGRAS, M., LE MOAL, M. & PIAZZA, P. V. 2002. The neurosteroid allopregnanolone increases dopamine release and dopaminergic response to morphine in the rat nucleus accumbens. *Eur J Neurosci,* 16**,** 169-73.

ROUGEOT, J., ZAKRZEWSKA, A., KANWAL, Z., JANSEN, H. J., SPAINK, H. P. & MEIJER, A. H. 2014. RNA sequencing of FACS-sorted immune cell populations from zebrafish infection models to identify cell specific responses to intracellular pathogens. *Methods Mol Biol,* 1197**,** 261-74.

RUSSO, S. J., MURROUGH, J. W., HAN, M., CHARNEY, D. S. & NESTLER, E. J. 2012. Neurobiology of Resilience. *Nat Neurosci,* 15**,** 1475-84.

RYU, M. H., MOSKVIN, O. V., SILTBERG-LIBERLES, J. & GOMELSKY, M. 2010. Natural and engineered photoactivated nucleotidyl cyclases for optogenetic applications. *J Biol Chem,* 285**,** 41501-8.

SANDI, C. & HALLER, J. 2015. Stress and the social brain: behavioural effects and neurobiological mechanisms. *Nat Rev Neurosci,* 16**,** 290-304.

SAPOLSKY, R. M., ROMERO, L. M. & MUNCK, A. U. 2000. How do glucocorticoids influence stress responses? Integrating permissive, suppressive, stimulatory, and preparative actions. *Endocr Rev,* 21**,** 55-89.

SARRAZIN, A. F., NUNEZ, V. A., SAPEDE, D., TASSIN, V., DAMBLY-CHAUDIERE, C. & GHYSEN, A. 2010. Origin and early development of the posterior lateral line system of zebrafish. *J Neurosci,* 30**,** 8234-44.

SATO, N. & MORISHITA, R. 2015. The roles of lipid and glucose metabolism in modulation of β-amyloid, tau, and neurodegeneration in the pathogenesis of Alzheimer disease. *Front Aging Neurosci,* 7.

SAWCHENKO, P. E. 1987. Adrenalectomy-induced enhancement of CRF and vasopressin immunoreactivity in parvocellular neurosecretory neurons: anatomic, peptide, and steroid specificity. *J Neurosci,* 7**,** 1093-106.

SCHMIDT, M. V. 2010. Molecular mechanisms of early life stress--lessons from mouse models. *Neurosci Biobehav Rev,* 34**,** 845-52.

SCHMIDT, M. V., WANG, X. D. & MEIJER, O. C. 2011. Early life stress paradigms in rodents: potential animal models of depression? *Psychopharmacology (Berl),* 214**,** 131-40.

SCHMITTGEN, T. D. & LIVAK, K. J. 2008. Analyzing real-time PCR data by the comparative C(T) method. *Nat Protoc,* 3**,** 1101-8.

SECKL, J. R. & MEANEY, M. J. 2004. Glucocorticoid programming. *Ann N Y Acad Sci,* 1032**,** 63-84.

SEEBURG, P. H., SINGLE, F., KUNER, T., HIGUCHI, M. & SPRENGEL, R. 2001. Genetic manipulation of key determinants of ion flow in glutamate receptor channels in the mouse. *Brain Res,* 907**,** 233-43.

SELYE, H. 1936. A syndrome produced by diverse nocuous agents. *Nature,* 138**,** 32-32.

SELYE, H. 1956. *The stress of life,* New York, McGraw-Hill.

SIMMICH, J., STAYKOV, E. & SCOTT, E. 2012. Zebrafish as an appealing model for optogenetic studies. *Prog Brain Res,* 196**,** 145-62.

SINGH-TAYLOR, A., KOROSI, A., MOLET, J., GUNN, B. G. & BARAM, T. Z. 2015. Synaptic rewiring of stress-sensitive neurons by early-life experience: a mechanism for resilience? *Neurobiol Stress,* 1**,** 109-115.

SMEDLEY, D., HAIDER, S., DURINCK, S., PANDINI, L., PROVERO, P., ALLEN, J., ARNAIZ, O., AWEDH, M. H., BALDOCK, R., BARBIERA, G., BARDOU, P., BECK, T., BLAKE, A., BONIERBALE, M., BROOKES, A. J., BUCCI, G., BUETTI, I., BURGE, S., CABAU, C., CARLSON, J. W., CHELALA, C., CHRYSOSTOMOU, C., CITTARO, D., COLLIN, O., CORDOVA, R., CUTTS, R. J., DASSI, E., DI GENOVA, A., DJARI, A., ESPOSITO, A., ESTRELLA, H., EYRAS, E., FERNANDEZ-BANET, J., FORBES, S., FREE, R. C., FUJISAWA, T., GADALETA, E., GARCIA-MANTEIGA, J. M., GOODSTEIN, D., GRAY, K., GUERRA-ASSUNCAO, J. A., HAGGARTY, B., HAN, D. J., HAN, B. W., HARRIS, T., HARSHBARGER, J., HASTINGS, R. K., HAYES, R. D., HOEDE, C., HU, S., HU, Z. L., HUTCHINS, L., KAN, Z., KAWAJI, H., KELIET, A., KERHORNOU, A., KIM, S., KINSELLA, R., KLOPP, C., KONG, L., LAWSON, D., LAZAREVIC, D., LEE, J. H., LETELLIER, T., LI, C. Y., LIO, P., LIU, C. J., LUO, J., MAASS, A., MARIETTE, J., MAUREL, T., MERELLA, S., MOHAMED, A. M., MOREEWS, F., NABIHOUDINE, I., NDEGWA, N., NOIROT, C., PEREZ-LLAMAS, C., PRIMIG, M., QUATTRONE, A., QUESNEVILLE, H., RAMBALDI, D., REECY, J., RIBA, M., ROSANOFF, S., SADDIQ, A. A., SALAS, E., SALLOU, O., SHEPHERD, R., SIMON, R., SPERLING, L., SPOONER, W., STAINES, D. M., STEINBACH, D., STONE, K., STUPKA, E., TEAGUE, J. W., DAYEM ULLAH, A. Z., WANG, J., WARE, D., et al. 2015. The BioMart community portal: an innovative alternative to large, centralized data repositories. *Nucleic Acids Res,* 43**,** W589-98.

SOLITO, E., MULLA, A., MORRIS, J. F., CHRISTIAN, H. C., FLOWER, R. J. & BUCKINGHAM, J. C. 2003. Dexamethasone induces rapid serine-phosphorylation and membrane translocation of annexin 1 in a human folliculostellate cell line via a novel nongenomic mechanism involving the glucocorticoid receptor, protein kinase C, phosphatidylinositol 3-kinase, and mitogen-activated protein kinase. *Endocrinology,* 144**,** 1164-74.

STEENBERGEN, P., METZ, J., FLIK, G., RICHARDSON, M. & CHAMPAGNE, D. 2012. Methods to Quantify Basal and Stress-Induced Cortisol Response in Larval Zebrafish. *In:* KALUEFF, A. V. & STEWART, A. M. (eds.) *Zebrafish Protocols for Neurobehavioral Research.* Humana Press.

STEENBERGEN, P. J., RICHARDSON, M. K. & CHAMPAGNE, D. L. 2011. The use of the zebrafish model in stress research. *Prog Neuropsychopharmacol Biol Psychiatry,* 35**,** 1432-51.

STIERL, M., STUMPF, P., UDWARI, D., GUETA, R., HAGEDORN, R., LOSI, A., GARTNER, W., PETEREIT, L., EFETOVA, M., SCHWARZEL, M., OERTNER, T. G., NAGEL, G. & HEGEMANN, P. 2011. Light modulation of cellular cAMP by a small bacterial photoactivated adenylyl cyclase, bPAC, of the soil bacterium Beggiatoa. *J Biol Chem,* 286**,** 1181-8.

SULI, A., WATSON, G. M., RUBEL, E. W. & RAIBLE, D. W. 2012. Rheotaxis in larval zebrafish is mediated by lateral line mechanosensory hair cells. *PLoS One,* 7**,** e29727.

SUN, Y., LUO, Z. M., GUO, X. M., SU, D. F. & LIU, X. 2015. An updated role of microRNA-124 in central nervous system disorders: a review. *Front Cell Neurosci,* 9.

SWANSON, L. W. & SAWCHENKO, P. E. 1980. Paraventricular nucleus: a site for the integration of neuroendocrine and autonomic mechanisms. *Neuroendocrinology,* 31**,** 410-7.

SWANSON, L. W. & SAWCHENKO, P. E. 1983. Hypothalamic Integration: Organization of the Paraventricular and Supraoptic Nuclei. *Ann. Rev. Neurosci.,* 6**,** 269-324.

TASKER, J. G. & HERMAN, J. P. 2011. Mechanisms of rapid glucocorticoid feedback inhibition of the hypothalamic-pituitary-adrenal axis. *Stress,* 14**,** 398-406.

TAYLOR, S. E. 2010. Mechanisms linking early life stress to adult health outcomes. *Proc Natl Acad Sci U S A,* 107**,** 8507-12.

TO, T. T., HAHNER, S., NICA, G., ROHR, K. B., HAMMERSCHMIDT, M., WINKLER, C. & ALLOLIO, B. 2007. Pituitary-interrenal interaction in zebrafish interrenal organ development. *Mol Endocrinol,* 21**,** 472-85.

TRAPNELL, C., HENDRICKSON, D. G., SAUVAGEAU, M., GOFF, L., RINN, J. L. & PACHTER, L. 2013. Differential analysis of gene regulation at transcript resolution with RNA-seq. *Nat Biotechnol,* 31**,** 46-53.

TRAPNELL, C., PACHTER, L. & SALZBERG, S. L. 2009. TopHat: discovering splice junctions with RNA-Seq. *Bioinformatics,* 25**,** 1105-11.

UHT, R. M., MCKELVY, J. F., HARRISON, R. W. & BOHN, M. C. 1988. Demonstration of glucocorticoid receptor-like immunoreactivity in glucocorticoid-sensitive vasopressin and corticotropin-releasing factor neurons in the hypothalamic paraventricular nucleus. *J Neurosci Res,* 19**,** 405-11, 468-9.

ULRICH-LAI, Y. M. & HERMAN, J. P. 2009. Neural regulation of endocrine and autonomic stress responses. *Nat Rev Neurosci,* 10**,** 397-409.

VERKUYL, J. M., HEMBY, S. E. & JOELS, M. 2004. Chronic stress attenuates GABAergic inhibition and alters gene expression of parvocellular neurons in rat hypothalamus. *Eur J Neurosci,* 20**,** 1665-73.

VIJAYAN, M. M. & LEATHERLAND, J. F. 1990. High stocking density affects cortisol secretion and tissue distribution in brook charr, Salvelinus fontinalis. *J Endocrinol,* 124**,** 311-8.

VIJAYAN, M. M., REDDY, P. K., LEATHERLAND, J. F. & MOON, T. W. 1994. The effects of cortisol on hepatocyte metabolism in rainbow trout: a study using the steroid analogue RU486. *Gen Comp Endocrinol,* 96**,** 75-84.

VIRU, A. & VIRU, M. 2004. Cortisol--essential adaptation hormone in exercise. *Int J Sports Med,* 25**,** 461-4.

VISVANATHAN, J., LEE, S., LEE, B., LEE, J. W. & LEE, S. K. 2007. The microRNA miR-124 antagonizes the anti-neural REST/SCP1 pathway during embryonic CNS development. *Genes Dev,* 21**,** 744-9.

VOM BERG-MAURER, C. M., TRIVEDI, C. A., BOLLMANN, J. H., DE MARCO, R. J. & RYU, S. 2016. The Severity of Acute Stress Is Represented by Increased Synchronous Activity and Recruitment of Hypothalamic CRH Neurons. *J Neurosci,* 36**,** 3350-62.

WAMSTEEKER CUSULIN, J. I., FUZESI, T., WATTS, A. G. & BAINS, J. S. 2013. Characterization of corticotropin-releasing hormone neurons in the paraventricular nucleus of the hypothalamus of Crh-IRES-Cre mutant mice. *PLoS One,* 8**,** e64943.

WANG, A., NIE, W., LI, H., HOU, Y., YU, Z., FAN, Q. & SUN, R. 2014. Epigenetic upregulation of corticotrophin-releasing hormone mediates postnatal maternal separation-induced memory deficiency. *PLoS One,* 9**,** e94394.

WANG, Z., GERSTEIN, M. & SNYDER, M. 2009. RNA-Seq: a revolutionary tool for transcriptomics. *Nat Rev Genet,* 10**,** 57-63.

WEAVER, I. C., CERVONI, N., CHAMPAGNE, F. A., D'ALESSIO, A. C., SHARMA, S., SECKL, J. R., DYMOV, S., SZYF, M. & MEANEY, M. J. 2004. Epigenetic programming by maternal behavior. *Nat Neurosci,* 7**,** 847-54.

WEAVER, I. C., SZYF, M. & MEANEY, M. J. 2002. From maternal care to gene expression: DNA methylation and the maternal programming of stress responses. *Endocr Res,* 28**,** 699.

WENDELAAR BONGA, S. E. 1997. The stress response in fish. *Physiol Rev,* 77**,** 591-625.

WESTERFIELD, M. 2000. *The zebrafish book. A guide for the laboratory use of zebrafish (Danio rerio).* Eugene, University of Oregon Press.

WILLIAMS, G., HARROLD, J. A. & CUTLER, D. J. 2000. The hypothalamus and the regulation of energy homeostasis: lifting the lid on a black box. *Proc Nutr Soc,* 59**,** 385-96.

WILSON, K. S., TUCKER, C. S., AL-DUJAILI, E. A., HOLMES, M. C., HADOKE, P. W., KENYON, C. J. & DENVIR, M. A. 2016. Early-life glucocorticoids programme behaviour and metabolism in adulthood in zebrafish. *J Endocrinol,* 230**,** 125-42.

WIRTH, M. M. 2011. Beyond the HPA Axis: Progesterone-Derived Neuroactive Steroids in Human Stress and Emotion. *Front Endocrinol (Lausanne),* 2.

WISMER FRIES, A. B., ZIEGLER, T. E., KURIAN, J. R., JACORIS, S. & POLLAK, S. D. 2005. Early experience in humans is associated with changes in neuropeptides critical for regulating social behavior. *Proc Natl Acad Sci U S A,* 102**,** 17237-40.

WOLF, A. & RYU, S. 2013. Specification of posterior hypothalamic neurons requires coordinated activities of Fezf2, Otp, Sim1a and Foxb1.2. *Development,* 140**,** 1762-73.

YADAV, R. S. & TIWARI, N. K. 2014. Lipid integration in neurodegeneration: an overview of Alzheimer's disease. *Mol Neurobiol,* 50**,** 168-76.

YEH, C. M., GLOCK, M. & RYU, S. 2013. An optimized whole-body cortisol quantification method for assessing stress levels in larval zebrafish. *PLoS One,* 8**,** e79406.

YIN, L., MADDISON, L. A. & CHEN, W. 2016. Multiplex conditional mutagenesis in zebrafish using the CRISPR/Cas system. *Methods Cell Biol,* 135**,** 3-17.

YUEN, E. Y., WEI, J., LIU, W., ZHONG, P., LI, X. & YAN, Z. 2012. Repeated stress causes cognitive impairment by suppressing glutamate receptor expression and function in prefrontal cortex. *Neuron,* 73**,** 962-77.

ZHANG, Y. & EDWARDS, P. A. 2008. FXR signaling in metabolic disease. *FEBS Lett,* 582**,** 10-8.

ZHU, B. G., ZHU, D. H. & CHEN, Y. Z. 1998. Rapid enhancement of high affinity glutamate uptake by glucocorticoids in rat cerebral cortex synaptosomes and human neuroblastoma clone SK-N-SH: possible involvement of G-protein. *Biochem Biophys Res Commun,* 247**,** 261-5.

ZIEGLER, D. R., CULLINAN, W. E. & HERMAN, J. P. 2005. Organization and regulation of paraventricular nucleus glutamate signaling systems: N-methyl-D-aspartate receptors. *J Comp Neurol,* 484**,** 43-56.

9. LIST OF ABBREVIATIONS

ACTH - adrenocorticotropic hormone

AEA - anandamide

2-AG - 2-arachidonoylglycerol

AVP - arginine vasopressin

BDNF - brain derived neurotrophic factor

BNST - bed nucleus of the stria terminalis

bPAC - *Beggiatoa* photoactivated adenylyl cyclase

CB1 - Cannabinoid receptor type 1

CRH - corticotropin releasing hormone

CRHR - corticotropin releasing hormone receptor

CREB - cyclic AMP response element binding protein

DNA - deoxyribonucleic acid

dp - dorsal parvocellular

dpf - days post-fertilization

ELS - early life stress

FACS - fluorescence activated cell sorting

FSC-A - forward scatter

GABA - gamma aminobutyric acid

GCs - glucocorticoids

GFP - green fluorescence protein

GluR5 - (also GRIK1) glutamate ionotropic receptor kainate type subunit 1

GR - glucocorticoid receptor

GRE - glucocorticoid responsive element

h - hours

HPA - hypothalamus-pituitary-adrenal axis

hpf - hours post-fertilization

HPI - hypothalamus-pituitary-adrenal axis

IPA - Ingenuity Pathway Analysis software (Qiagen)

mc2r - melanocortin 2 receptor

Met - metronidazole

min - minutes

miRNA - micro ribonucleic acid

mM - millimolar

mW - milliwatts

mpv - ventral division of the medial parvocellular regions

mpd - dorsal division of the medial parvocellular regions

MR - mineralocorticoid receptor

n.s. - non-significant

nfsB - nitroreductase (dihydropteridine reductase, NAD(P)H-dependent, oxygen-insensitive)

NaCl - Sodium chloride

NM - nitroreductase-metronidazole

NMDA - N-methyl-D-aspartate

NPO - neurosecretory preoptic area

Otp - orthopedia

OXT - oxytocin

p - pulses

PFC - prefrontal cortex

pg - picograms

pm - posterior magnocellular

pomc - proopiomelanocortin

PVN - paraventricular nucleus

q-PCR - quantitative polymerase chain reaction

RFP - red fluorescence protein

RNA - ribonucleic acid

rpm - revolutions per minute

SSC-A - side scatter

StAR - steroidogenic acute regulatory protein

10. ACKNOWLEDGEMENTS

I am deeply grateful to Dr. Soojin Ryu, my supervisor, for she has always been supportive and helpful. I thank her for her advice and guidance through this process and for the opportunity she has given me to learn and grow. I genuinely thank her for always being interested in the progress of my project and for always being willing to answer my questions, providing assistance, and having scientific discussions. Thank you Soojin for your time and for your words; thank you for your kindness. I express my gratitude as well to Dr. Jan Lohmann, Dr. Ilme Schlichting, and Dr. Anton Meinhart, whose advice contributed to the development of this work and kept me motivated to move forward on my project. My sincere gratitude as well to the National Council of Science and Technology in Mexico (CONACYT), and to the Instituto de Innovación y Transferencia de Tecnología of Nuevo León (I2T2), Mexico, for their support.

I would like to express my gratitude to all the people who contributed to this project: to David Ibberson for providing assistance in the evaluation of RNA quality; to Dr. Monika Langlotz and the Flow Cytometry & FACS Core Facility of the Center for Molecular Biology at Heidelberg University (ZMBH), for their support concerning fluorescence activated cell sorting (FACS); to Dr. Ana Martin-Villalba and Dr. Enric Llorens-Bobadilla for generating the cDNA libraries for transcriptome analysis; to Dr. Juan Mateo for his valuable contributions and comments concerning bioinformatics and for his advice on statistical analysis.

Many thanks to all the current and former members of our team for always providing a nice atmosphere and sharing knowledge and experiences. Thanks to Boris Knerr and Chen-Min Yeh for providing help when I needed at the beginning of my project. Special thanks to Antonia Groneberg for her advice and discussions about data analysis and for the fruitful collaborations; I appreciate your willingness to always listen to our challenges, either scientific or personal. I am grateful that I had the chance to meet Markus Lutz; your soul is pure and patient, there is much that one can learn from you! Thanks to Laura Flores, for her commitment and hard work as a master student, it was always pleasant to work with you. Special thanks as well to Theresa Thiemann, for her outstanding and efficient help with screenings and cortisol experiments. It was always a pleasure to work with you.

I am deeply thankful to Ulrich Herget, because he was always willing to provide help and listen to what I had to say, not only about work, but also about life. I am extremely glad I had the opportunity to work with you, and I am thankful for the fruitful collaborations. Thank you for all your help with experiments and for sharing with us all your stories!

I express my gratitude to Rodrigo de Marco, whose advice and insights were essential for the development of my project. I really appreciate the time you invested in our discussions and the knowledge you shared not only with me, but with our whole team. Thank you for your support and guidance. I am also grateful to Arturo Gutierrez for his outstanding support regarding molecular biology and for always keeping a joyful atmosphere in the lab. It was always pleasant to work with you and I am extremely glad that our work together was productive and efficient. My gratitude goes as well to Colette vom Berg-Maurer, thank you for your genuine interest in helping every time that it was needed.

Thanks to Heidrun Krabbenhöft, Marcel Kegel, Peter Steenbergen, and Patrick Lichtner, for always being good colleagues and for providing a nice atmosphere in which it was always nice to work.

Many thanks to Regina Singer for always providing technical support, for keeping our lab running with all necessary reagents and stock solutions, and for taking care of the fish. Thanks as well to Gabi Shoeman and Angelika Schoell for their assistance with fish care.

At this point, I will express my gratitude to my family, whose unconditional support has contributed significantly to the accomplishment of this work.

Estoy profundamente agradecido con mis padres, Martha Elva Ramírez González y Juan Castillo Montemayor, quienes siempre me han brindado lo que necesito y más. Estoy agradecido por su apoyo en todas mis decisiones y su confianza incondicional. Gracias por su amor, cariño, afecto, tiempo y atención a lo largo de este proceso. Gracias por los valores de trabajo y respeto que me enseñaron y que me han permitido realizar este proyecto. Han invertido gran parte de su vida en mi hermano y en mí; ahora, los frutos que nosotros colectamos son también producto de su labor. Este trabajo es también de Uds. Gracias a mi hermano, Juan Alejandro Castillo Ramírez, y a mi

cuñada Jannet Mares Vidal, por su apoyo, respeto, y por siempre ser un ejemplo de trabajo duro, planeación, y determinación para alcanzar las metas laborales y personales.

Gracias a la nueva familia de la que también soy parte, Elia Nancy Mendivil Molina, Jaime Otañez Hurtado, Elisa María Otañez Mendivil y Andrea María Otañez Mendivil. Gracias por su apoyo, cariño, respeto y confianza a lo largo de este proceso. Gracias por abrirme las puertas de su hogar y su familia.

Finalmente, mi más grande agradecimiento hacia mi esposa, Nancy María Otañez Mendivil, quien me ha acompañado y apoyado totalmente sin reservas durante este tiempo y con quien he compartido cada una de las experiencias vividas a través de este proceso. Gracias por siempre recordarme lo que realmente es importante en la vida, tanto en lo laboral como en lo personal. Gracias por siempre escucharme y por tu consejo incondicional. Gracias por compartir tu amor, tu tiempo, y atención. Gracias por regalarme sonrisas y reconfortarme cada uno de nuestros días. Gracias por alimentarme el alma. Haber compartido esta experiencia contigo ha sido alentador y gratificante. Hemos crecido y aprendido juntos durante estos años y es así como deseo seguir a tu lado: siempre aprendiendo y sirviendo.